UNIVERSITÀ DEGLI STUDI DI PALERMO

Dottorato di ricerca in Oncologia e Chirurgia Sperimentali
Dipartimento di Medicina di Precisione in Area Medica, Chirurgica e Critica (Me.Pre.C.C.)

Molecular mechanisms underlying the ability of colorectal cancer derived small extracellular vesicles to induce epithelial to mesenchymal transition of normal hepatocytes: new insight on liver metastases formation

Doctoral Dissertation of:
Marco Loria

Tutor:
Prof. Riccardo Alessandro

Co-Tutor:
Prof. Alice Conigliaro
Prof. Simona Fontana

The Chair of the Doctoral Program:
Prof. Antonio Russo

2025 – XXXVII Ciclo

"Nulla di ciò che si ottiene senza dolore e senza lavoro è veramente prezioso." (Joseph Addison, 1672-1719).

Index

Abstract

Colorectal cancer (CRC) is one of the most common tumor diseases, accounting for two million new cases every year [1]. Epidemiological data show that almost 50% of the CRC patients will develop liver metastases, which are still the leading cause of CRC related deaths [2]. Many literature data have shown the role of Tumor derived small extracellular vesicles (TD_sEVs) in the definition of the pre-metastatic niche (PMN) in the liver, promoting morpho-functional alterations which pave the way for the establishment of a favorable microenvironment for future organ colonization by metastatic cells [3]. Although the studies have highlighted the effect of TD_sEVs on the PMN formation in the liver, most of them focused on the intervention of the non-parenchymal component of the liver (Hepatic Stellate Cells and Kupffer cells), while the active role of the parenchymal cells, the hepatocytes (which account for almost 80% among the liver cell population), has been mostly neglected [4]. Our research group already demonstrated the effects of CRC-derived small extracellular vesicles (CRC_sEVs) in the promotion of the epithelial-to mesenchymal transition (EMT) of human healthy hepatocytes, particularly focusing on TGF-β1 signaling activation, but the inhibition of this pathway only partially blocked the EMT program on the hepatocytes [5]. Non-coding RNA cargo in the EVs is gaining particular interest, due to their activity in gene expression regulation [6]. I focused my attention on the role of lncH19 carried by CRC_sEVs and its involvement in biological processes associated with the establishment of a favorable microenvironment for metastatic cell organ colonization. Moreover, in the context of EV research, the current methodology deployed in the field can rarely reproduce the chronic effects of the sEVs on recipient cells. In fact, in most studies focusing on the role of TD_sEVs in PMN formation, the effect of the vesicles on recipient cells is evaluated through immediate and acute treatment, which due to high lipid dose delivery can trigger unspecific responses in target cells, altering the downstream results [7]. Recently, new microfluidic devices are gaining the attention of EV-researchers, partly because of the possibility of interconnecting the different organ cytotypes through different chambers and channels in these innovative culture systems. These Organ-on-a-Chip platforms (OoCs) also offer the opportunity to perform chronic delivery of the EVs to the recipient cells, using syringe or peristaltic pumps, mimicking a condition more similar to the *in vivo* condition, contextually reducing the number of animal models deployed for biomedical research, in accordance with the 3R ethical guidelines [8]. The data reported in this thesis show, for the first time, the role of Colorectal cancer derived sEVs (CRC_sEVs) in promoting alternative splicing (AS) mechanisms of mRNAs related to the Epithelial-To-Mesenchymal transition (EMT), a biological process required for the establishment of organ fibrosis, with a particular focus on EV-associated lncH19, which role in the PMN definition has not been deeply investigated [9, 10]. Moreover, I developed an advanced OoC culture system which offers the possibility to increase hepatocyte differentiation, prolonging their maintenance in vitro, and performing a chronic delivery of the CRC_sEVs, which overcomes the limitations of the acute treatment normally performed for the majority of EV studies.

CHAPTER 1

Colorectal Cancer and Liver Metastases

Colorectal Cancer (CRC) represents approximately the third most common malignant neoplastic transformation for incidence and the second cause of cancer-related deaths in both males and females, with a total of 19.29 million new cases and 9.96 million deaths in 2020, [11, 12]. Geographical differences were registered in mortality and incidence rates and age of diagnosis across different genders and regions of the world, and many factors like diet, lifestyle, inflammations disorders and family history can affect the incidence rate in the population (***Figure 1***) [13, 14]. This cancer form comprises colon and/or rectum cancer and is caused by aberrant proliferation of glandular epithelial cells [15]. Like many solid tumors, CRC is a heterogeneous disease which can be classified according to molecular and clinical features in sporadic, hereditary, and colitis-associated [16, 17]. Metastasis is the primary cause of CRC-related mortality in these patients [18], the prevention of tumour metastasis can delay the progression of cancers by preventing metastatic cells from colonizing other organs [19]. Population-based studies show that almost 25-30% of patients affected by CRC will develop liver metastases during their pathology [20]. Despite the medical advances made in the recent years, only the 25% of CRC patients are amenable for metastases resection, which until now represents the only way for their cure [1, 21].

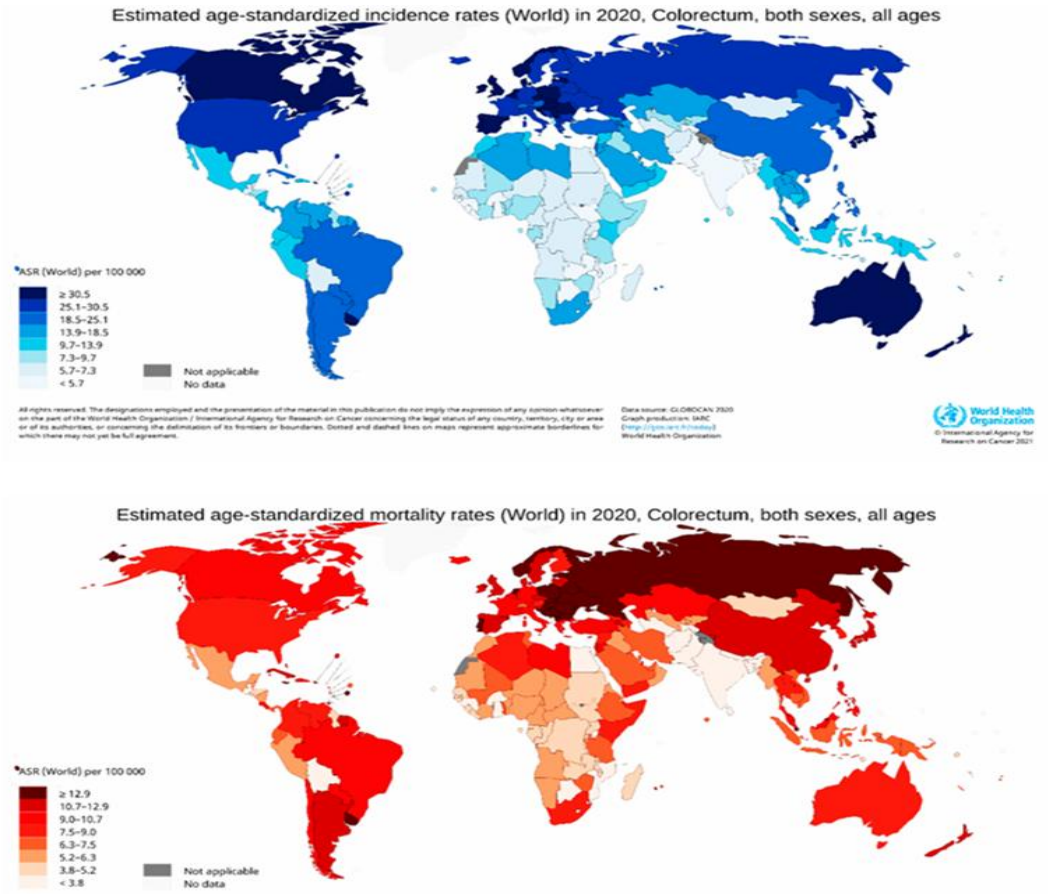

Figure 1 *Map showing the global distribution of estimated age-standardized incidence rates (top) and mortality rate (bottom) of CRC in 2020 for both sexes and all ages. Sanower Hossain et al.2022.*

In a pioneer model proposed by Fearon and Vogelstein, the sequential accumulation of mutations in onco-suppressors and oncogenes (APC, KRAS, BRAF, TP53) explained colorectal tumorigenesis by describing the progression from normal colonic epithelium to adenoma (early and late), and eventually carcinoma, which in worst case scenario can culminate in distant organ metastases [22, 23]. The normal colon epithelium is composed of crypts containing a variety of cytotypes: at the bottom, colonic stem cells reside in the crypt, establishing a microenvironment known as "stem cell niche". The stemness of these cells is maintained by their epigenetic state and by the interaction with surrounding cytotypes, which have a deep role in preserving this environment. For instance, myofibroblast (surrounding colonic stem cells) release signalling factors with crucial role in maintaining their stemness. Colonic stem cells divide through asymmetrical division, leading to the formation of a colonic stem cell, and another cell which will be the precursor of the different cell types of the colon [24]. This precursor cell will differentiate into enterocytes (nutrient uptake), globet cells (muchus production) and enteroendocrine cells (hormone secretion). In their stemness potentiality, colonic stem cels share some common traits with CRC stem cells [25]. The chronic evolution of CRC indicates that it is likely originated form an aberrant crypt, which degenerate into a polyp, initially benign [26]. After a certain amount of time (10 to 15 years), the benign polyp can ultimately transform into CRC [27, 28]. In 70-90% of cases, this represents the canonical adenoma-carcinoma metastasis model discovered by the scientific community (***Figure 2***) [16]. As mentioned above, for all these degenerative steps to take place, specific mutations ned to occur. The general signature genetic of "APC-TP53-KRAS" has been now established as the Vogelstein model [29].

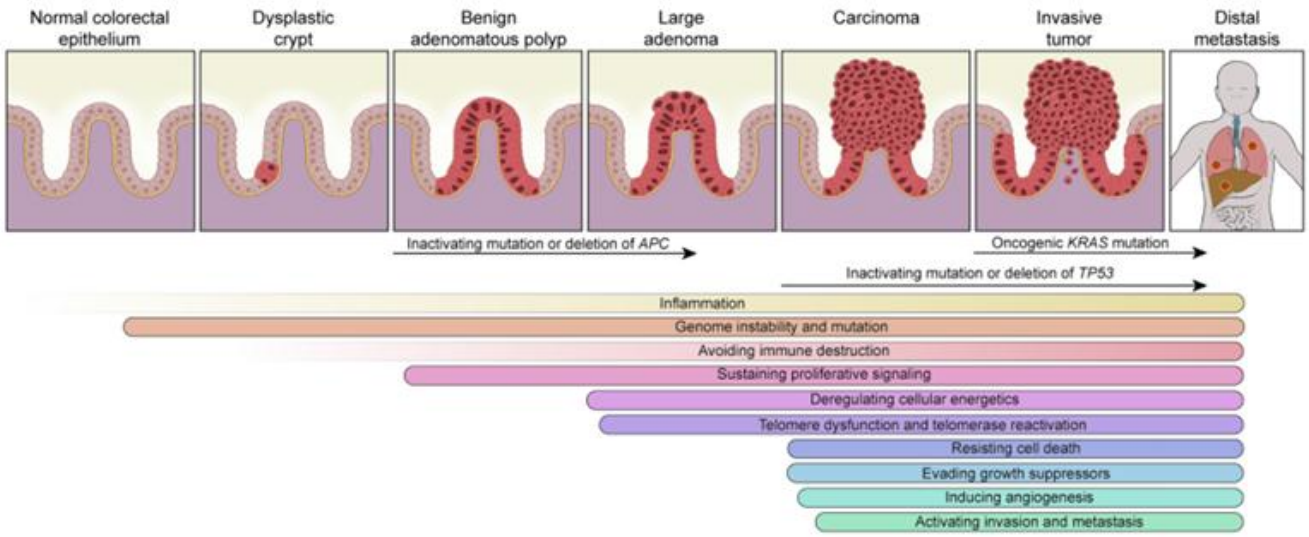

Figure 2 *CRC "adenoma-carcinoma-metastasis" conventional model and corresponding hallmarks. Li Jiexi et al. 2021.*

The liver is the most common site of CRC metastases. Up to 25% CRC patients may have synchronous Colorectal cancer-liver metastases (CRC-LM) [30]. Metastasizing cancer cells show site-specific tropism upon encountering a unique tissue microenvironment to adapt and survive. Since 1889, when Paget proposed the "seed and soil" hypothesis, unravelling how disseminating tumour cells show a selective preference for specific organs, the different molecular mechanism underlying tumour invasion have been extensively studied. In fact, during CRC progression, a subpopulation of CRC cells acquires the capacity to evade from the primary tumour, due to the activation of biological processes like EMT, ECM degradation, intravasation, survival in the blood stream, extravasation and eventually colonizing the distant organ, such as the lung or the liver (***Figure 3***) [31]. This process is strictly related to genome instability of cancers, which leads to the activation of oncogenes and the simultaneous inactivation of tumour suppressor genes. The development of CRC-LM is extremely complex and requires the activation of different molecular mechanism (TGF-β1 signalling pathway, non-coding RNAs, c-MET signalling pathway, Notch signalling [32, 33]. Different studies have demonstrated the mechanisms driving specific organ colonization by CRC circulating cells, and the colonized organ also plays an important role in the process. In fact, being an immunological fortress and given its role in the regulation of complex metabolism processes, the liver is a highly metastasis-compatible organs [34, 35]. The rich and slow venous supply connection between the liver and the gut, and the immune tolerance of the liver are part of the reasons for the metastatic colonization [2]. Moreover, the right side of the colon is adjacent to the liver, which may also cause direct spread of CRC metastases. The expression of chemokines further enforces the colonization of this organ; in fact, the high expression of CXCL12 deliver specific homing signals for disseminating CRC cells (especially the subtypes with high expression of CXCR4 receptors) [34]. Recent studies have demonstrated the importance of the interaction between the tumoral cells and the extracellular matrix (ECM) in every step of liver metastasis formation. The ECM comprises a complex collection of extracellular proteins organized in a three-dimensional architecture in which cells establish complex structural interactions [36]. For circulating tumour cells (CTCs), liver ECM provides a favourable microenvironment to survive and proliferate [37, 38]. All these reasons taken together contribute to establish the previously described fertile "soil" for metastasizing CRC cells (the seeds) [39, 40].

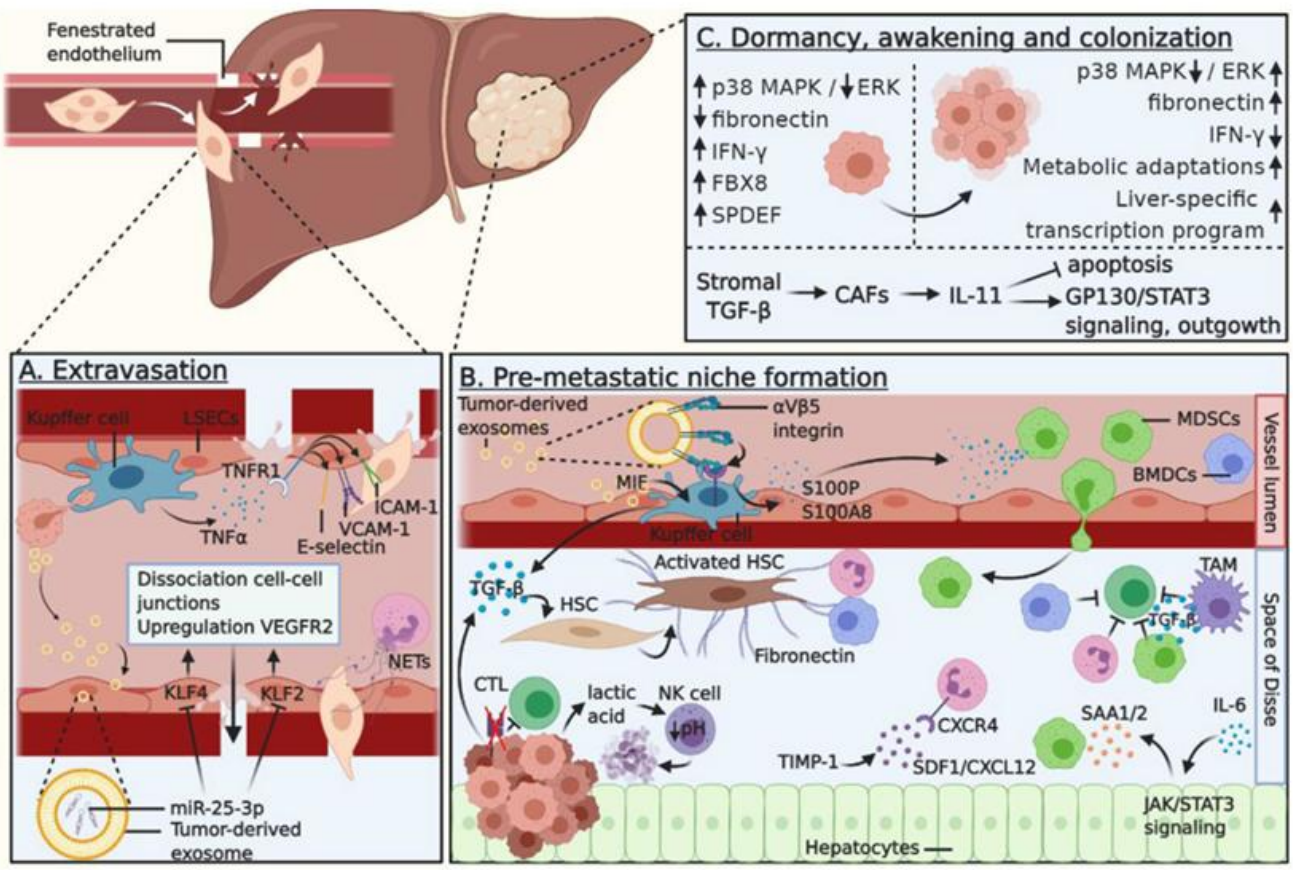

Figure 3 *Colorectal Cancer Liver metastases interaction in the Liver: from extravasation to organ colonization. Shasha Tal et al. 2022.*

CHAPTER 2

Extracellular Vesicles

2.1 Structure, Biogenesis, Isolation and Function of the EVs

Extracellular Vesicles (EVs) are membrane delimited particles released by almost all cell types in the extracellular space [41]. Although they were initially considered particles involved in "garbage disposal", they have gained increasing interest by the scientific community due to their role in cell-to-cell communication. They were firstly described in 1967 by P.Wolf as "platelet dust" in platelet-free plasma after ultracentrifugation, and even though they have been firstly described around 60 years ago, only in the last few decades the EVs have been considered by researchers, investigating their biogenesis, release, functions and possible applications [42]. Depending on their origin, EVs can be grouped in three different classes: Apoptotic bodies (100-5000 nm) which originate from apoptotic pathways activated in apoptotic cells, Microvesicles (100-1000 nm) which originate from the shedding of the cytomembrane, and Exosomes (50-200 nm) which originate from multi-vesicular bodies (MVBs). Since the terminology regarding Extracellular vesicles has been very often misleading and confusing in the last decade, the Internation Society for the Study for Extracellular Vesicles (ISEV) has put its efforts in organizing some minimal guidelines for the young scientists working with EVs. ISEV endorses "extracellular vesicle" (EV) as a generic term for particles naturally released from the cell delimited by a lipid bilayer and unable to replicate. Since assigning an EV to a particular biogenesis is extremely difficult, it's more practical to use operational terms for EV subtypes that refer to physical characteristics of EVs, such as size, like "small EVs" (sEVs with a diameter $\leq$200 nm) and "large EVs" (with diameter $\geq$ 200 nm) [43].

Exosomes are generated as intraluminal vesicles (ILVs) through inward budding into endosomes, which are referred to as MVBs: after fusing with the plasma membrane, the exosomes are released in the extracellular space (Figure 4) [44]. Experimental data has demonstrated that the formation of ILVs requires the function of a protein machinery named the endosomal sorting complex required for transport (ESCRT). This complex is composed of four different protein ESCRTs (0, I, II, III) working simultaneously to promote MVB formation, followed by vesicle budding and sorting of protein cargo [45]. This machinery is typically initiated by the recognition and binding of ubiquitinated proteins to ESCRT-0 [46]. This complex interacts with ESCRT-I and ESCRT-II, and finally the complete machinery combines with ESCRT-III (this subunit is particularly involved in the budding process). After the cleavage of the buds to generate the ILVs, The ESCRT complexes is separated from the MVB at the cost of energy distributed by the sorting protein Bps4. Alix, a typical EV-related protein, is associated with different ESCRT proteins, such as TSG101 and CHMP4, and has been described to take part in the endosomal budding and abscission processes, and with the selection of the exosomal cargo (through interaction with syndecan). Even if the ESCRT complex is important for sEVs biogenesis, new evidence has highlighted an alternative pathway, ESCRT Independent, for sorting sEVs related cargo inside MVBs. This alternative pathway seems to be related on raft-based microdomains associated with the segregation of cargo inside the endosomal membrane (***Figure 4***) [47].

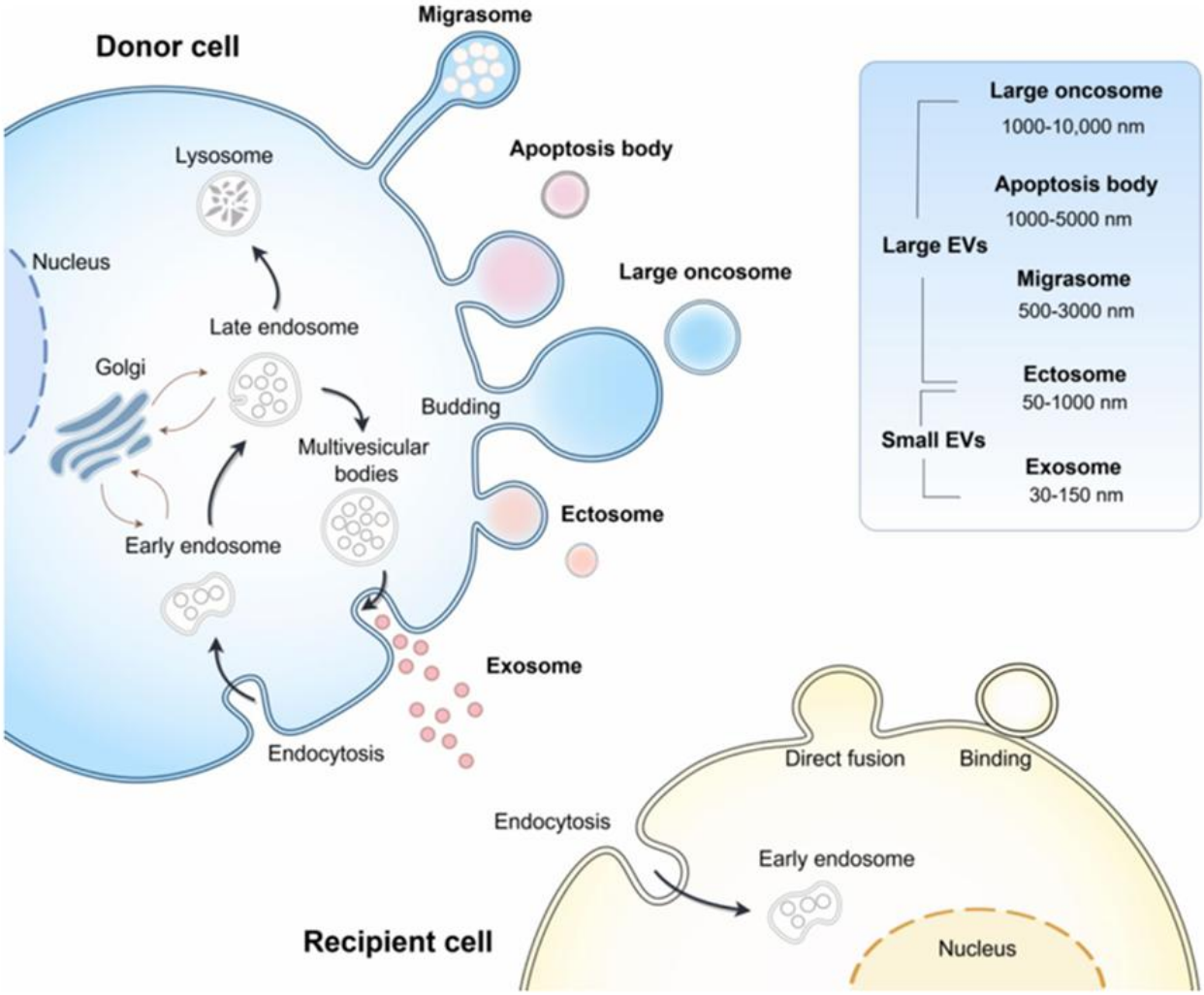

Figure 4 *Biogenesis of extracellular vesicles. Dai Wei et al. 2024.*

A critical step in the study of Extracellular Vesicles regards the isolation methodology. In fact, many different methods have been proposed in the last decades to increase the purity of the EVs isolated from different starting material (cell culture media, plasma, urine, solid tissue etc.). Traditional methods for isolating the sEVs are ultracentrifugation (UC), ultrafiltration (UF), size exclusion chromatography (SEC), immune affinity capture and precipitation. While some methods are based on the size and density of the vesicles, the others are based on the specific binding antibody-aptamers, so on the specific protein signature of the EVs. Differential ultracentrifugation (dUC), consisting in differential centrifugations adopted to remove cell debris and large vesicles, followed by a final ultracentrifugation, has been considered a "gold standard" for many years. Although this technique is still valid, researchers have been trying to combine different techniques in order to improve the preparation purity. For instance, SEC followed by iodixanol density gradient, or also SEC combined with UF have shown promising results [48]. The combination of different methods can indeed reduce nanoscale contaminants in the EVs preparation, and obtain different subpopulations of the EVs, so many researchers have been developing combined methodology techniques [49]. In recent years, commercially produced qEV size-exclusion columns are being taken in higher account by EV-research community; these columns, which use is very often coupled with tangential flow filtration (TFF), allow to obtain extremely rich preparation of EVs in a very short amount of time, and very often deploying low starting material, compared to other methods [50]. Researcher have also been studying and optimizing different methods for isolating EVs from solid tissue, which requires further processing step in order to extract the EVs which subsequently need to be collected [51] . EVs can transport an heterogenous array of substances: lipids, proteins, nucleic acids (mRNA,DNA, lncRNA, circRNA and microRNA) [52].

Categorizing all the biological molecules contained in the EVs is surely a difficult task, for these reasons, during the years, Database such as ExoCarta and EVpedia have been created to collect all data regarding EVs and their molecular cargo, but they need to be constantly updated by EV researchers [53, 54].

The proteins contained in the EVs have interesting roles, they can be grouped in two main categories: the first group regards tetraspanin superfamily members (CD63, CD81, CD82, CD9 etc.), proteins related to the cytoskeleton, flotillins, TSG101, Alix, annexins and heat shock proteins (HSP90 and HSP70). While the second group comprises, proteins associated with the cellular source of the EVs. TD_sEVs will be enriched in proteins known to play a role in tumor processes such as TGF-β, BMPs, EpCAM, while EVs derived from immune regulatory cells (lymphocytes, macrophages) will be enriched in proteins like MHC-I and MHC-II [55]. Also, the nucleic acids cargo inside the EVs can be translated into functional proteins if horizontally transferred to recipient cells. Several lipids can be found in the sEVs membranes, they can be classified in different categories according to their structure [56]. The main representative lipids superfamily includes steroids, sphingolipids and glycerophospholipids. Different studies have highlighted those changes in cell condition (for instance, form physiological to pathological conditions) can affect the lipid composition of EVs, and this could be useful for identifying new biomarkers in different diseases [56, 57]. In the context of nucleic acids, we can distinguish among DNA and RNA inside the EVs [58]. Until 2014, only mitochondrial DNA (mtDNA), single-stranded DNA and repetitive transposon presence was reported in the EVs. Thakur et al. demonstrated for the first time the presence of dsDNA in TD_sEVs [59]. Cai et al, reported that EV-DNA may have a biological effect on target cells, since they demonstrated the horizontal transfer of BCR/ABL hybrid gene, involved in chronic myeloid leukemia, to HEK293 cells and neutrophils. Guescini et al demonstrated that mtDNA in EVs could be delivered to other cells, proposing this as a mechanism of DNA horizontal transfer in several pathologies [60].

NcRNAs are among the most abundant component of the EVs, and their specific content can influence the functionaliy and effects of the vesicles. These ncRNA comprise different types of RNA molecules, like long non coding RNA (lncRNAs), small ncRNAs (sncRNAs) and circular RNAs (circ RNAs) [61, 62]. Through advanced RNA sequencing techniques, the RNA content of the EVs has been deeply studied, revealing their regulatory activity in many biological pathways in healthy and pathological conditions [58]. Their packaging inside the EVs has been extensively investigated, and even though not all the molecular mechanism are known, some molecular actors have been identified during the years (***Figure 5***). For instance, Santangelo et al, have identified an RNA-binding protein (RBP), named Synaptotagmin-binding cytoplasmic RNA-interacting protein (SYNCRIP) as a component of hepatocyte exosomal miRNA sorting machinery. The knockdown of this protein lead to the depletion of miRNA loading inside the EVs [63]. Other proteins have been identified in this sorting process, for instance, EV-loading of miR-223 strongly depends on its binding to Y-box protein 1 (YBX1) in HEK293T cells. Vps4A also regulates the packaging of different ncRNAs inside EVs. For heterogenous nuclear ribonucleoprotein A2/B1 (hnRNPA2/B1), an RBP that regulates the EV packaging miRNAs through a specific “EXOmotif” domain, SUMOylation process seems to be crucial in the efficiency of this binding. This EXOmotif domain was also identified in other RBP involved in the loading of ncRNAs in the EVs, such as SYNCRIP [64, 65].

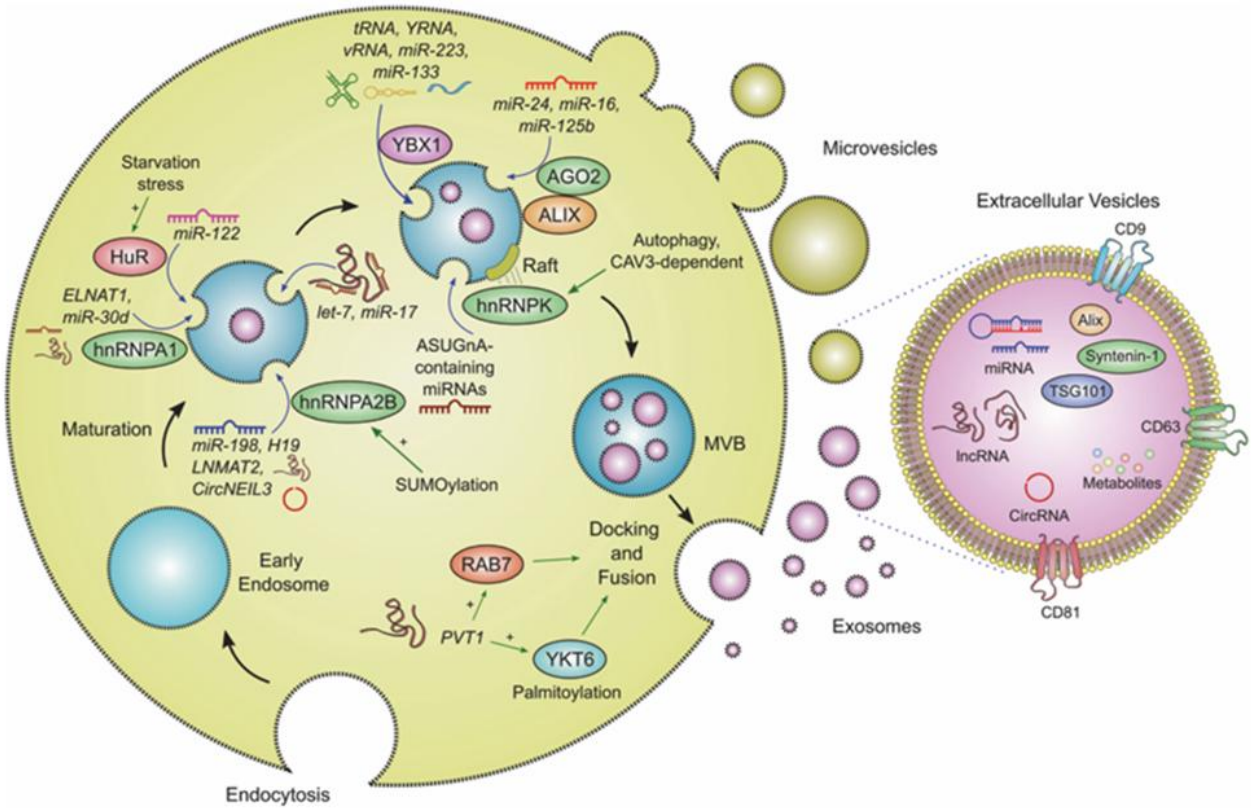

Figure 5 *ncRNAs packaging inside the extracellular vesicles. Samuels et al. 2023.*

2.2 Tumor Derived EVs and Pre Metastatic Niche Formation

In the last decades, the role of the tumour microenvironment in cancer progression has gained increasing interest. In this picture, tumour derived small extracellular vesicles (TD_sEVs) have been studied because of their role in cell-cell communication and in the promotion of the tumour microenvironment, both directly surrounding the primary tumour and affecting distant sites, favouring the establishment of a receptive microenvironment for metastatic cells colonization [66]. In fact, TME in not only composed of cancer cells, but also normal cell types (stromal cells) which surround the tumour and can sustain its growth and survival. In addition to transfer information between cancer cells, EVs have also been reported to transfer oncogenic-like properties to non-tumour cells, affecting their behaviour [41]. In the recent years, in addition to the generally know "metastatic niche", recent studies have begun to highlight a new aspect of cancer microenvironment, known as "pre-metastatic niche" (PMN) [67]. Since then, this concept has been extensively investigated and now its common knowledge that primary tumours can prime the sites of future metastasis through delivering signals even before tumour cells intravasation step [68]. Among the "signals" spread by the primary tumour, TD_sEVs play a crucial role, due to their important role in cell communication, they have been studied in the promotion of metastatic cascade [69]. In fact, among the different roles played by TD_sEVs in tumour progression, the most notable involve the regulation of immunoregulatory processes, angiogenesis, EMT and fibrosis, and finally PMN formation (***Figure 6***) [70]. In fact, EVs can transfer the oncogenic cargo from tumour cells to normal cells, enforcing a pro-tumour microenvironment and delivering cancer-specific traits (such as enhanced survival and anchorage independent growth) [72]. For example, hypoxic melanoma-derived EVs can activate mitogen-activated protein kinase pathways in recipient cells, while glioma-derived EVs can induce pro-angiogenetic processes, and EVs derived A431 cells can horizontally transfer epidermal growth factor (EGFR) to endothelial cells, inducing angiogenetic cascade [73]. TD_sEVs carrying Tissue factor (TF) and P-selectin glycoprotein ligand-1 (PSGL-1) can also affect coagulation processes and promote thrombosis in cancer patients [74]. The

ability of these non-cancerous cell types to acquire cancerous-like traits transferred by TD_sEVs require the continuous exposure of the cells to the EVs [75]. As previously described, the liver represents one of the major "hub" for disseminating cancer cells; CRC, but also gastric and pancreatic carcinomas have a strong tendency for metastasizing the liver (as well as melanomas and sarcomas) [42]. CRC_sEVs can induce in the hepatocytes the release of hepatocyte growth factor (HGF) through SPINT1 suppression. CRC_sEVs can also modulate stromal cells surrounding the hepatocytes, for instance they can be up taken by Kupffer cells and hepatic stellate cells (HSCs) and activate specific signalling pathways, inducingTGF-1 upregulation and fibronectin deposition [76]. The deposition of fibronectin by activated HSCs promotes macrophages infiltration in the liver, worsening the PMN condition through the establishment of a pro fibrotic and immunosuppressive environment, mainly acting on HSCs and Kupffer cells, but not hepatocytes [77, 78]. In fact, despite counting about 70-80% among the cell populations in the liver, the role of the hepatocytes in the PMN formation is relatively poorly understood, especially compared to the stromal counterpart. Their intervention is mostly described after the PMN is already established. In fact, in murine model of breast cancer metastasis, they're described to directly interact with metastasizing cells through claudin-2 and contributed to establishment of a pro-fibrotic environment after activation by PDAC-derived-IL6 [79, 80].

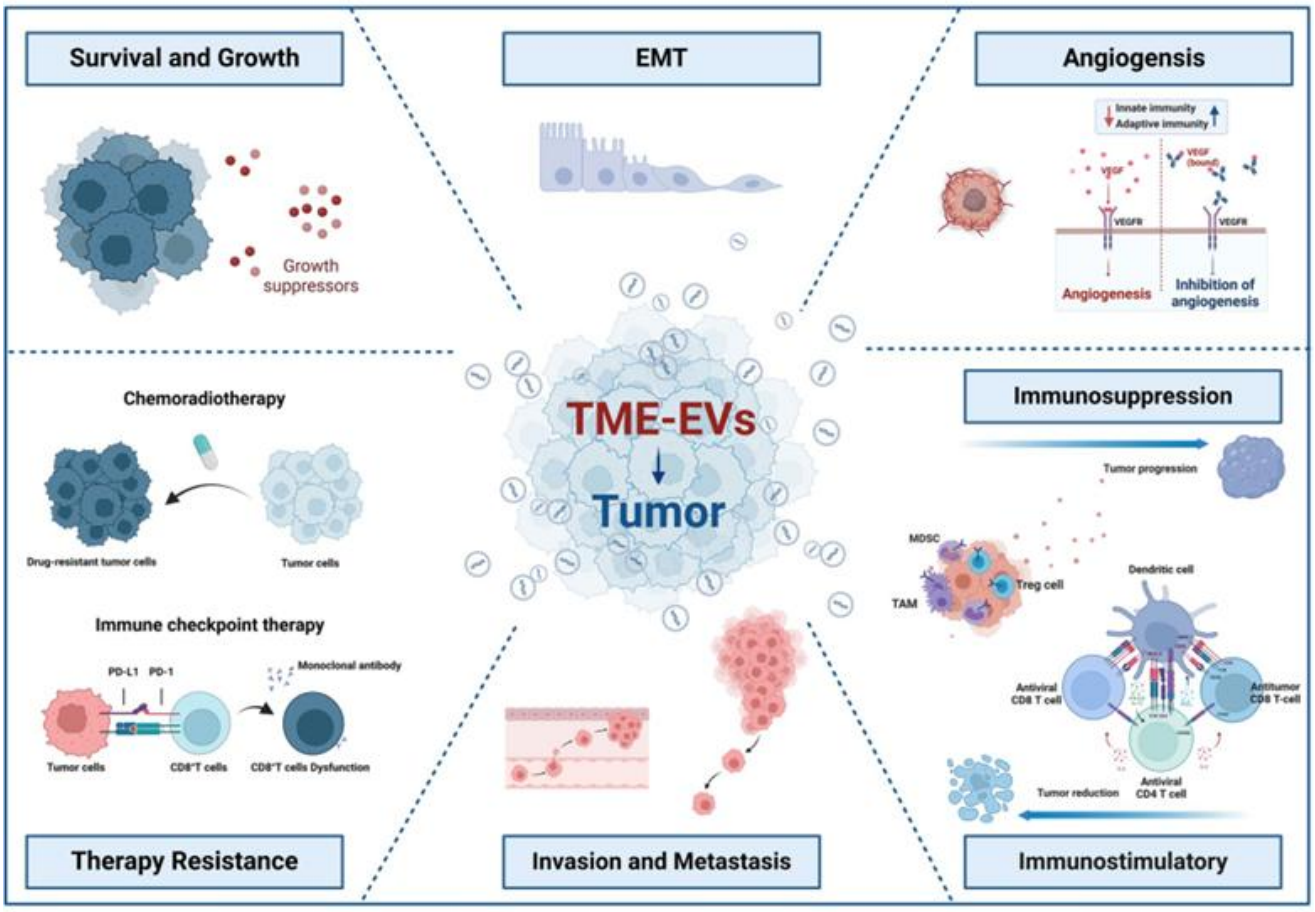

Figure 6 *TD_sEVs multifaceted roles in tumour progression. Hou Pei-Pei et al. 2021.*

CHAPTER 3

Non-Coding RNA in Tumour Biology

3.1 Non-Coding RNA Biology and tumour progression

Long non-coding RNAs (lncRNA) comprises a category of transcripts longer than 200 nucleotides with generally no protein-coding ability. Most of them are transcribed by the RNA polymerase II, so they share structural similarities with mRNAs (occasionally like cap structures and poly A tails). Among them, a subclass is represented by long intergenic non-coding (linc)-RNAs, long intronic noncoding RNAs and long non-coding antisense RNAs [81]. Their expression is generally lower than mRNAs expression levels and are poor in their sequence conservation. In the recent years, many lncRNAs have been studied and identified in animals and plants through different biotechnological techniques: RNA-seq, microarrays, expressed sequence tags (ESTs), tiling arrays. Different studies focusing on lncRNAs functions have showed their multiple roles in the regulation of epigenetic mechanisms, post transcription, translation and post-translation modifications. Moreover, lncRNAs play regulatory roles in chromatin remodelling, genomic imprinting, alternative splicing, cycle regulation and cell differentiation [82]. These RNAs also affects gene expression acting as competitive endogenous RNAs (ceRNAs) decoys or sponge. They can act through two main mechanisms: one of them in involved in the sequester of miRNAs, blocking their binding to specific mRNAs targets. The other one regards their direct interaction with transcripts, sequestering them and avoiding their binding with specific miRNAs as well as their enrolment in the translation machinery (***Figure 7***). These molecular mechanisms are important for the regulation of many homeostatic biological processes, though the dysregulation of some of these mechanisms can lead to pathological conditions [83, 84].

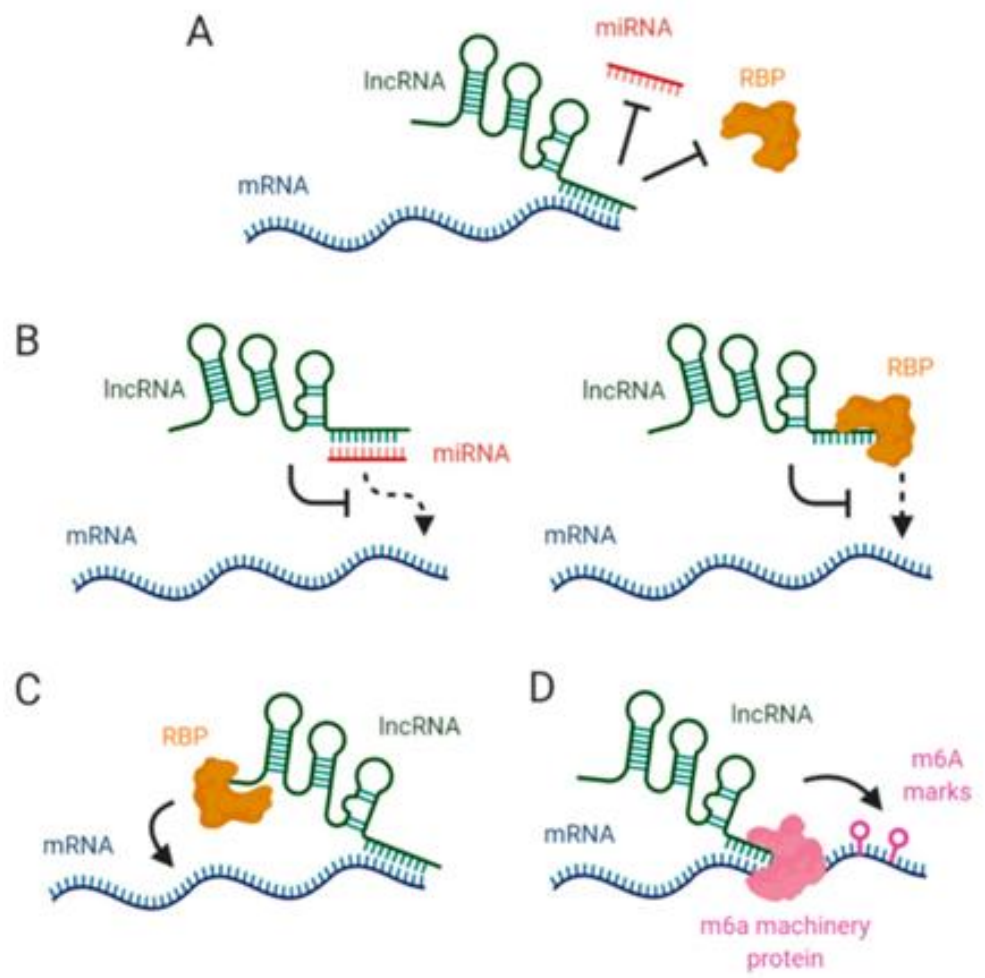

***Figure** 7 LncRNA-mediated mRNA stability regulation. Sebastain-delaCruz et al. 2021.*

Despite being powerful gene expression regulators, lncRNAs rarely act alone. In fact, their molecular action is very often coupled with different "partnerships", among these, RBPs are the most common. lncRNAs and RBPs can establish molecular complexes (name ribonucleoproteins, RNPs) and act synergistically to impact gene expression in both normal and pathogenic conditions. Among the most important examples, we can find linc HOXA1 RNA, which represses Hoxa1 interacting with the protein PURB. Also, P21-associated ncRNA DNA damage activated (PANDA) can block apoptosis interacting with NF-YA, a transcription factor, thus inhibiting pro-apoptotic genes expression, while Linc-RoR has been described to interact with hnRNP I to suppress p53 (activated following DNA damage) [85, 86]. Among the different processes regulated by the molecular complex lncRNAs-RBPs, alternative splicing (AS) has gained increasing interest in the recent years. AS in a crucial mechanism for temporal and spatial regulation of gene expression and to expand proteome diversity of our cells. Most of the genes (more than 90 %) are subjected to AS mechanism in human cells. This biological process is regulated by different RBPs and Splicing factors (SFs), and many of them contain serine/arginine structural domains which are evolutionary conserved for RNA recognition functions. Since these SFs contain RNA binding domains, they can also interact with lncRNAs which also affect AS processes [87]. For example, ENOD40 and lnc351 can regulate AS interacting with nuclear selective splicing regulator nuclear speckle RNA-binding proteins (NSRs). NSRr are a group of RBPs that are involved in the nuclear AS regulation in Arabidopsis. LncRNA MALAT1 is also involved in AS regulation, this lncRNA localizes primarily in nuclear speckles and possesses a binding site for SR protein splicing factor 1 (SRSF1), which can simultaneously bind the 5' region of the lncRNA [88]. RIP experiments demonstrated MALAT1 binding with different subsets of SR proteins moreover, it affects the distribution and localization of SR proteins in the nuclear speckles (as well as their phosphorylation/dephosphorylation

state). MALAT1 has also been described to recruit different SF proteins toward the transcription active region in the nucleus and regulating the cleavage of the transcript precursors [82]. Due to their ability to form RNA-DNA duplexes, lncRNAs may also affect AS processes through the establishment of splicing-specific chromatin tags, so also in a independent mechanism from SFs (***Figure 8***) [89]. LncRNA and RBPs can bind specific chromatin sites, named regulatory chromatin domains, which are subjected to structural remodelling by RNPs complexes. Still, the complex molecular interactions between lncRNAs and chromatin domains remain largely unknown, but some studies have revealed that an evolutionary conserved lncRNA generated form FGFR2 locus in humans (lncRNA-asFGFR2) recruits the histone demethylase KDM2a and polycomb repressive complex 2 into the FGFR2 locus. AS result, a splicing-specific chromatin tag is formed in the genetic locus which affects chromatin environment and inhibiting the binding of different chromatin binding complex (such as MRG15-PTB) [90]. Eventually, this mechanism leads to the inclusion of exon IIIb of FGFR2, thus affecting the epithelial or mesenchymal isoforms of this gene [91].

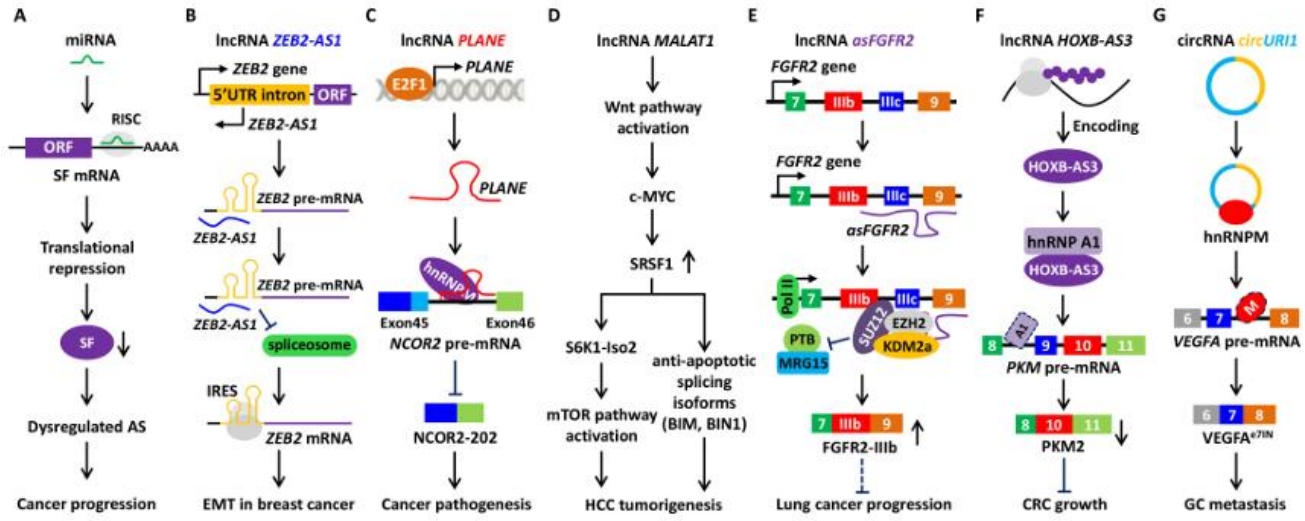

Figure 8 *Molecular mechanism of ncRNA-mediated AS in human cancers. Wang et al. 2022.*

3.2 LncH19 in Cancer and in TD_sEVs

LncH19 is a 2.3-kb lncRNA encoded by a gene locus on an imprinted region of chromosome 11p15.5. This locus has been described to produce different products in addition to lncH19, such as H19 opposite tumour suppressor protein (HOTS), miR-675 and 91HlncRNA. MiR-675 is derivative from H19 (the first exon) and was described to be up-regulated in colorectal cancer. This miRNA can act by inhibiting tumour suppressor protein retinoblastoma, while lncRNA 91H is antisense to H19 and has an oncogenic role in tumours [92]**.** H19 is an oncofetal transcript which role in the progression of many tumours has been largely confirmed, in fact, it's involved in the regulation of key steps of neoplastic transformation and confers pro-migratory and pro-proliferative properties to tumour cells. in the TME, lncH19 increases the angiogenic capacity of cancer cells and promotes epithelial-to-mesenchymal transition (EMT), increasing the chances of intravasation and metastatic cascade. H19 is also described to increase chemoresistance of malignancies, enforcing their capability of survival in the presence of anti-cancer drugs through different molecular mechanism (***Figure 9***) [93].

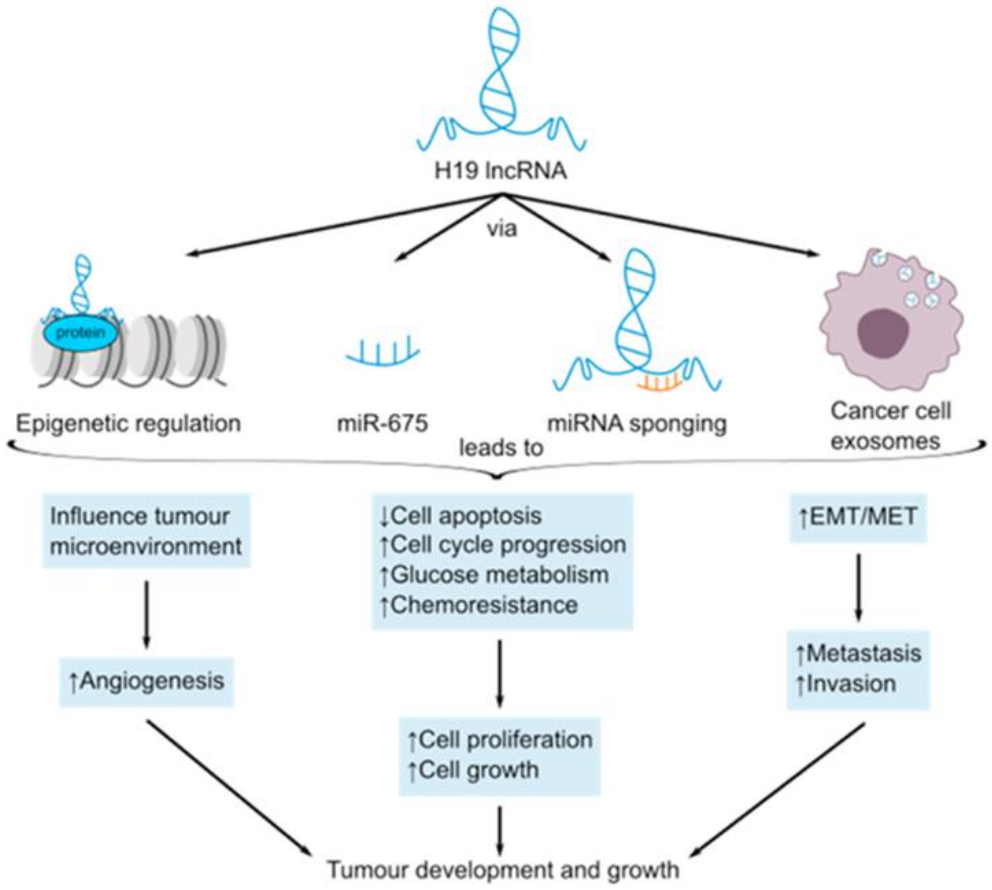

Figure 9 *LncH19's multifaceted roles as oncogene. Shermane Lim et al. 2021.*

Metastasis is a challenging step for the medical community, as this critical event enhances survival and dissemination of metastatic cells, significantly worsening prognosis of the patients. LncH19 is described to increase migration of cancer cells, affecting their epigenetic profile and thus enforcing the malignant transformation [94]. For example, in colorectal cancer, H19 increases hnRNPA2/B1 expression, which ultimately triggers the EMT cascade [95] (***Figure 10***). EMT is a biological process through which a polarized epithelial cell undergoes morphological/biochemical changes that trigger its de differentiation in a mesenchymal phenotype. Epithelial cells normally establish interactions with basement membrane via their basal surface; during EMT they gain enhanced migratory traits, resistance to apoptosis, loss of cell junctions. Invasiveness and increasing ECM components production [96]. Generally, three different types of EMT are generally described in literature. Type 1 EMT is associated with embryogenesis and organ development and is characterized by the generation of mesenchymal cell (primary mesenchyme) that can undergo mesenchymal-to epithelial transition (MET) to generate secondary epithelia in organogenesis. Type 2 EMT is instead associated with tissue regeneration, wound healing and, in pathological conditions, organ fibrosis. This type of EMT is associated with repair-related mechanisms and characterized by fibroblast activation following inflammation stimuli. These mechanisms have the crucial role of reconstructing damaged tissues, and are commonly balanced in healthy conditions, but if the inflammation injury is persistent (chronic inflammation), fibroblasts can be over-activated, leading to the massive deposition of extracellular matrix proteins and ultimately organ fibrosis [97]. Finally, type 3 EMT is typical of cancer cells which accumulated genomic abnormalities (affecting oncogenes and tumour suppressor genes). In these cells, migratory and invasive capabilities are enhanced during EMT, thus enabling these tumour cells to invade and metastasize in distant organs [98, 99].

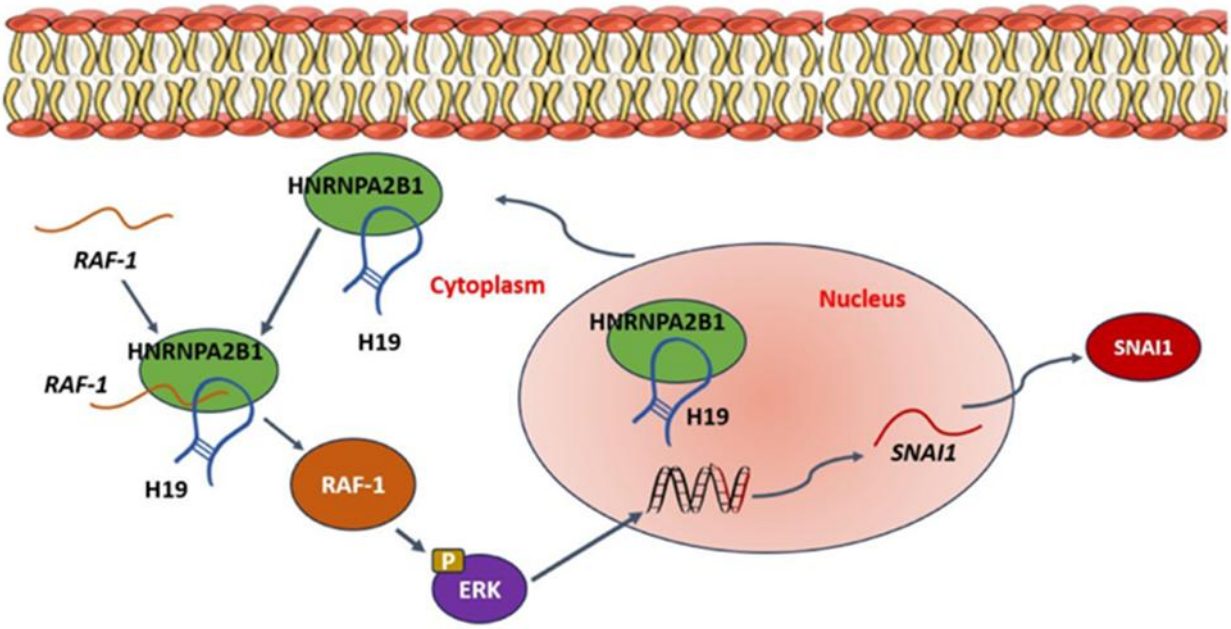

Figure 10 *Mechanisms of lncH19 interaction with hnRNPA2/B1 in CRC metastases and EMT. Chowdhury et al. 2023.*

As previously cited, lncH19 can trigger EMT processes through intervening in different molecular pathways. For instance, lncH19 has been described to down-regulate mir-29b-3p, increasing the expression levels of PGRN which leads to the activation of Wnt signaling thus triggering EMT processes. In gastric cancers LncH19 also stimulates Wnt/ß-catenin signalling which strongly increases the metastatic capability of tumour cells. In oesophageal cancer, H19 can promote the interaction between STAT3 and EZH2, finally inducing SOX4/b catenin signalling [100]. LncH19 has also been described to be overexpressed in retinoblastoma (both in vitro and in vivo models), promoting in this tumour the up-regulation of Vimentin and matrix metalloproteinase-9 (MMP-9), increasing again the metastatic phenotype of these cancer cells. Also, in breast and bladder cancer, H19 is strongly up-regulated, and can affect different hallmarks of cancer, sponging miR-29b-3p and leading to the up-regulation of DNMT3B which in turns increases the invasive capabilities of tumour cells. LncH19 can directly affect β-catenin, triggering EMT in oesophageal and breast cancers, where the lncRNA can influence different steps of cancer progression [101]. Experimental data has shown that silencing lncH19 impairs migration and invasion and blocks EMT in different cancer cells. LncH19 can also induce p53 down regulation, increasing the expression levels of TNFAIP8, which in turns induces the EMT and metastatic cascade. One of the most important transcription factors regulating EMT and promoting metastasis is ZEB1, and H19 is described to have an indirect role in ZEB1 mRNA stabilization. Mechanistically, miR-200a targets ZEB1 suppressing its levels, noteworthy, lncH19 can sponge miR-200a, thus leading to an up-regulation of ZEB1 and a downstream enhancement of EMT-related processes in TME [92, 102]. In CRC, lncH19 overexpression correlates with metastasis and poor prognosis. H19 can promote CRC progression through different mechanism: it can act as a ceRNA for miRNAs, indirectly affecting downstream transcripts, it can bind and act as scaffold for different proteins (such as SFs), promoting malignant transformation in vivo and in vitro models. H19 can bind eIF4AIII, obstructing its recruitment to CDk4, cyclin D1 and E1 transcripts, blocking their degradation and influencing cell cycle regulation. As with the other cancers discussed above, lncH19 can activate Wnt/β-catenin pathway also in CRC, sponging miR-200a, which is involved in the repression of β catenin by endogenously targeting its mRNA. Since miRNA is sequestered by lnch19 in CRC, this sponging activity results in an over expression of β-catenin, which in turns over stimulates proliferation and EMT activation [103, 104]. In hypoxic conditions, H19 and its intragenic miR-675-5p have shown to be up regulated, and the loss of this miRNA lead to a reduction of β-catenin nuclear localization and transcriptional activities. Since miR-675-5p could

target PP2CA, this inhibition restored the activity of Glycogen Synthase Kinase 3β (GSK-3β), ultimately regulating β-catenin nuclear translocation [105].

In addition to the already described multifaceted roles in the promotion of the different hallmarks of cancer, in the last years lncH19 has also been studied for its presence in the TD_sEVs. Despite a few studies focusing on H19 EV-associated (EV-H19), its role in the progression of neoplastic transformation is still largely unknown. From our current knowledge, H19 inside the TD_sEVs seems to propagate the tumoral properties already displayed in cancer cells (angiogenesis, chemoresistance, fibrosis and inflammation). H19 has been found to be enriched in EVs derived from CD90+ cancer cells, and endothelial cells treated with the EVs from CD90+ cells show an up-regulation of VEFG, indicating the capability of EV-H19 to induce pro angiogenetic stimuli [106]. EV-H19 has also been shown to promote gefitinib resistance in non-small cells lung cancer (NSCLC) cell lines, where H19 seems to be up-regulated (especially the gefitinib-resistant cells) and to be packaged into the NSCLSC-dervied-EVs by hnRNPA2/B1. Finally, the horizontal transfer of EV-H19 induced gefitinib resistance to recipient NSCLC [107, 108]. In other studies, H19 transported by Multiple Myeloma Derived EVs was described to regulate osteogenesis both in vivo and vitro models. In this study MM-EVs enhanced the osteolysis in C57BL6/kawRij mice and promoted the differentiation of RAW264.7 cells into osteoclast, reducing the osteogenic differentiation of BMSCs, where the lncRNA acted as ceRNA for BRD2 and BRD4 mRNA, regulating their action in chromatin modification and gene expression. The authors also demonstrated that lncH19 regulates hnRNPA2/B1 accumulation in the cytoplasm, and the protein knockout reduced osteoclast differentiation promoted by lncH19. Finally, the author confirmed the role of hnRNPA2/B1 in the EV-loading of H19 by performing a knockdown of the protein, thus obtaining H19 depleted MM-EVs [109]. Liu et al also demonstrated that EV-H19 released by cholangiocytes promotes cholestatic liver injury in Mdr2-/- mice and could induce hepatic stellate cells (HSCs) trans-differentiation and over-activation. The HSC educated by the EVs increased the ECM deposition in the liver of mice with mild cholestatic liver fibrosis, but still the underlying molecular processes under the fibrotic cascade promoted by EV-H19 must still be clarified [110]. Ultimately EVs isolated from cirrhotic mice models present high levels of lncH19, and different studies have highlighted its role on hepatocarcinoma (HCC) development, [111, 112]. Still, the role of EV-H19 in the morpho functional alterations of healthy hepatocytes need to be further elucidated.

CHAPTER 4

Organ on a Chip Culture System

4.1 Organ on a Chip Culture Systems as bridge between *in vitro* and *in vivo* models

Studying the complex tridimensional organization existing in human organs has always represented a demanding challenge for biomedical research. In fact, one of the key obstacles in the study of human pathology is represented by unravelling the complex molecular alterations, which are gradually established in the organ microenvironment. These alterations are very often the outcome of different dysregulations chronically established in the complex cytoarchitecture defining the organ. The origin of 2D cell culture is attributed to Ross Harrison, a scientist who investigated neural tissue growth in the early years of 1900. The era of 2D cell cultures exploded in the mid-1950s, thanks to the establishment of the first cell lines used in scientific research, such as "L" and Hela cell lines. 2D cell cultures surely represented a fundamental pillar in the study of a vastity of human physiological and pathological molecular processes, but they also present different disadvantages, for example the inability to mimic the in vivo scenario where the cell types interact in a complex 3D structure with the extracellular matrix component [113, 114]. Since *in vitro* systems can not properly depict this complex three-dimensional (3D) structure, animal models have been extensively used by the scientific community. Animal models represent more suitable systems for studying complex pathologies and cell responses in their native microenvironment**,** but this intense application of the animal model, on the other hand, increased ethical interest concerning animal wellbeing. In fact, inside the European Union (EU), animal testing regarding cosmetology has been totally prohibited since 2013. It is logical to assume that this progressive restriction regarding animal testing will also affect drug discovery in the next years [115, 116]. As a result, the development of 3D culture systems have gained increasing interest, the attractiveness of the 3D models lies in their potential to better recapitulate the in vivo cellular organization and tissue structure in comparison to the canonical 2D systems. In order to overcome the limitations of the 2D culture systems and the ethical instances regarding the use of animal models, the development of new tridimensional culture systems through the employment of advanced technologies and biomaterials is gaining increasing interest. Among these advanced systems, Organ-on-Chip (OoC) are fastly advancing in the biomedical research community (**Figure *11*).**

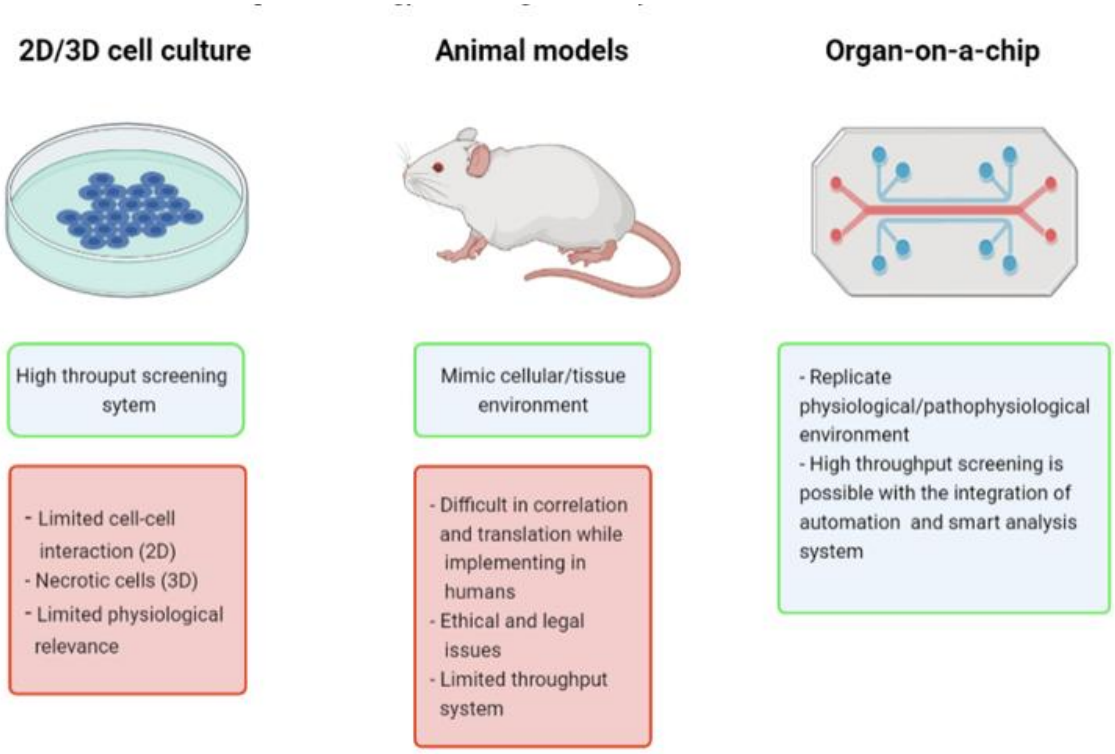

Figure 11 *Summary of advantages of OoC technology over cell cultures and animal models. Koyilot et al. 2022 [117].*

These systems represent an optimal bridge between in vitro culture systems and animal models, since they can mimic the physiological conditions of different organs in controlled and stable environments [118]. OoCs can be generally described as microfluidic devices which contain organ specific cells and can simulate their functionality. These microdevices offer excellent opportunities in advancing research fields such as drug discovery, organ pathology, disease etiopathogenesis, infections, drug screening and personalized medicine **(Figure 12)**. These devices represent innovative platforms for studying complex organ cytoarchitecture and functions, including heart, lung, liver brain and other organs, while maintaining controlled environmental conditions which can be easily analyzed in a miniaturized volume [118, 119]. Currently, new devices are advancing, enabling to interconnect multiple cell types of different organ models, for this reason described in literature as multi-organ on a chip (MoC), leading in vitro research to a next level of complexity [120, 121].

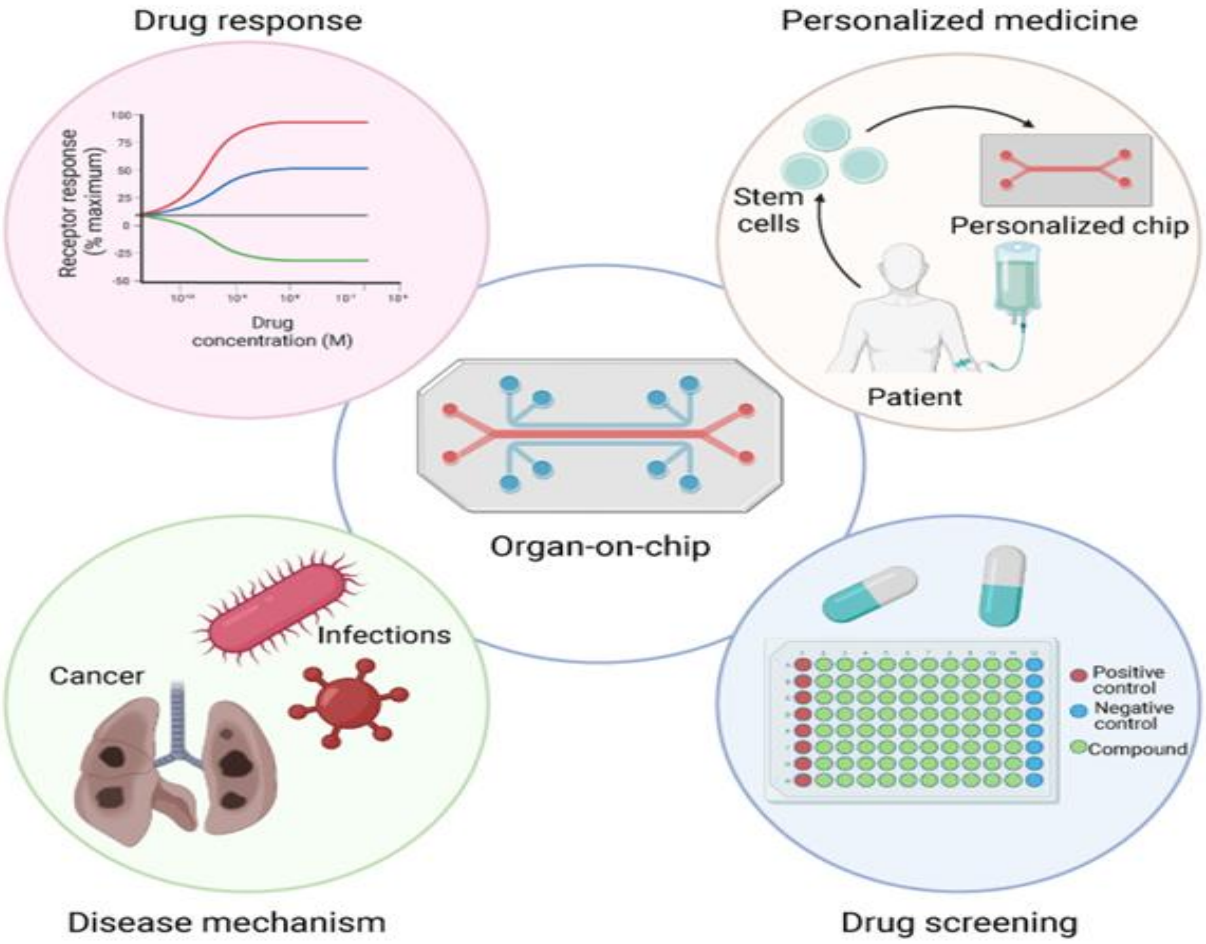

Figure 12 *Schematic diagram describing the different opportunities offered by OoC technology in the fields of drug response, personalized medicine. Srivastava et al. 2024.*

4.2 Liver on a Chip Systems for studying the chronic effects of TD_sEVs

Preserving the physiology of healthy differentiated hepatocytes over extended timepoints is often challenging. Since the complex role in drug/toxin metabolism performed by these cells in the liver is due to the its cytoarchitecture organization (liver lobule), maintaining their differentiations often requires the use of specific enriched culture media and complex in vitro systems. In this context, OoCs platforms allow promising opportunities for increasing hepatocytes differentiation for studying the molecular alterations and de-differentiation processes induced by CRC_sEVs. The first Liver on Chip (LoC) described in literature goes back to 2007 by Philip Lee et al., this system was described three years before the first lung on a chip, reported by Huh et al., which gained much interest due to the introduction of tuneable mechanical forces which mimicked the breathing patterns [122]. Common LoC devices typically contain the hepatocytes as the main (and sometimes the only) cell type. Of course, monocellular culturing is not enough for depicting the complexity of organ physiology, but still, they represent important milestones for the development of such modern culture systems. Researchers are currently trying to introduce other liver-resident cell types, to better recapitulate the intercellular interactions existing in the organ [123]. This possibility, offered by LoC devices, allowed researchers to obtain interesting results in this field. For instance, rat derived hepatocytes cultured in LoC could efficiently synthesize albumin and activate hepatocyte-related metabolism. Through the design of a LoC which could mimic the interstitial space of endothelial cells, Lee et al cultured primary hepatocytes increasing their differentiation and promoting substance exchange. Scientists also fabricated multi layers chip, with independent channels, using a polyethylene terephthalate (PET) membrane and

perfusing the hepatocytes with mixtures of collagen and fibronectin from the lower chamber to the upper chamber, where they were seeded. These devices have also been deployed for 3D cultures recently: Ma et al produced a platform to analyse hepatocytes spheroids, while Lu et al. developed microfluidic systems for studying liver tumours [119]. One of the major research fields in which OoCs are emerging and gaining increasing attention by the research community, is EV research. In fact, the OoCs devices allow to simulate chronic physiological and pathological stimuli, which cannot easily be reproduced by canonical in vitro systems, where the flow of fluids (containing drugs or EVs) cannot be precisely controlled. When studying the effects of TD_sEVs in tumour progression, target cells are often treated with a single administration, analysing the downstream morpho-functional alterations. However, it is widely recognized that these methods cannot fully mimic the physiological conditions for the lack of a continuous and low exposure of the recipient cells to the EVs [124, 125]. The acute administrations of the vesicles, unavoidable in the 2D cell culture systems, are often considered too high for their significant lipid load, and this limitation represents a recurrent controversy emerging during the revision steps for paper publication or grant funding, since these kinds of exposures can lead to stressful "unrealistic" conditions and elicit unspecific biological responses (***Figure 13***).

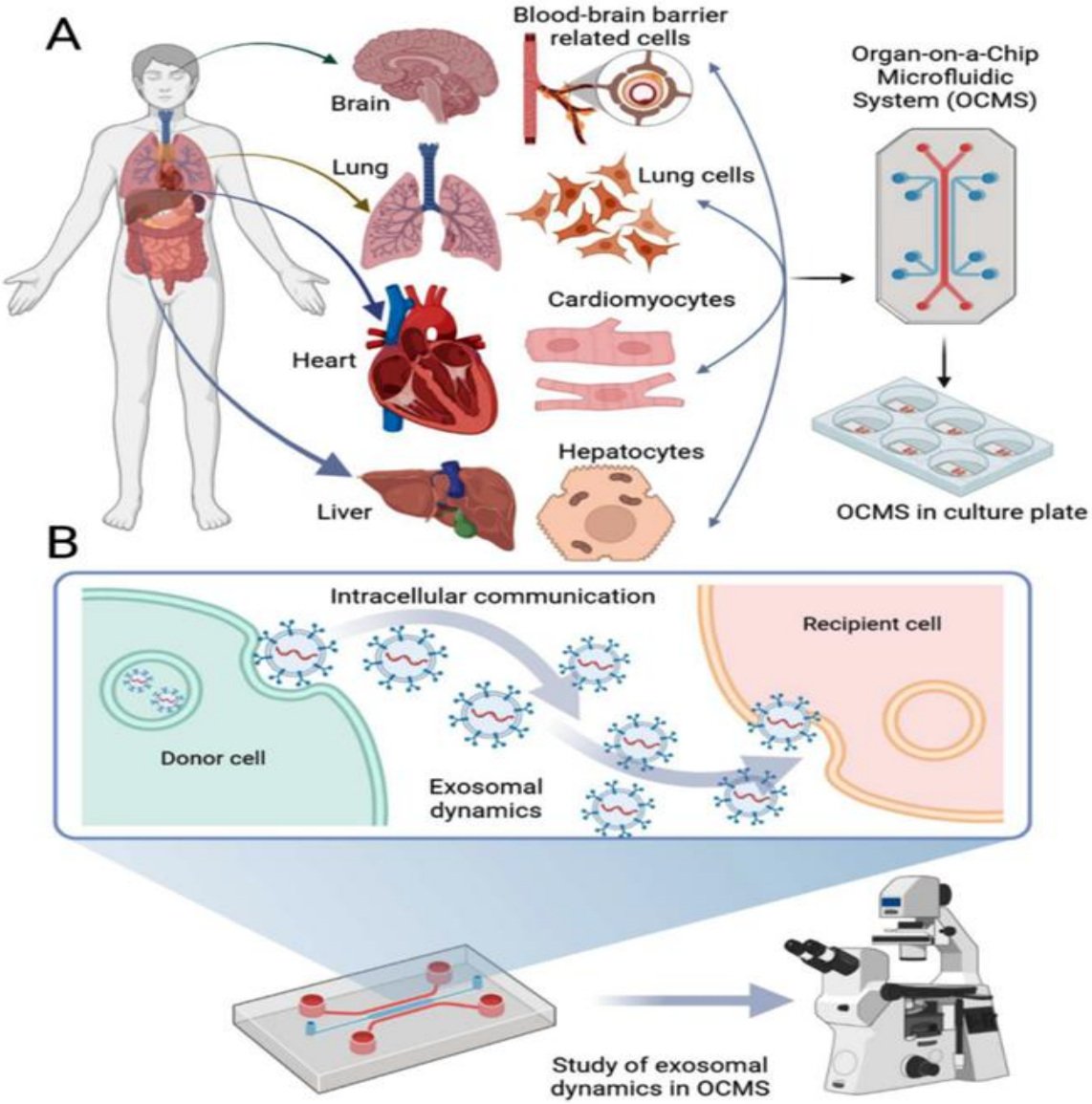

Figure 13 *Organ-on-a-chip systems (OCMS) for modelling various human body organ systems and exosomal dynamics for intracellular communication. Abhimanyu Thakur, 2023.*

To solve these problems, as a proof-of-concept, we efficiently developed a Hepatocyte-on-Chip (HoC) device composed of two chambers in order to dynamically flow cancer-derived small extracellular vesicles (EVs) on human healthy hepatocytes (THLE2 cells). The produced thermoplastic device integrates a poly-lactic acid electrospun scaffold as a culture substrate closely resembling the in vivo liver ECM. To enable a direct comparison between static and dynamic culture conditions (named Insert-like PLA and HoC respectively), custom 3D-printed insert-like devices that incorporate the same PLA scaffold were also fabricated. This versatile design provided a valuable tool for laboratory applications, supporting well-oxygenated environments under static conditions to serve as a benchmark against the scaffold based OoC systems like HoC. In the HoC, hepatocytes were cultured in the upper compartment of culture chamber for 24 hours under static fluidic conditions to allow cell adhesion on the electrospun scaffold and for additional 48 hours with a medium flow rate of 41.7 µL/h, to renew the culture medium within the culture chamber once per hour and ensure adequate oxygen supply for the cell culture.

Our novel method enables the versatile fabrication of OoC platforms that can be tailored to the native environment of the target tissues. This is achieved by employing electrospun scaffolds as effective

membranes to support cell cultures within a OoC system. Due the well-known low absorption of PMMA [126] leading almost absence of gas exchange, oxygen carried by liquid flow medium it proves sufficient to sustain the vitality and functionality of human hepatocytes. As a result, our approach yields outcomes closely resembling those achieved in more conventionally oxygenated static cultures while simultaneously providing maximum control and automation over the culture performed on a physiologically relevant substrate like electrospun scaffolds.

CHAPTER 5

OBJECTIVES

As described in the introduction, the aim of this PhD thesis involves the study of the effect of CRC_sEVs in the definition of the PMN in the liver, particularly focusing on their role on the parenchyma component of the liver, the hepatocytes. I focused my study on the molecular cargo of the CRC_sEVs and on the development of advanced technologies for the study of their effect on these cells. Different studies have highlighted the role of CRC_sEVs in the priming of the PMN in the liver, but mainly focusing on the non-parenchymal cells residing in the liver, such as hepatic stellate cells and Kupffer cells, but the intervention of the hepatocytes at this stage of the PMN formation has been mostly neglected, while it is only described in their interaction with metastasizing CRC cells (when the PMN is already established) [127]. In the light of this knowledge, the two main objectives faced during my PhD thesis involve:

- The study on the molecular cargo of the CRC_sEVs, particularly focusing on lncH19 and how this ncRNA could promote underrated de-differentiation processes in the hepatocytes, shedding light on its molecular action alongside other RBPs in the promotion of AS splicing of EMT-related mRNAs. The investigation of the underestimated molecular effects promoted by EV-H19 on the hepatocytes could lead to a deeper understating on the biological alterations induced by the primary tumour on the distant site of metastasis, offering better opportunities for tackling the tumour in the early onset phase.

- The development of innovative technologies, such as OoCs, in order to investigate the chronic effect of the CRC_sEVs on the hepatocytes, overcoming the limitations of the canonical in vitro models, where the acute treatment doesn't allow to study the realistic effects of the vesicles on the recipient cells. These modern technologies offer the opportunity to interconnect the different cytotypes composing the organ, allowing to study the complex interactions of the cells in their environment, reducing the animal models required for cancer research.

CHAPTER 6

MATERIAL AND METHODS

6.1 Cell cultures

The colorectal cancer cell lines SW480 (ATCC CCL 228), SW620 (ATCC CCL-227) and HCT-116 (ATCC CCL-247) were used for sEVs isolation. SW480 and SW620 were maintained in RPMI 1640 medium (Euroclone, UK), while HCT-116 in McCoy's 5A medium (Euroclone, Uk), both supplemented with 10% fetal bovine serum (FBS; Corning), 2 mM l-glutamine (Euroclone, UK), 100 U/ml penicillin, and 100 µg/ml streptomycin (Euroclone, UK). Before use, FBS (South America origin EU approved, Euroclone, UK) was ultracentrifuged for 1h and 45 min at 100,000 × g in a Type 70 Ti fixed angle rotor to eliminate bovine sEVs. The SV40 large T antigen-immortalized healthy human liver epithelial cell line THLE2 (ATCC, Manassas, VA) was cultured in Airway Epithelial Cell Basal Medium (ATCC, Manassas, VA) with the Bronchial Epithelial Cell Growth Kit (ATCC PCS-300–040, Manassas, VA) supplemented with 5 ng/ ml epidermal growth factor (EGF), 70 ng/ml phosphoethanolamine, 10% fetal bovine serum, 100 U/mL penicillin, and 100 µg/ml streptomycin (Euroclone, UK) at 37 °C with 5% CO2. THLE2 were cultured in precoated flasks with a collagen coating made of a mixture 0.03 mg/ml bovine collagen type I (Advanced Biomatrix, San Diego region, California, USA), and 0.01 mg/ml bovine serum albumin (Sigma Aldrich, St Louis, MO, USA). All cell lines were tested for Mycoplasma using Hoechst staining and N-GARDE Mycoplasma PCR reagent set (Euroclone). Moreover, morphology and proliferation rate were constantly evaluated.

Before cell culturing, all HoCs, tubing, and accessories were sterilized using an aqueous solution of EtOH 70% v.v. for 30 minutes followed by a wash with PBS to remove any EtOH residuals, followed by UV light treatment for 2 h under the laminar fume hood [128]. In 2D system cells were seeded at the density of 50000/well (25000 cells /cm2). The same cell number was maintained on both Static Insert-like PLA and in the HoC since. Indeed, even if the cell seeding area is only 0.33 cm2, the structure of the PLA offers a 3D environment for cell growth.

6.2 Chip Design and Fabrication

Microfluidic devices and accessories were designed using Autodesk Fusion 360 ™ software (Autodesk, San Rafael, CA, USA). The HoC was designed to emulate a barrier tissue by including two independently perfusable chambers separated by an electrospun scaffold. The HoC device was designed in Fusion 360 as a 3D CAD model and subsequently segmented into six functional layers, each with a distinct thickness. To implement this design, the 3D model was digitally "sliced" into individual 2D profiles, corresponding to each layer. The profiles and scaffold shape model were then converted from STL to DXF file to be imported in Autolaser software for laser micromachining. Laser cutting was performed using a CO_2 Laser Cutter (Maitech, 40 W, Milan, Italy) with a z-adjustable stage, which allowed for precise machining of both the PMMA layers and the electrospun (ES) scaffold Materials were cut and engraved according to computer-designed laser paths at 1 cm focal distance using different power and speed parameters. Laser parameters were controlled with Autolaser software by adjusting the laser power and speed. The obtained layers were

immersed in a water:EtOH solution (70:30 vol) and subjected to ultrasonic treatment for 3 minutes to remove residual dust. Engraved PMMA layers were exposed to TCM vapor to furtherly finish their surface. In particular, the sheets were exposed to TCM vapor for 3 minutes at a distance of 2 mm from the liquid surface at room temperature, under fume hood [129, 130]. The functional PMMA layers were aligned in specific custom-made aluminium plates endowed with metallic pins adding EtOH. The scaffolds were positioned in the proper layer and then the bonding process was conducted at 70 °C and 100 bar for 3 minutes in a laboratory hot-press (Carver Laboratory Press, Fred S. Carver, Inc., Menominee Falls, WI) [131].

6.3 Lactate Dehydrogenase (LDH) Cytotoxicity Assay

The bioluminescent LDH-cytotoxicity assay (LDH-Glo™ Cytotoxicity Assay kit - Promega) was performed to assess the biocompatibility of the PLA for the THLE2 cells. The levels of the released LDH were measured in the conditioned medium of cells grown in 2D system and on PLA in both static and dynamic conditions, respectively using the Insert-like and the HoC systems. After 72h from seeding, the medium was recovered from each growth condition and diluted 1:50 in LDH Storage Buffer. Then, 50 µL of the diluted medium was transferred into wells of a 96-well plate, 50 µL of LDH Detection Reagent were added to each well and incubated for 60 minutes at room temperature. Finally, the bioluminescence was recorded using Glomax. The data obtained were plotted as % of cytotoxicity applying the formula: 100 x [(Experimental LDH Release- Medium Background)/ (Maximum LDH Release Control-Medium Background)] following manufacturer's instructions. The reported data are the mean of at least three independent replicates.

6.4 Cell proliferation assay

Proliferation rate of THLE2 cells grown in 2D system and on Static Insert-like PLA was assessed by measuring DNA content through the Quant-iT™ PicoGreen™ assay (ThermoFisher Scientific, cat. numb. P11496) according to the manufacturer's instructions. Briefly, at the indicated time points (24h, 48h and 72h) conditioned medium was removed and adherent cells were rinsed two times with PBS. Subsequently, to lyse cells, 300 µl of TE buffer supplemented with 0.1% Triton-X THLE2 were used by direct addiction to cells in 2D system, or by submerging the PLA scaffold. To facilitate DNA release, samples were vortexed for 15 s every 5 min for 20 min while kept on ice. The samples were subsequently centrifuged for 8000 g for 5 min to eliminate cell debris. The recovered supernatants were diluted 1:10 in TE buffer and loaded into a white flat bottomed 96 well plate. After adding PicoGreen working solution to each standard and sample, fluorescence was measured with a microplate reader (Glomax) at excitation and emission wavelengths of 480/520.

6.5 Proteomic profile analysis: Sample Preparation and LC-MS/MS and bioinformatic analysis

All the chemicals used for protein extraction and digestion were of analytical grade, and Milli-Q water was employed in all buffers and solutions. THLE2 cells grown for 72h in 2D, Static Insert-like PLA and HoC systems were lysed in RIPA buffer (NaCl 5M, Tris HCl pH 7.6 1M, 5% Triton X-100) containing protease and phosphatase inhibitors for 90 minutes in ice; lysates were centrifuged at 14000 g for 12 minutes at 4°C and protein concentration was measured using a Pierce Bicinchoninic Acid (BCA) assay kit (Thermo Fisher Scientific, Waltham, Massachusetts, US) and a plate reader from Tecan (Mannedorf, CH). For each sample, a protein amount of 30 µg was subjected to proteolytic digestion using filter-assisted sample preparation (FASP) protocol with 10 kDa Vivacon spin filters (Sartorius, Göttingen, Germany)[132]. Briefly, samples were concentrated by centrifugation (14,000 x g; 10 min) and then reduced by adding 1 M Dithiothreitol (DTT, Sigma-Aldrich, part of Merck Group, St. Louis, Missouri, US) in 100 mM Tris/HCl, 8 M urea pH 8.5 for 30 min at 37 °C. Subsequently, proteins were alkylated in 50 mM iodoacetamide (IAA, Thermo Fischer Scientific) for 5 min at room temperature. After reduction and alkylation, samples were washed three times in 100 mM Tris/HCl, 8 M urea pH 8.0 at 14,000 × g for 30 min. Proteins were then digested with LysC (1:50 enzyme-to-protein ratio, from Promega, Madison, Wisconsin, US) in 25 mM Tris/HCl, 2 M urea pH 8

overnight and with trypsin (1:100 enzyme-to-protein ratio, Promega) in 50 mM ammonium bicarbonate for 4 h. Resulting peptides were then eluted from the filter columns by centrifugation (14,000 x g; 60 min) and acidified with 20 µl of 8% formic acid. Peptides were desalted by stop-and-go extraction (STAGE) on reverse-phase tips packed with Empore C18 disks in-house (Sigma-Aldrich), as previously described [133]. Peptides were eluted, vacuum-dried, and resuspended in 20 µl of 0.1% formic acid. Their concentration was measured using a Nanodrop 2000 (Thermo Scientific). 1 µg of peptides was separated using a nanoLC system (Vanquish Neo UHPLC, Thermo Scientific) equipped with an Acclaim PEPMap C18 column (25 cm x 75 µm ID, Thermo Scientific) in a 130-minute binary gradient of water and acetonitrile containing 0.1% formic acid. Separated peptides were ionized using a nano-electrospray ion source and analysed using an Exploris 480 mass spectrometer (Thermo Fisher Scientific) for tandem mass spectrometry analysis. Data independent acquisition (DIA) was performed using an MS1 full scan (400 m/z to 1200 m/z) followed by 60 sequential DIA windows with a 1 m/z overlap and the window placement optimization option enabled. Full scans were acquired with a resolution of 120,000, AGC of 3 x 10^6, and a maximum injection time of 50 ms. Subsequently, 60 isolation windows were scanned with a resolution of 30,000, an AGC of 8 x 10^5, and the maximum injection time was set to auto to achieve the optimal cycle time. Collision-induced dissociation fragmentation was induced with 30% normalized HCD. The data were analysed using the DIA-NN software (version 1.8.1) with a predicted library generated from in silico digestion of the Homo sapiens proteome (UP000005640) from the Uniprot reference database, with cleavages at K* and R*, two missed cleavages allowed, and a minimal peptide length set at 6 residues. The false discovery rate (FDR) for peptide and protein identification was set at 0.01%. Label-free quantification (LFQ) was used for protein quantification. Using Perseus software (v2.0.9.0; [134], the LFQ values were filtered based on valid values: values were considered valid when detected in at least the 50% of the biological replicates of at least one of the compared groups (“2D vs Static Insert-like” and “2D vs HoC”). GraphPad Prism 10.3.0 was used for (i) performing the p-value correction (Benjamini, Krieger, and Yekutieli method); (ii) making a volcano plot scaling in which the Log2 Fold Change (FC) was centred on zero. FC threshold at ±2 with a FDR-adjusted p-value (q-value) ≤ 0.05 were used to consider a protein significantly modulated in the indicated pair-wise comparisons. The enrichment analysis of the Biological Pathways of proteins modulated in the performed comparisons (“2D vs Static Insert-like” and “2D vs HoC”) was carried out using the stand-alone enrichment analysis tool FunRich 3.1.3 (Functional Enrichment analysis tool; http://www.funrich.org) [135].The tissue expression enrichment of the modulated proteins was analysed within the integrative web resource on mammalian tissue expression TISSUES 2.0 (http://tissues.jensenlab.org/) [136] by STRING v12 (Search Tool for the Retrieval of Interacting Genes/Proteins; http:// string-db.org/).

6.6 Shear Stress Test

THLE2 cells were seeded in the upper chamber of the HoC device. The following day, the medium was removed and through a syringe pump, PBS was delivered to the lower chamber at the flux of 2000µl/min for 5 minutes. The outgoing PBS was collected and was subjected to cell counting in a Burker chamber before and after centrifugation. Meanwhile cells in the HoC were fixed in PFA 4%, and after three washes in PBS, cells were stained with Actin Green (Molecular Probes, Life Technologies, Carlsbad, CA, USA) and Hoechst (Molecular Probes, Life Technologies, Carlsbad, CA, USA). The samples were analysed through Fluorescence microscopy (Nikon Eclipse Ti).

6.7 Infection with lentiviral vectors to stably silence hnRNPA2/B1 and lncH19

SW480, SW620 and HCT-116 cells were stably silenced for hnRNPA2/B1 by lentiviral infection with hnRNPA2/B1 lentiviral particles (Cat. n° TL312380VC, OriGene Technologies, Inc., Rockville, MD, United States). Only HCT-116 cells were also stably silenced for lncH19 by lentiviral infection with H19 human shRNA lentiviral particles (Cat. n° TL318197VB, OriGene Technologies, Inc., Rockville, MD, United States), while relative control cells were infected with control shRNA lentiviral particles (Cat. n° TR30021V, OriGene Technologies, Inc., Rockville, MD, United States). Subsequently, infected cells were selected by

cell sorting (BD FACSAria™ III Sorter, ATeN Center) and maintained in culture under selective pressure with 2µg/ml of puromycin (Gibco™ puromycin dihydrochloride, cat. n°A1113802, Thermo Fisher® Scientific, United States). Silencing efficiency was regularly tested by qRT-PCR and Western Blot, and the fluorescence signal relative to the GFP expression frequently observed with Fluorescence Microscopy (Nikon Eclipse Ti).

6.8 Extracellular Vesicles Isolation

SEVs were isolated from the conditioned media of wt- and sh-SW480, SW620 and HCT-116 cells maintained in the presence of EV-depleted FBS. The conditioned medium was collected after a culture period of 48 h and then subjected to differential centrifugation followed by ultracentrifugation according to the described protocol: the conditioned medium was centrifuged at 4 °C for 5 min at 300 × g, 15 min at 3,000 × g and 30 min at 10,000 × g. The supernatant was then ultracentrifuged at 4 °C for 1h and 45 min at 100,000 × g in a Type 70 Ti fixed angle rotor. The obtained sEV pellet was resuspended in a range of 60–120 µl PBS, quantified by the Bradford protein assay (Pierce, Rockford, IL, USA) aliquoted and stored at − 80 °C.

6.9 SW620_sEVs Internalization in HoC

SW620-EVs were incubated with PKH 26 Red Fluorescent Cell Linker Kits (Merck KGaA, Darmstadt, Germany) for 20 min, washed three times with PBS, and after centrifugation resuspended in RPMI medium. Labelled EVs were delivered in the lower chamber of HoC in which THLE2 were seeded in the upper chamber. After 4 h of treatment, cells were fixed with PFA 4%, washed three times, permeabilized with 0.1% TritonX-100 and stained with Actin Green (Molecular Probes, Life Technologies, Carlsbad, CA, USA), and Hoechst (Molecular Probes, Life Technologies, Carlsbad, CA, USA). To gain clearer visualization of the EV signal, the HoC Device was disassembled to extract the PLA membrane that was mounted in two coverslips. The samples were observed through Fluorescence microscopy (Nikon Eclipse Ti).

6.10 Acute Treatment of the THLE2 with CRC_sEVs

To investigate the effects induced by CRC_sEVs on hepatocytes, the following treatment protocol was performed. After reaching sub confluence, THLE2 cells were treated for the indicated time-points with approximately 1.5*E10 particles of sEVs derived from wt- and sh-SW480, SW620 and HCT-116 cell lines corresponding to 20 µg/ml, biological dose which was found effective in previous studies[137]. After treatment, the cells were harvested for real-time quantitative PCR, *RNA in situ* or immunofluorescence analysis by confocal microscopy.

6.11 Chronic Treatment of the THLE2 with CRC_sEVs

After 24h from seeding in both 2D system and HoC as described in the 4.2 paragraph, the THLE2 cells were treated for the following 48h with 20 µg/ml of SW620_sEVs. While the treatment was performed as unique and acute administration in the 2D system, the HoC allowed to set a chronic system of administration as following described. THLE2 were seeded on the upper chamber of the HoC and after 48h a syringe pump was connected to the chamber and set to deliver 1 ml of medium per day to the lower chamber of the HoC (41.67 µl/h), in the presence or absence of the EVs isolated from the SW620 cells (SW620_sEVs). After 48 hours of this chronic treatment, the experiment was stopped for the indicated analyses.

6.12 RNA Isolation and Real-time quantitative PCR

Total RNA was extracted using Macherey–Nagel™ NucleoSpin™ miRNA Kit (Cat. n°740971.250, Macherey–Nagel, Germany), according to the manufacturer's instructions. The RNA was reverse transcribed to cDNA using the High-Capacity cDNA Reverse Tran scription kit (Applied Biosystems, Foster City, CA, USA). Then, the cDNA was used to perform quantitative real-time reverse transcriptase-polymerase chain reaction (qRT-PCR) analysis. The sequences of the primers used are reported in **Table 1**. The qRT-PCR was performed using a Step One™ Real-time PCR System Thermal Cycling Block (Applied Biosystems, Waltham, MA, USA) in a 20 µl reaction containing 300 nM of each primer, 2 µl template cDNA, and 18 µl

2X SYBR Green I Master Mix. Gene expression levels were normalized using β-actin as an endogenous control. Finally, the data are presented as 2^-ΔCt and 2^-ΔΔCt compared with the untreated control.

Gene	Forward	Reverse
LncH19	TCGTGCAGACAGGGCGACATC	CCAGCTGCCACGTCCTGTAACC
RbFOX2	CCAGCTTTCAAGCAGATGTGTCC	CAAATGGGCTCCTCTGAAAGCG
HnRNPA2/B1	CAGCAACCTTCTAACTACGGTCC	CACTGCCTCCTGGACCATAGTT
ENAH	GACACTTGTCTCCCGTCTCC	TCTGTTCACTCATGGTGCCG
ENAHex6	TGCTGGGAGACTCTTCTGCT	CCTGTTGGGATGGAGTCTCG
ENAHex11a	CCAGACGGGATTCTCCAAGG	TTTGGTCTGTGTAATGAATCATAGG
CTTN	CCGACCGAGTAGACAAGAGC	GTCGATACCGTATTTGCCGC
CTTNex11	GACAAATGTGCCCTTGGCTG	CTGCCTCTCCGACTGAACAC
PARD3	TTCGCTGTTGAGAAGCACCA	ATCTGCATCTGGCTTGGCTC
PARD3ex18	AGCAATTTTCAGATGCCAGTCA	TTCTGGTCATCCACTGTATTGAGTT
β-ACTIN	CAAGAGATGGCCACGGCTGCT	TCCTTCTGCATCCTGTCGGCA

Table 1 *qRT-PCR primers list.*

6.13 THLE2 transfection for lncH19 over expression

THLE2 cells were seeded at 1.5 x 10^4 in 6 well plates. After 24 h from seeding, cells were transfected with 1.2 µg/ml of H19-pFLAG-CMV-2 expression vector (cat. n° E7033, Sigma-Aldrich, USA), or empty pFLAG-CMV-2 as Negative Control (Sigma-Aldrich). HiPerFect Transfection Reagent (cat. n° 301704, Qiagen, Germany) was used following the manufacturer's standard instructions. Eighteen hours after transfection, the cells were processed for the indicated experiments.

6.14 Protein Lysates preparation and Western blot

Colorectal cancer or sEVs were lysed using RIPA buffer with protease inhibitor cocktail (Thermo Fisher Scientific, Waltham, MA, USA) (1:100 dilution) with gentle shaking for 1h on ice and then centrifuged at 18,800 × g for 15 min at 4 °C. The extracted proteins were quantified through Bradford protein assay (Pierce, Rockford, IL, USA). Protein lysates were separated on Bolt 4–12% Bis–Tris Plus precast polyacrylamide gels (Invitrogen by Thermo Fisher Scientific, Waltham, MA, USA) in reducing conditions. After the electrophoresis, proteins were transferred to a nitrocellulose blotting membrane (Amersham Protran Premium 0.45 µm NC by GE HealthCare Life Science, Little Chal font, Buckinghamshire, UK), blocked in 5% Milk Blocking Solution and incubated with primary antibodies overnight at 4 °C with gentle shaking. The following primary antibodies were used for detecting the proteins of interest: anti-RBM9/ rbFOX2 (1:1000, cat. n° A300-864 A Bethyl Fortis, Montgomery, Texas) and anti-hnRNPA2/B1 **(**Invitrogen, 1.1000 cat. n° PA5-30960). Primary antibodies used for sEV characterization [43]were: anti-CD81 (1:1000 dilution; Santa Cruz Biotechnology, Dallas, TX, USA), anti-HSC70 (1:1000 dilution; Santa Cruz Biotechnology, Dallas, TX, USA), anti-Calnexin (1:1000; Santa Cruz Biotechnology, Dallas, TX, USA), anti-cytochrome c (1:1000; Cell Signaling Technology, Danvers, MA, USA) anti-HSP70(1:1000, Santa Cruz Biotechnology, Dallas, TX, USA) anti-TSG101(1:1000, Santa Cruz Biotechnology, Dallas, TX, USA). Anti-β actin (1:1000 dilution; Santa Cruz Biotechnology, Dallas, Tx, USA) and anti-Tubulin (1:1000 dilution; Santa Cruz Biotechnology, Dallas, TX, USA), were used for housekeeping proteins used as loading control. Subsequently, membranes were washed with Tris-buffered saline + Tween-20 (TBS/T) three times and

incubated with horseradish peroxidase (HRP)-conjugated goat anti-rabbit, anti-mouse or anti-chicken secondary antibodies (1:1000 dilution; Thermo Fisher Scientific, Waltham, MA, USA) at room temperature for 1 h in gentle shaking. Finally, the protein bands were visualized through enhanced chemiluminescence (ECL™ Prime Western Blotting System Cytiva RPN2232) with Chemidoc imaging system (Bio-Rad, Milan, Italy).

6.15 Immunofluorescence and Confocal Microscopy

After the treatment, the medium was removed and after washing three time in PBS, cells were fixed by adding 4% PFA, then permeabilized for 5 min with 0.1% Triton X-100 and after blocking for 1h with BSA 3%, were incubated for 1 h at room temperature with the following antibodies: anti-RbFOX2 primary antibody (1:300 dilution, cat. n° A300-864 A Bethyl Fortis, Montgomery, Texas), anti-Albumin (1:100 dilution; Santa Cruz Biotechnology) and anti-Vimentin (1:100 dilution; Cell Signaling Technology). Unbound primary antibody was removed by washing three times with PBS, and the cells were incubated with DyLight 488 or DyLight 594 secondary antibody (1:500 dilution; Thermo Fisher Scientific,). Unbound secondary antibody was removed by washing with PBS. Nuclei were stained with Hoechst (Molecular Probes, Life Technologies), and F-actin with Actin Green (1:125 dilution, Thermo Fisher). Finally, the samples were analysed by fluorescence microscopy (Nikon Eclipse Ti) and confocal fluorescence microscopy (Nikon A1 confocal microscope). Mean Fluorescence Intensity (MFI) of Albumin, Vimentin and Actin expression was measured analysing three Regions of Interest (ROIs) of at least three different images with ImageJ Software.

6.16 RNA in situ Hybridization (RNA Scope)

In order to visualize the lncH19 localization in THLE2 treated by the CRC_sEVs, RNA in situ protocol was applied as described. After the indicated time-points of treatment, media was removed, and cells were washed two times with PBS. Cells were subsequently fixed with 10% Neutral Buffered Formalin (NBF) for 30 min at room temperature, and after fixation were washed twice with PBS and RNAscope® Protease III (diluted 1:15 with PBS) was added for 10 min incubation. Subsequently, cells were washed with PBS and RNAscope® Multiplex Fluorescent v2 Assay combined with Immunofluorescence (Cat. No. 323100) was applied according to manufacturer's instructions.

6.17 Bioinformatic analysis

In order to predict the interactions between lncH19 and its targets in the THLE2, bioinformatic analyses were conducted using DIANA tools (Rincon-Riveros et al., 2021). LncH19–miRNA interactions were identified using DIANA-LncBase v.3, as well as the miRNAs involved in the EMT process. DIANA-miTED software was used to identify the miRNAs expressed by healthy liver tissue, and all the datasets obtained were intersected using FunRich software. Finally, through mirPATH database, the mRNAs targets of the obtained miRNAs were identified.

6.18 Statistical analysis

Statistical analysis was performed using GraphPad Prism software (GraphPad software, Inc., La Jolla, CA). Values reported in all graphs are the mean ± standard deviation (SD) of three replicates, unless otherwise stated. The statistical significance of the differences was analysed using a one-way Anova test. p-values were indicated in the graphs as follows: * = $p < 0.05$; **= $p < 0.001$; and **** = $p < 0.0001$. A p-value$\leq$0.05 was considered significant.

CHAPTER 7

RESULTS AND DISCUSSION

7.1 The long non-coding RNA H19 is contained in the CRC_sEVs and is horizontally transferred to the hepatocytes with RBFOX2.

Small EVs have been isolated from CRC cell line through differential ultracentrifugation (dUC), HCT-116_sEVs were characterized for protein markers according to MISEV 2023 guidelines (***Figure 14a***) [43], SW480_sEVs and SW620_sEVs characterization has been published in our previous research study [5]. As shown in ***Figure 14a***, the protein lysate of HCT-116_sEVs show the presence of EV-specific markers (HSC70, CD81) and the absence of cellular markers, which is instead present in the HCT-116 cell lysate (Cytochrome C). QRT-PCR allowed us to reveal that CRC_sEVs are enriched in lncH19 compared to relative EV-producing cells (***Figure 14b***). Our previous study demonstrated that CRC_sEVs promote liver pre-metastatic niche formation inducing EMT in hepatocytes [5]. The EMT process is strictly associated with morphological alterations, especially the loss of cell polarity and intercellular junctions [98], which are present in the hepatocytes after the CRC_sEVs treatment. Here, with aim to investigate if transported lncH19 might take part to EVs liver premetastatic niche formation, we treated THLE-2 cells for 18h. As expected, treated cells showed mesenchymal like phenotype. Q*RT-PCR and RNA* in situ demonstrated that EVs' treatment induced lncH19 increase in THLE2 cells *(**Figure 14c-d***).

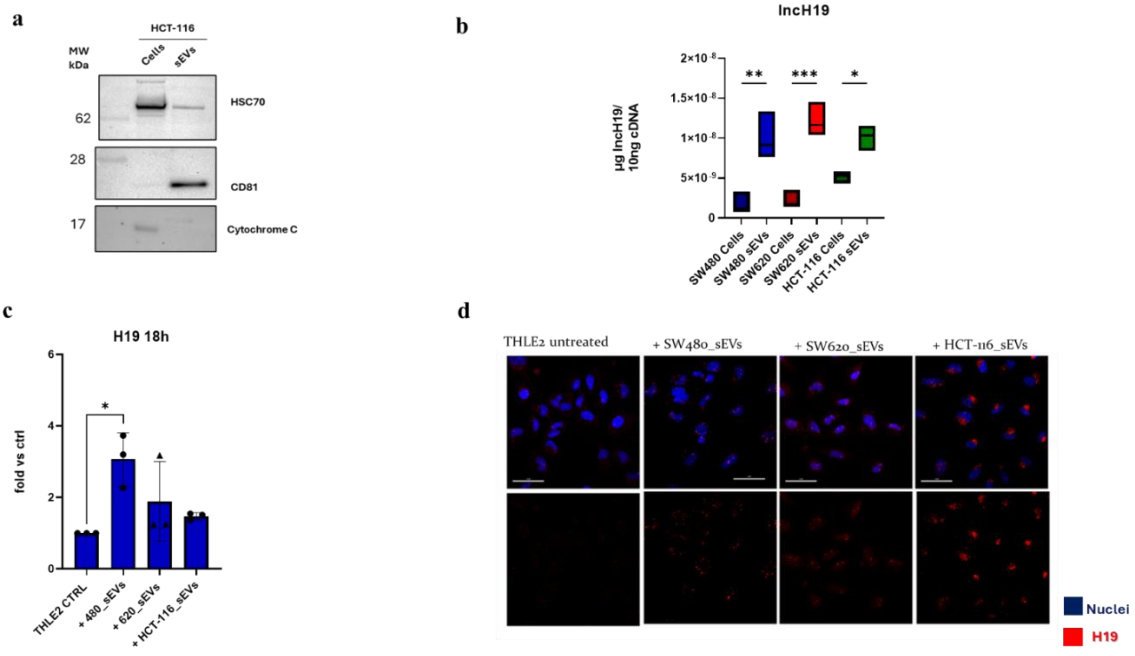

Figure 14 (a) *Western Blot showing the characterization of HCT-116_sEVs through EV-specific markers (HSC70 and CD81) and the absence of cellular marker (Cytochrome C).* ***(b)*** *qRT-PCR showing the quantification of lncH19 inside the CRC_sEVs and CRC_cells.* ***(c-d)*** *qRT-PCR and RNA in situ showing the increase of lncH19 in the THLE2 treated for 18h with the CRC_sEVs.*

As already demonstrated in our recent manuscript [138], in CRC, lncH19 directly takes part to RNA maturation by delivering splicing the factors RBFOX2 and hnRNPM directly to mRNA targets thus inducing pro-metastatic Alternative Splicing. We then wondered whether splicing factors travel into EVs via H19 and then to recipient cells. As shown in **Figure 15a**, we demonstrated for the first time to our knowledge, that RbFOX2 is transported by CRC_sEVs. The western blot from EVs'protein lysate show the presence of RBFOX2, moreover the treatment of the THLE2 with the CRC_sEVs lead to an increase of RBFOX2 at 6h and even more at 18h after treatment ***Figure 15b-d.*** Interestingly, we did not observe any increase in RBFOX2 mRNA levels in the THLE2 cells treated with the CRC_sEVs, as shown in ***Figure 15c***. This supports the idea that RBFOX2 is directly transferred from the CRC_sEVs to the THLE2 cells, rather than being induced at the transcriptional level within the hepatocytes.

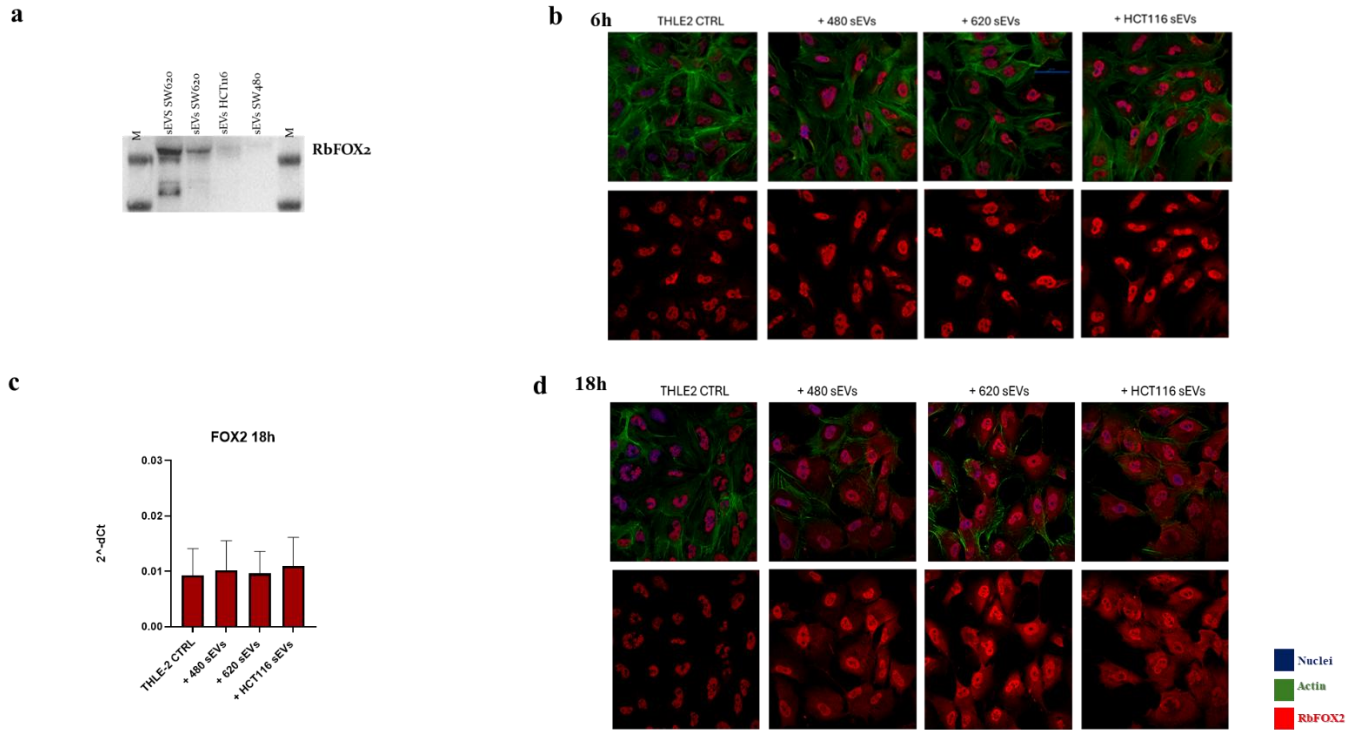

Figure 15 (a) *western blot showing the presence of RBFOX2 in the CRC_sEVs protein lysates.* ***(b-d)*** *Confocal micrographs showing the increase of RBFOX2 in the THLE2 treated with the CRC_sEVs for 6h and 18h respectively.* ***(c)*** *qRT-PCR showing the levels of RBFOX2 mRNA in the THLE2 treated with the CRC_sEVs.*

After evaluating the increase of RBFOX2 and lncH19 in the THLE2 cells treated with the vesicles, as well as the morphological alteration induced by the treatment (***Figure 16b***), to understand whether the molecules were transported together we analyzed the presence of both after only three hours of treatment with the EVs. To achieve this, an RNA in situ hybridization combined with immunofluorescence was performed. As shown in the confocal images, there was a co-localization between the two signals (***Figure 16a***), supporting the idea of the direct transfer of lncH19 and RBFOX2 from the sEVs to the recipient cells (***Figure 16c***). This data further enforces the experimental hypothesis regarding the EV transfer of RBFOX2 and lncH19 to the hepatocytes.

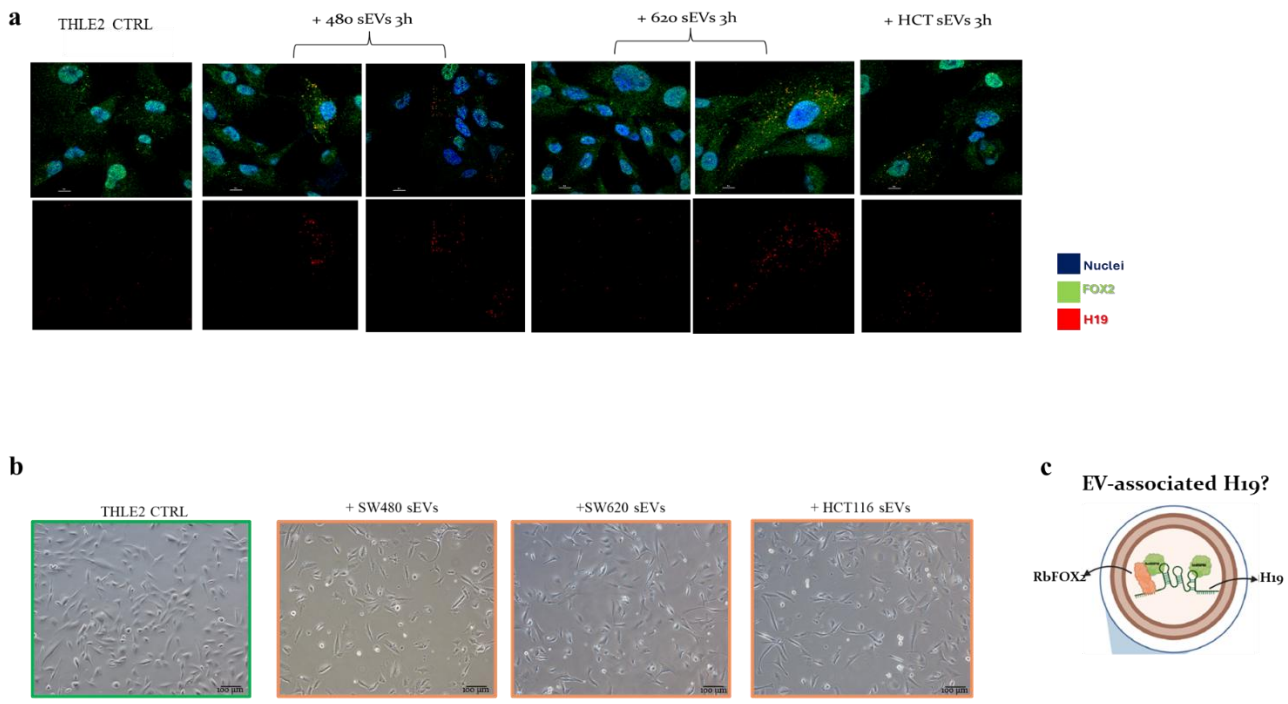

Figure 16 (a) *Confocal micrographs of RNA in situ combined with Immunofluorescence showing the increase of RBFOX2 (green) and lncH19(red) in the THLE2 treated with the CRC_sEVs for 3h.* ***(b)****Microscopy images showing the morphological changes in the THLE2 educated by the CRC_sEVs for 18h.* ***(c)*** *Representative Image showing the proposed mechanism of lncH19 acting as shuttle RNA transferring RBFOX2 inside the EVs.*

7.2 CRC_sEVs induce AS mechanism in the THLE2

As already mentioned, the vesicles promote a morphological alteration of the THLE2, as well as an increase of RBFOX2, confirmed by the confocal images in ***Figure 17a***. Among the different AS mechanism regulated by RBFOX2, in literature is extensively described its role in regulating the AS of mRNAs involved in the promotion of the EMT process [139]. We focused our further investigation on RBFOX2 targets involved in the definition of the cell shape and morphology: ENAH (hMENA), PARD3 and CTTN [140]. It has been demonstrated for these three mRNAs that alternative splicing controls the switch from epithelial to mesenchymal isoforms. In particular, the mRNA of ENAH is described to be subjected to the skipping of exons 6 an 11A during the EMT process [141], while for CTTN mRNA the inclusion of exon 11 is associated with EMT and increased aggressiveness in colon cancer forms [142]. Finally, PARD3 mRNA undergoes exon 18 skipping during EMT. By designing exon-specific primers, we evaluated the expression of AS variants as well as the common gene isoforms. As shown by the qRT-PCR in Figure 17b, the common genes do not show an increase in the THLE-2 cells treated with the CRC_sEVs, except for PARD3. In contrast, the AS variants seem to be affected by the treatment, which results in the skipping of exons 6 and 11a of ENAH, the inclusion of exon 11 of CTTN, and the skipping of exon 18 of PARD3 (***Figure 17b-c***). Overall, the data here showed indicated that CRC_sEVs treatment induced AS in hepatocytes, favouring mesenchymal isoforms. Here remain to understand if the presence of the complex lncH19-RBFOX2 plays a role in this process.

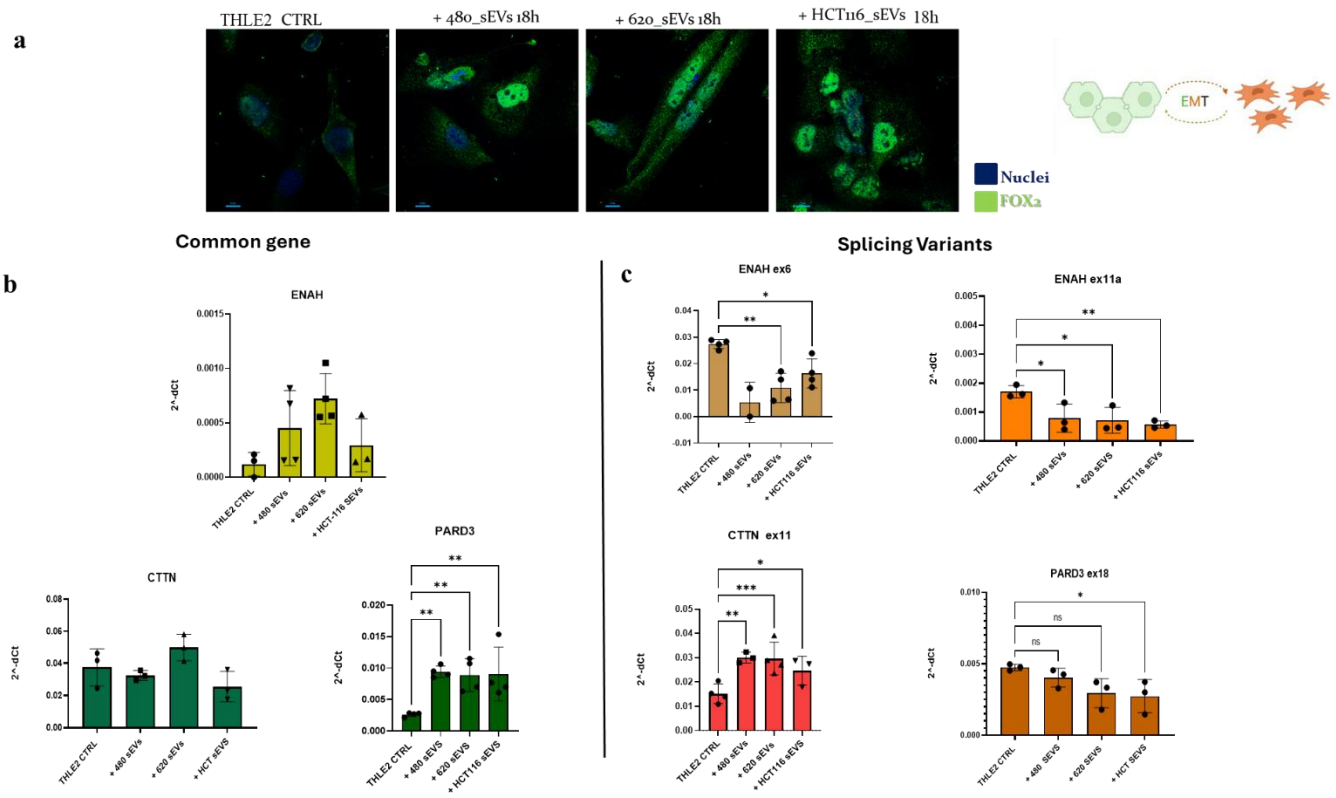

Figure 17 (a) *Confocal micrographs showing the increase of RBFOX2 and the morphological alterations in the THLE2 treated with the CRC_sEVs for 18h.* ***(b)*** *qRT-PCR showing the levels of RBFOX2 splicing targets alteration in the hepatocytes after the treatment with the CRC_sEVs for 18h* ***(c)*** *as long as their splicing counterparts.*

7.3 hnRNPA2/B1 is crucial for the EV-loading of lncH19 and RBFOX2

To investigate the role of EV-associated lncH19 in orchestrating the molecular processes previously described, we silenced hnRNPA2/B1 in CRC cell lines (***Figure 18a***), since has been demonstrated that the RNA binding protein is responsible for lncH19 loading in EVs [143]. The efficiency of hnRNPA2/B1 silencing has been validated through qRT-PCR and W.B (***Figure 18b***).

We isolated the EVs from the sh-CRC_cells (sh-CRC_sEVs) and characterized them for EV specific markers (TSG101, CD81, HSC70, HSP70) and the absence of cell-specific markers (Calnexin). Subsequently, lncH19 levels were evaluated in the wild type- and sh- CRC_sEVs through qRT-PCR. As shown in ***Figure 18d***, wt-CRC_sEVs contain higher levels of lncH19 compared to their sh- counterparts, as further control we included EVs isolated from lncH19 silenced HCT-116, previously established in our laboratory [144]. We investigated the presence of RBFOX2 in wt- and sh- sEVs. The western blot in ***Figure 18d*** show that also RBFOX2 levels decrease in HCT-116_sEVs obtained from shA2B1 silenced cells, thus enforcing our hypothesis of lncH19 as shuttle for SF in EVs.

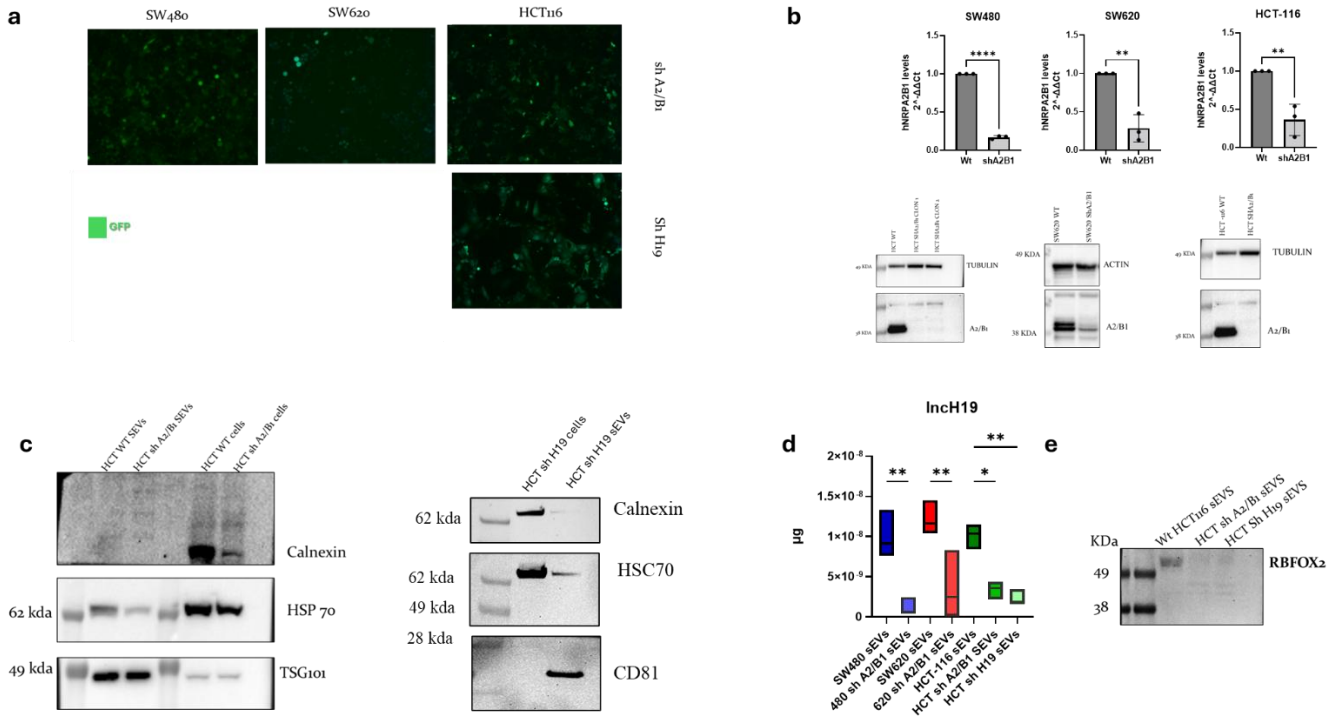

Figure 18 (a)*Fluorescence Images showing the GFP expression of CRC_cells infected with -sh lentiviral particles.* ***(b)*** *qRT-PCR and W.B. showing the downregulation of hnRNPA2/B1 at both mRNA and protein level in sh-CRC_cells (SW480, SW620 and HCT-116).* ***(c-d)*** *Characterization of sh-HCT_sEVs through W.B. for sEVs specific markers (HSP70, TSG1201, HSC70 and CD81) and the absence of cellular marker (Calnexin).*

After characterizing and confirming the different molecular cargo inside the wt-and sh-CRC_sEVs, in order to investigate the different biological activities elicited in the THLE2, cells were treated for 18h with the different CRC_sEVs and the lncH19 increase was evaluated through RNA *in situ (and its densitometric analysis)* and qRT-PCR. As shown by ***Figure 19a-b-c***, the increase of lncH19 elicited by the wt-CRC-sEVs is reverted with the treatment with the sh-CRC_sEVs, consistent with the lower levels of the RNA in these sEVs, as previously shown. Finally, also the levels of the RBFOX2 were analysed in the treated hepatocytes, and after 6h and 18h the protein increase detected is significantly lower when treating with the sh-sEVs (***Figure 19d***).

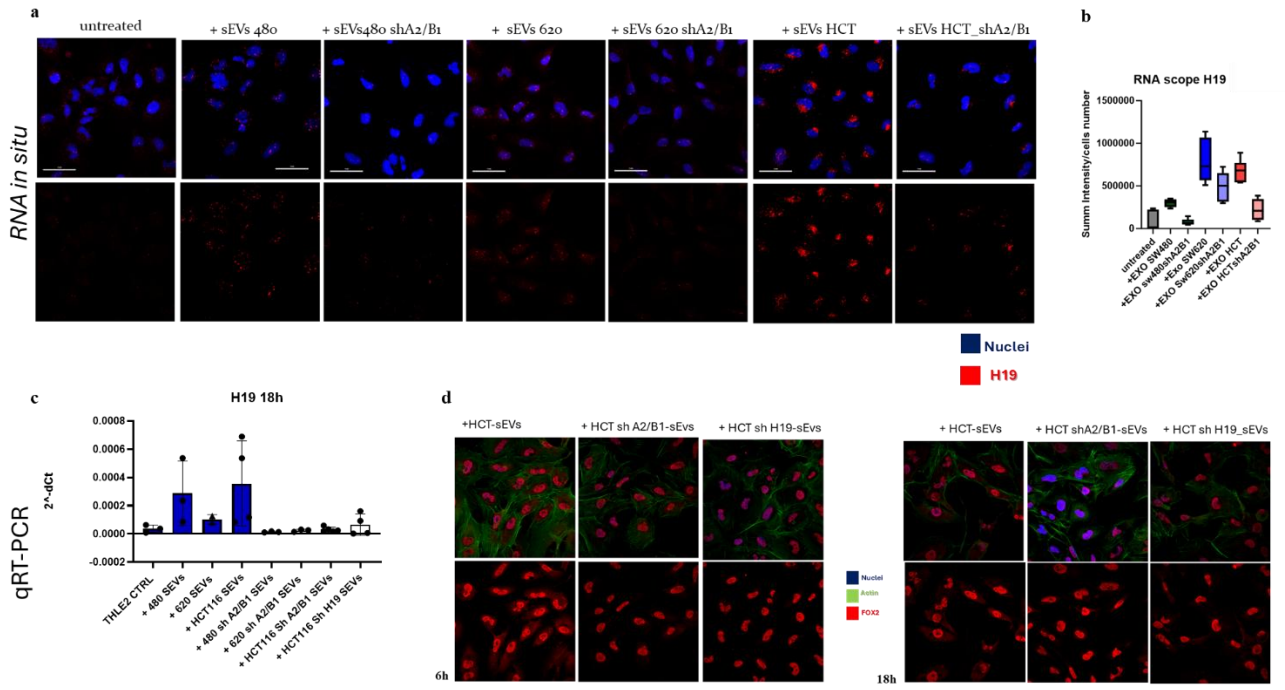

Figure 19 (a) *Confocal Micrographs with* ***(b)*** *relative densitometric analysis and* ***(c)*** *qRT-PCR showing the levels of RBFOX2 in the THLE-2 treated for 18h with the wt-CRC_sEVs and the sh-CRC_sEVs. (d)Confocal micrographs showing the increase of RBFOX2 in the THLE-2 treated with the HCT wt- and sh- sEVs for 6h and 18h.*

Finally, to validate the data regarding the AS mechanism induced by the CRC_sEVs, after treating the hepatocytes with the -wt and -sh CRC_sEVs, the splicing targets of RBFOX2 were evaluated. The results on the common gene and the splicing variants shown in ***Figure 20a-b*** show that the mechanism induced by the wt-CRC_sEVs seem to be only partially induced by the sh-CRC_sEVs, further confirming the key role of lncH19 and RBFOX2 in the promotion of EMT-associated AS. In fact, while the treatment with the wt-CRC_sEVs induce the AS of the exon 6, 11a and 18 of PARD3, promoting the skipping of these exons, when THLE2 were treated with sh-CRC_sEVs, the effects of this AS mechanism were significantly reduced for exon 6 of ENAH and partially for exon 18 of PARD3. Regarding CTTN, the inclusion of exon 11 promoted by the wt-CRC_sEVs doesn't seem to be induced by the treatment with sh-CRC_sEVs.

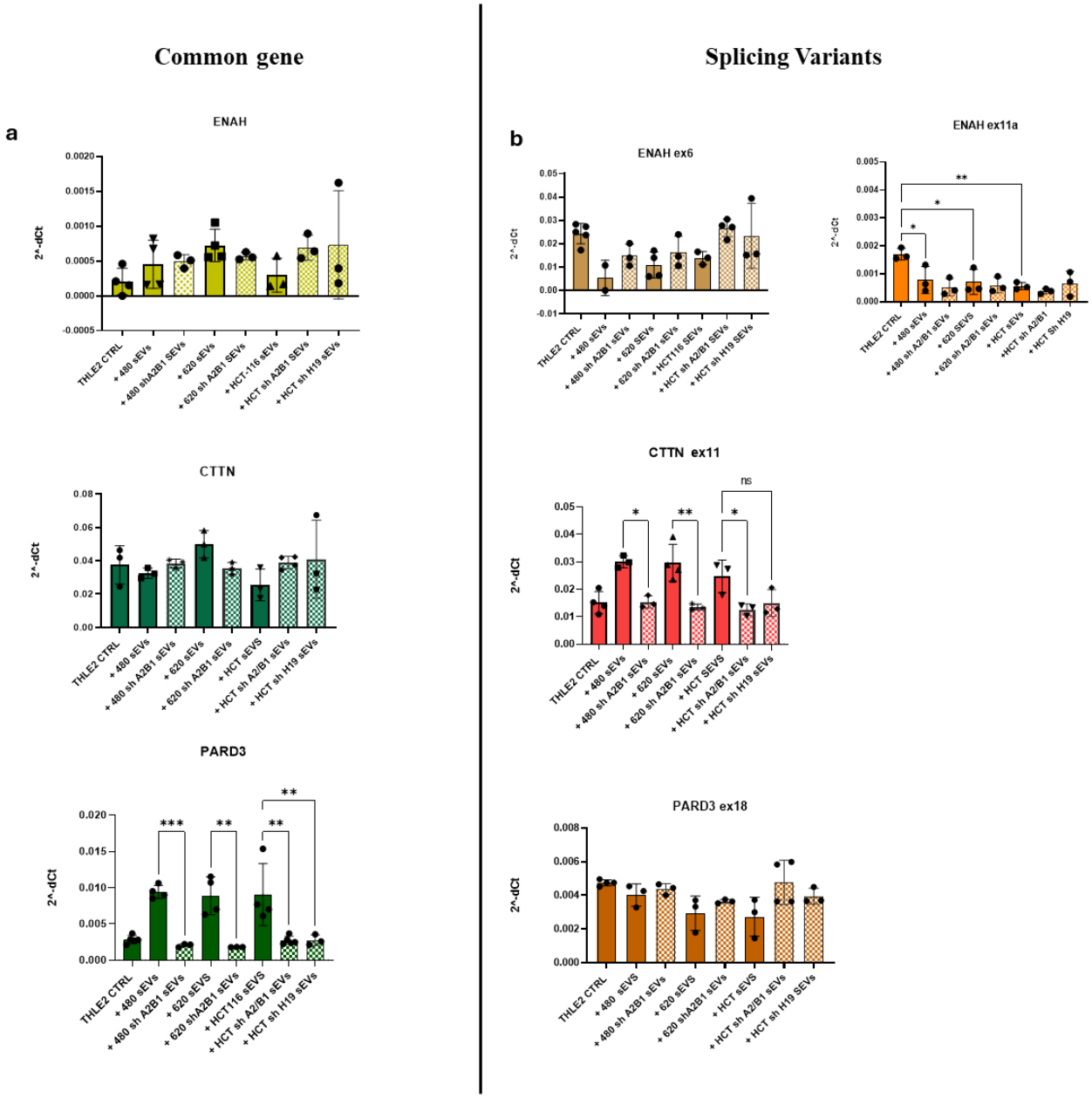

Figure 20 (a) *qRT-PCR graphs showing the levels of ENAH, CTTN and PARD3 genes in the THLE2 treated with the wt- and sh-CRC_sEVs.* ***(b)*** *qRT-PCR graphs showing the AS mechanism induced by the wt-CRC_sEVs and the sh-CRC_sEVs on the splicing isoforms of ENAH, CTTN and PARD3.*

7.4 LncH19 transported by EVs acts as a miRNA sponge in the target cells

Finally, after studying the AS mechanism promoted by RBFOX2 horizontally transferred from the CRC_sEVs to the hepatocytes, the molecular activity of lncH19 in the THLE2 was investigated. LncRNAs are described to regulate gene expression through different mechanism: formation of nuclear structures, acting as lncRNA guide or decoy, scaffolding chromatin modifying complexes, binding RBPs or DBPs regulating their localization and finally acting as sponge for miRNAs [145]. Among all these mechanisms, I focused my attention on lncH19 action as miRNA sponge, affecting hepatocytes differentiative status through gene expression regulation. To gain a clearer picture of the miRNAs eventually sponged by lncH19 in the THLE2, through the deploy of different Bioinformatic tools, a bioinformatic analysis evaluating all the miRNAs sponged by lncH19 which were involved in the EMT process in the healthy liver was performed (***Figure 21a-b***). Performing a Funrich analysis, these three datasets obtained were intersected identifying 11 miRNAs which were analysed to identify the mRNAs targeted by their molecular activity. Out of the 11 miRNAs identified, 4 share PARD3 mRNA as a common target (***Figure 21c***). To validate this computational

analysis, lncH19 over expression was performed in the hepatocytes. After confirming the success of the transfection, PARD3 mRNA was evaluated, resulting in an increase of PARD3 mRNA in the THLE2 overexpressing lncH19 (***Figure 21d***).

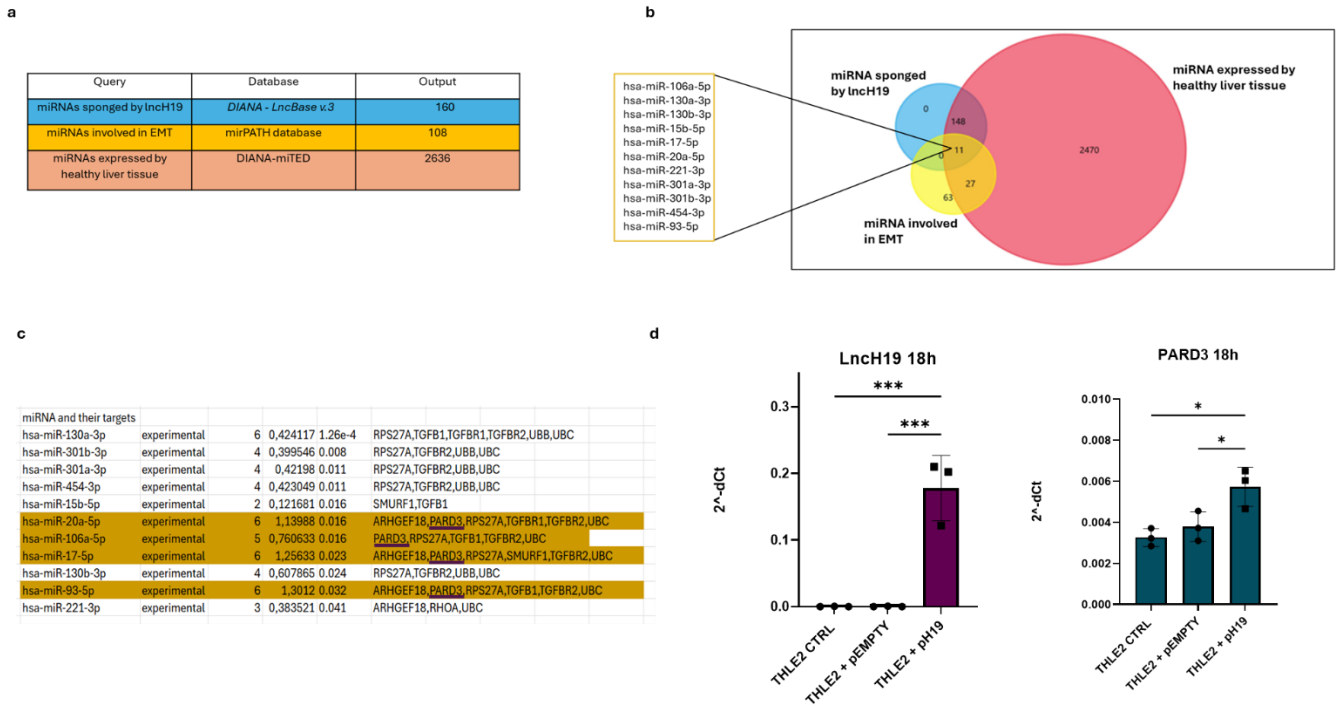

Figure 21 (a) *table showing the different miRNAs identified in the three different analyses (sponged by lncH19, involved in EMT and expressed by healthy liver tissue).* ***(b)*** *Venn Diagram showing the identification of the 11 miRNAs in common by intersecting the three datasets through FunRich analysis.* ***(c)*** *Table showing the different mRNAs targets of the 11 miRNAs identified.* ***(d)*** *qRT-PCR showing the successful over expression of lncH19 in the THLE2 and the increase of PARD3 mRNA in the H19-overexpressing hepatocytes.*

7.5 Hepatocyte-on-Chip design fabrication and evaluation of scaffold-hepatocytes biocompatibility

The design of the HoC culture chamber proposed in the study consists of a top culture chamber cultured with immortalized human hepatocytes, a bottom chamber where CRC_sEVs are flow injected, and a middle layer composed of a thin electrospun scaffold interfacing with the top and bottom chamber **(Fig. 22a)**. The electrospun scaffold serves both as a separator between the two compartments and as a biomimetic substrate for cell culture. Additionally, it acts as an extra barrier to the passage of EVs from the lower to the upper chamber, mimicking the role of the basement membrane, to which hepatocytes adhere in vivo. The design of the whole device is presented in **Fig. 22b**. It is composed of two individual culture chambers presenting specific inlets and outlets for each semi-chamber. The total culture area of the hexagonal chamber is 0.417 cm^2, but it is 0.33 cm^2 by excluding the triangular inlet and outlet regions, making it comparable to the culture surface of a 96-well plate. The volume of the upper chamber is 41.7 µl, whereas the bottom chamber has a slightly lower volume (37.5 µl) due to the presence of an engraved 100 µm-deep recess designed to accommodate the electrospun scaffold, which reduces the overall volume. Alignment holes were also designed for layer alignment during the fabrication. Finally, holes for screw and nuts were also added to the design to ensure a secure seal of the tubes using the connectors. **Fig. 22c** represents the whole HoC platforms including the tubing connector, tubes, and ferrules (top) and the HoC holder and nuts (bottom). Since the fabrication technique proposed in this work is a multilayer-based assembly, the HoC CAD design was then sliced in six functional layers with different thicknesses, as reported in **Fig. 22d**. To assess the suitability of the PLA scaffold for hepatocyte culture, its biocompatibility with THLE2 cells was evaluated. This analysis aimed to determine whether the scaffold could provide a supportive and non-cytotoxic

environment for cell growth, particularly in comparison to conventional 2D systems. To evaluate the biocompatibility of the PLA scaffold for the THLE2 cells, cytotoxicity LDH assay was performed on conventional 2D and 3D systems (insert-like PLA and HoC) after 72h from seeding **(Fig. 22e)** [146]. Rather, the significant decrease % of cytotoxicity for cells grown on PLA suggests that the scaffold provide a more favourable environment for hepatocyte culture than the canonical 2D condition. According to these results, hepatocytes well adhere to PLA scaffold. Indeed, the shear stress experiment performed by giving a PBS flux of 2000 µl/min for 5 minutes, did not cause cell detachment from the scaffold as demonstrated by the absence of any pellet in the exiting PBS and by performing a manually counting cells through a Bürker chamber. Moreover, as demonstrated by the evaluation of the Actin Mean Fluorescence Intensity (MFI), the shear stress did not affect the number of adherent cells on HoC **(Figure 22g)**.

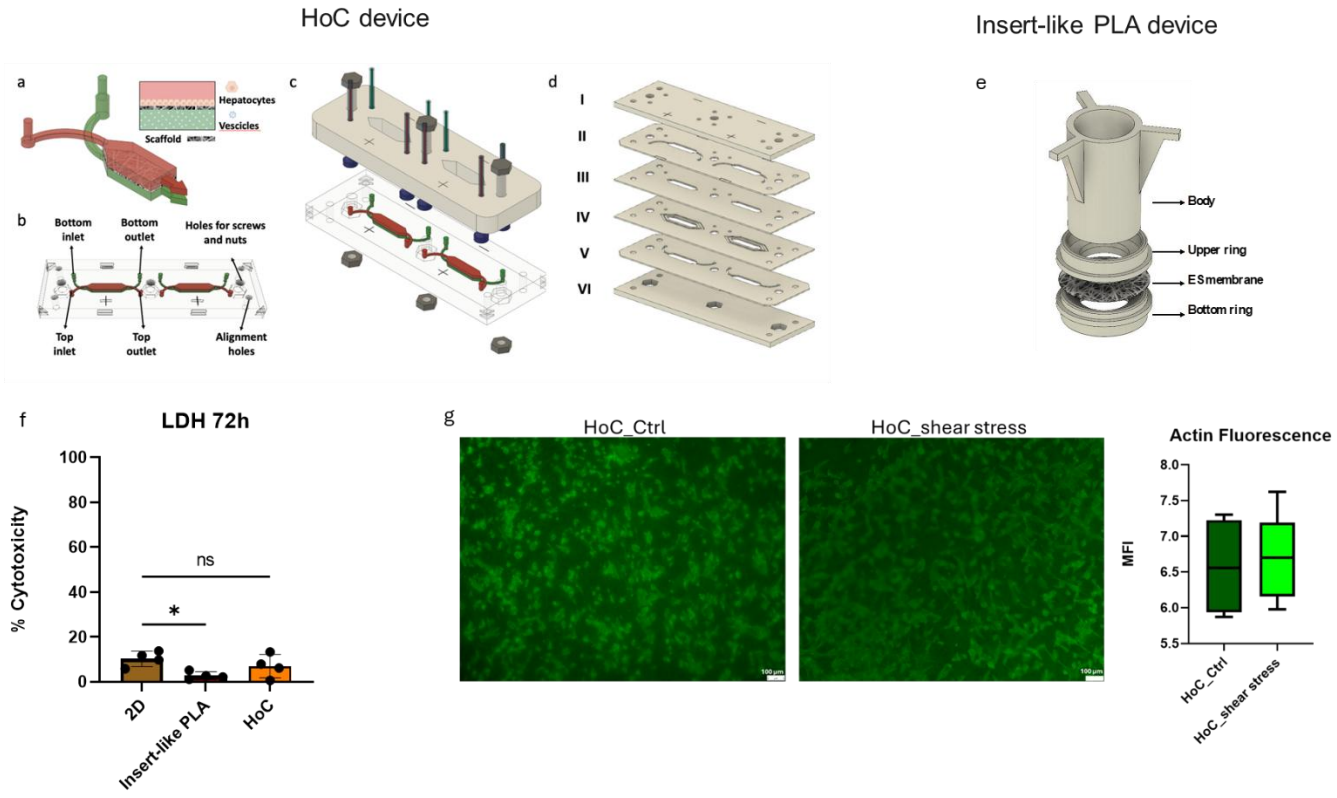

Figure 22 (a) *Perspective view of the fluid volume design of the double culture chamber and schematic of the of the biological validation of the HoC platform;* ***(b)*** *Design of the whole HoC system composed of two culture chamber and the inlet and outlet holes of the upper and bottom compartment on the side indicated by the plus and minus signs on the top of the HoC, respectively;* ***(c)*** *CAD design of the exploded view of the entire HoC platform composed by chip, connector, tubes, ferrules, screws, and nuts;* ***(d)*** *CAD design of the exploded view of the HoC into its six functional layers.****(e)*** *3D CAD design of the the insert-like device composed of a body, Upper ring, ES membrane and a final Bottom ring* ***(f)*** *Assay measuring the concentration of LDH enzyme (mU/mL) that demonstrates the no-cytotoxicity of PLA in both static (Insert-like PLA) and dynamic (HoC) condition in comparison to the 2D system. The data represent the means ± SD of four independent experiments (***$p \leq 0.001$).* ***(g)*** *Fluorescence images showing the hepatocytes attached to the HoC device after the shear stress test. HoC_Ctrl: hepatocytes untreated by shear stress.*

7.6 PLA based devices promote hepatocyte differentiation

To investigate the ability of the PLA scaffold to modulate the phenotypic traits of the hepatocytes, with a perspective analysis of a long-term treatment, an unbiased high-resolution mass spectrometry-based proteomics was used to analyse the proteome of THLE2 cells grown for 72h in 2D, Insert-like PLA and HoC systems. For protein identification, only the proteins that were detected in at least the 50% of the replicates of at least one among the analysed growth condition were taken into consideration, resulting in 7025 totally

identified proteins. Then, the expressed proteins were analysed with the aims to highlight the effects induced by the PLA on the hepatocyte phenotype. With this purpose, the proteome profile of cells grown in 2D system was compared to that of cells grown on Insert-like PLA ("2D vs Insert-like PLA comparison") and on HoC ("2D vs HoC comparison"). These analyses revealed a deep modification of the hepatocyte protein profile associated with the presence of the PLA scaffold. As detailed reported in **Supplementary Table S3**, in the comparison "2D vs Insert-like PLA" about the 70% of the total analysed proteins (4618/6774) were modulated, including both qualitative and quantitative differences. In particular I found that 1504 proteins were exclusively expressed in cells grown in the 2D system, while 144 were exclusively expressed in cells grown on Insert-like PLA (qualitative differences); moreover, significant changes in expression levels were detected for 2970 proteins (fold change $\geq \pm 2$ and q-value ≤ 0.05), including 2357 proteins up-regulated in the 2D system and 613 up-regulated in the Insert-like PLA (quantitative differences), as viewable in the volcano plot reported in **Fig. 23a**. To depict the functional meaning of the observed modulations, the whole set of modulated proteins (both qualitative and quantitative differences) was functionally categorized using the FunRich software which allows to perform a hypergeometric test for the enrichment of the Biological Pathhways of the KEGG Database, followed by the Benjamini & Hochberg (BH) method for multiple test adjustment (adjP.Value). The histogram in **Fig.23b** and the data reported in **Supplementary Table S4** shows that the most significantly enriched Biological Pathways (AdjP-Value) including the proteins positively modulated in cells grown in the insert-like PLA, were specifically related to differentiation mechanism (mesenchymal to epithelial transition) and to liver Haemostasis; Lipoprotein metabolism), as highlighted by the STRING analysis showed in **Fig. 23c** and widely reported in literature [147, 148]. This result provides interesting evidence about the ability of the PLA to enhance the differentiative potential of THLE2 cells. On the other side, the most significantly enriched Biological Pathways including the proteins positively modulated in cells grown in the 2D system, were related to cell division process (Cell Cycle, Mitotic; DNA Replication; PLK1 signalling events; S Phase; M Phase). Since the remarkable inverse relationship between cell proliferation and differentiation is well known [149], the proteomic results suggest that the canonical 2D system maintains a high proliferative rate of hepatocytes at the expense of the acquisition of a differentiated state that is instead promoted by the presence of PLA. According to that, the significant increase of DNA content found in cells grown in the 2D system during the 72h of culture was not observable in cells grown in the insert-like PLA **(Fig. 23d)**.

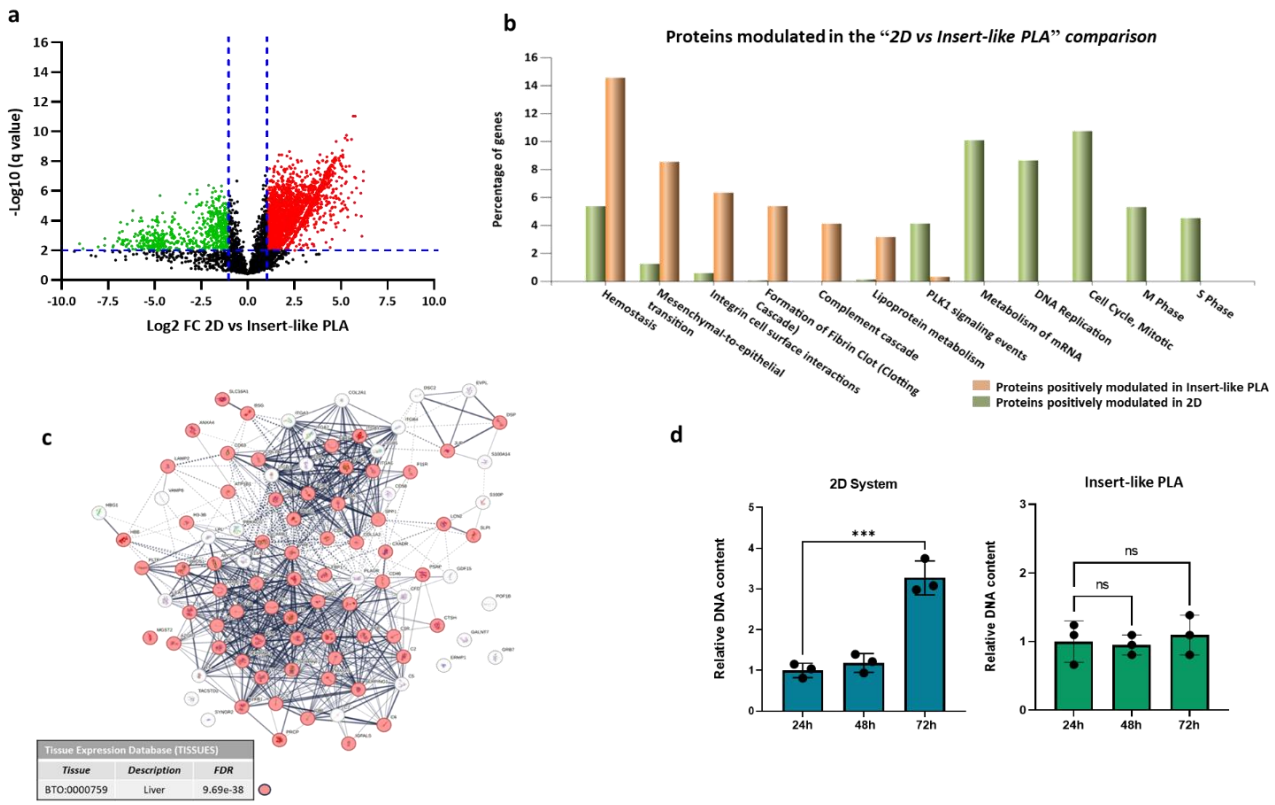

Figure 23 (a) *Volcano plot illustrating the significant protein expression modulation in the comparison "2D vs Insert-like PLA". The vertical and horizontal dashed lines respectively indicate the FC (≥ ±2) and q-value (≤0.05) threshold to consider proteins significantly up-regulated in 2D (red dots) and up-regulated in Insert-like PLA (green dots).* ***(b)*** *The histogram shows Biological Pathway enrichment analysis of the modulated proteins performed by FunRich. Extended data of the analysis is reported in Supplementary Table S4.* ***(c)*** *Network of proteins positively modulated in the Insert-like PLA obtained by String, in which the expression evidence in liver (red nodes) from TISSUES database is visualized. The FDR in the bottom panel refers to the significance of the liver expression enrichment.* ***(d)*** *The Picogreen DNA content assay was performed on cultures of THLE2 cells seeded in 2D system and the Insert-like PLA for 24h, 48h and 72h (n=5). The values reported in the graphs, normalized to DNA level at 24, are the mean ± standard deviation of three independent replicates. *** p≤0.001.*

In the comparison "2D vs HoC", the observed differences in protein expression, although numerically smaller, were functionally similar and overlapped, confirming the pro-differentiating effect of the PLA scaffold. As reported in **Supplementary Table S5**, between the 2D and the HoC systems the 27% of the analysed proteins (1877/6977) were modulated. Among them, as in the previous comparison, both qualitative differences (506 proteins exclusively expressed in cells grown in the 2D system and 115 exclusively expressed in cells grown on HoC system) and significant quantitative differences (867 up-regulated in the 2D system and 389 up-regulated in the HoC system, with fold change ≥ ±2 and q-value ≤ 0.05) were found, as summarized in the volcano plot reported in **Fig. 24a**. The functional analysis of the whole set of the modulated proteins performed by using the FunRich software again highlighted the pro-differentiating effect of the PLA scaffold. Indeed, similarly to that observed in the comparison "2D vs Insert-like PLA", the histogram in **Fig. 24b** shows that the most significantly enriched Biological Pathways (AdjP-Value ≤ 10−4) including the proteins positively modulated in cells grown in the HoC system, were specifically related to liver tissue activities regulated by the hepatocytes (Formation of Fibrin Clot); Complement cascade; Integrin cell surface interactions; Haemostasis), as highlighted by the STRING analysis showed in **Fig. 24c** and by literature evidence [148, 149], while the most significantly enriched Biological Pathways including the proteins positively modulated in cells grown in the 2D system, were related to cell division process (Cell Cycle, Mitotic; M Phase; Phosphorylation of Emi1; Mitotic M-M/G1 phases; DNA Replication). The Venn diagrams in **Fig. 24d-e** summarize the high level of overlapping of the results obtained within the two performed comparison. Furthermore, comparing our results with a dataset of hepatocyte markers

extrapolated from literature data [150, 151], it was interesting to note that over 30% of these markers (42/122).

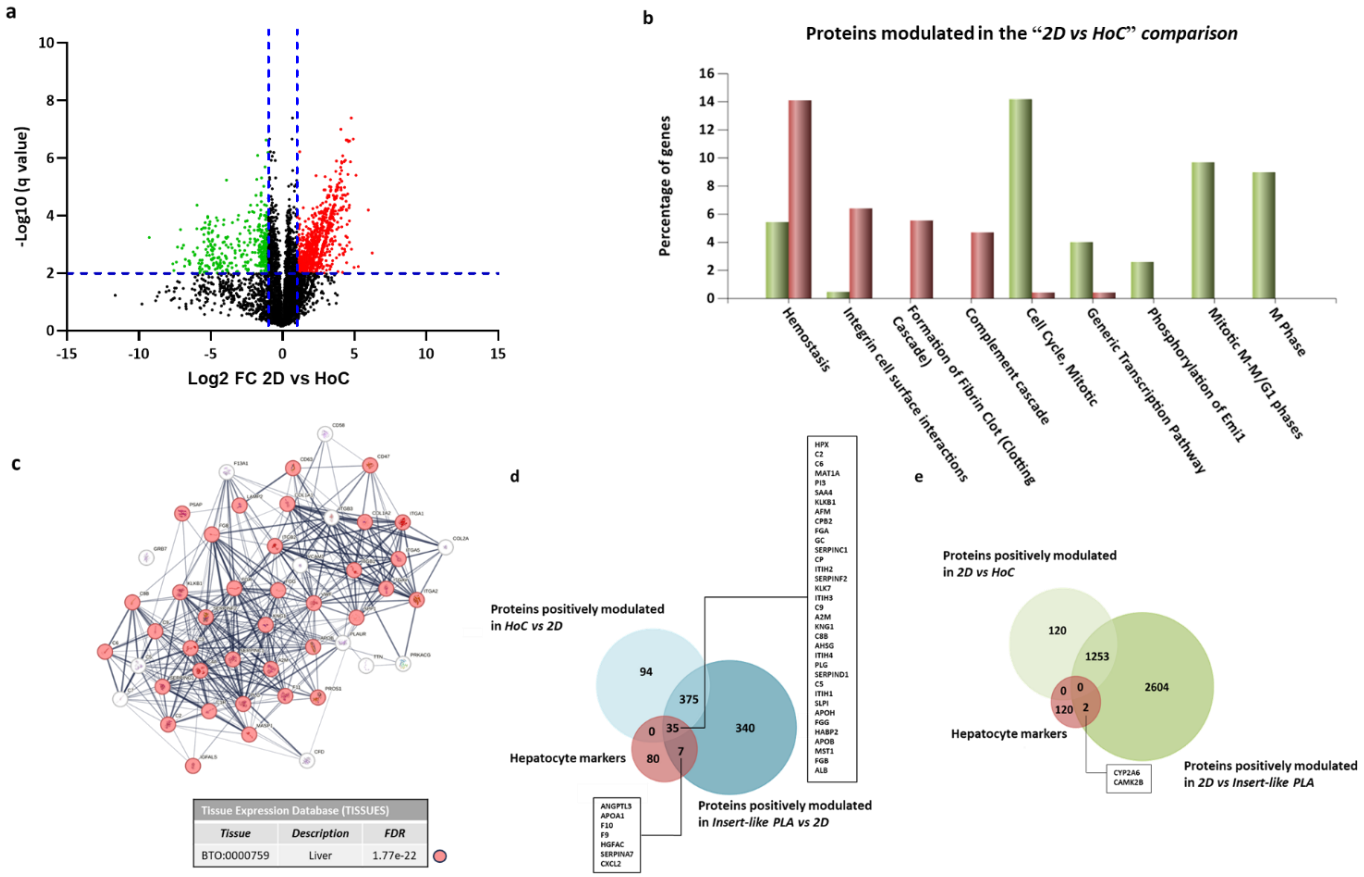

Figure 24 (a) *Volcano plot illustrating the significant protein expression modulation in the comparison "2D vs HoC". The vertical and horizontal dashed lines respectively indicate the FC (≥ ±2) and q-value (≤0.05) threshold to consider proteins significantly up-regulated in 2D (red dots) and up-regulated in HoC (green dots).* ***(b)*** *The histogram shows Biological Pathway enrichment analysis of the modulated proteins performed by FunRich. Extended data of the analysis is provided in Table 4.* ***(c)*** *Network of proteins positively modulated in the HoC obtained by String, in which the expression evidence in liver (red nodes) from TISSUES database is visualized. The FDR in the bottom panel refers to the significance of the liver expression enrichment.* ***(d)*** *Venn diagram showing the overlap among the proteins positively modulated in HoC vs 2D, in Insert-like PLA vs 2D and hepatocyte markers [152];* ***(e)*** *Venn diagram showing the overlap among the proteins positively modulated in 2D vs HoC, in 2D vs Insert-like PLA, and hepatocyte markers [148].*

To validate the proteomic data showing the higher differentiation level of hepatocytes grown on PLA in both static and dynamic condition, we assessed by fluorescence microscopy the expression level of albumin, a relevant hepatic lineage marker [152], found in the proteomic analysis among the proteins mostly up-regulated in cells grown on PLA **(Table in Fig. 25a)**. The representative images reported in **Fig. 25b**, and the relative MFI analysis **(Fig. 25c)** confirmed the increase of albumin expression by hepatocyte grown for 72h on both insert-like PLA and HoC in comparison to the canonical 2D culture. Thus, even if in comparison to the static condition, the differentiative level of THLE2 cells exposed to the dynamic flow was less pronounced, the HoC represents a vantage with respect to the 2D system in supporting the acquisition of the hepatocyte phenotype.

a

Proteomic data of Albumin Expression		
	COMPARISON	
	Insert-like PLA vs 2D	HoC *vs 2D*
Fold Change	16.68007846	9.93041745
q value	0.000103056	0.002923273

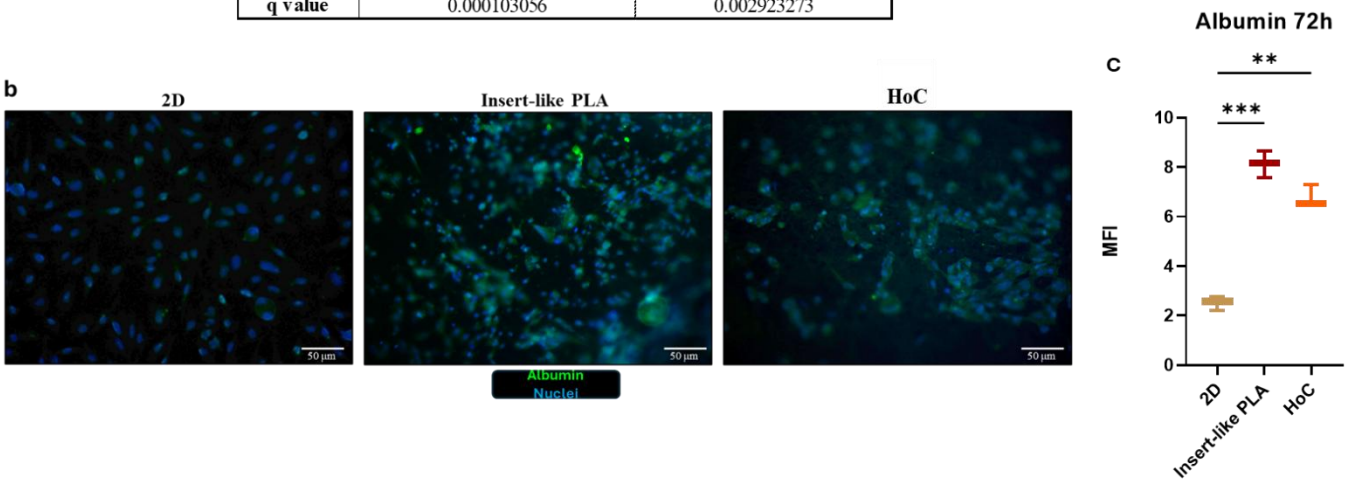

Figure 25 (a) *Table summarizing the proteomic data on Albumin expression. Extended data of the analysis is provided in Supplementary Table S3 and S4* ***(b).*** *Immunofluorescent staining of Albumin in THLE2 cells grown for 72h in the 2D, Insert-like PLA, and HoC systems. Nuclei were stained with Hoechst.* ***(c)****Box and whiskers plot on the right shows the Mean Fluorescence Intensity (MFI) ±SD of Albumin level in 2D, Insert-like PLA and HoC conditions measured with ImageJ Software (**p < 0.01; ***p < 0.001).*

7.7 The HoC as platform to develop a chronic stimulation system: proof of concept

The 2D cell culture systems are still extensively used to maintain the in vitro cell growth. However, it is widely recognized that these methods cannot fully mimic the physiological conditions for the lack of a 3D environment and of continuous and mechanical flow of nutrients or stimulating factors. For example, in the field of the extracellular vesicle (EV) research, the treatment of target cells with single and acute administrations, unavoidable in the 2D cell culture systems, requires biologic active doses of EVs frequently considered too high for their significant lipid load. This is a recurrent controversy emerging during the revision steps for paper publication or grant funding, since it is criticized that cells in their physiological setting are exposed to continuous low concentrations of EVs rather than to acute and high doses that could elicit unspecific response to a stress condition. To solve these problems and challenges, 3D dynamic culture systems could primarily provide a proper platform to develop continuous delivery systems better mimicking the real in vivo exposure of cells and tissue to stimulating factors as the EVs [153]. The pro-metastatic role that EVs released by primary tumours may have in promoting the formation of a microenvironment supporting the tumour cells colonization in the secondary sites (the so-called pre-metastatic niche – PMN –) have gradually attracted interest of cancer researchers [70]. With the purpose to better simulate the in vivo systemic condition in which the PMN formation is due to the chronic exposure of secondary site-resident cells (as hepatocytes in liver) to the EVs released from the primary colorectal cancer (***Fig. 26a***), we develop a HoC system suitable for simulating the EV chronic delivery (***Fig. 26b***). At steady-state conditions, after seeding and allowing the THLE2 cells to adhere in the upper chamber, culture medium containing EVs was introduced into the lower chamber to assess their effect on hepatic cells. The dual-chamber HoC system enables the perfusion of EVs through the lower chamber interacting with the electrospun scaffolds and then with the hepatic cells also due to the slight pressure difference between the chambers. The electrospun scaffold acts as a highly porous barrier to the passage of EVs from the lower to the upper chamber, mimicking the role of the basement membrane, to which hepatocytes adhere *in vivo*. To experimentally validate the diffusion of the EVs through the membrane from the lower to the upper chamber of the HoC where the THLE2 cells were seeded, the EV up-take assay was performed. As shown in ***Fig. 26c***, the PKH

26-labelled SW620_sEVs delivered in the lower chamber after already 4h were found in the upper chamber where colocalized with cells. This observation also indicates that THLE2 cells seeded on PLA can internalize the SW620_sEVs.

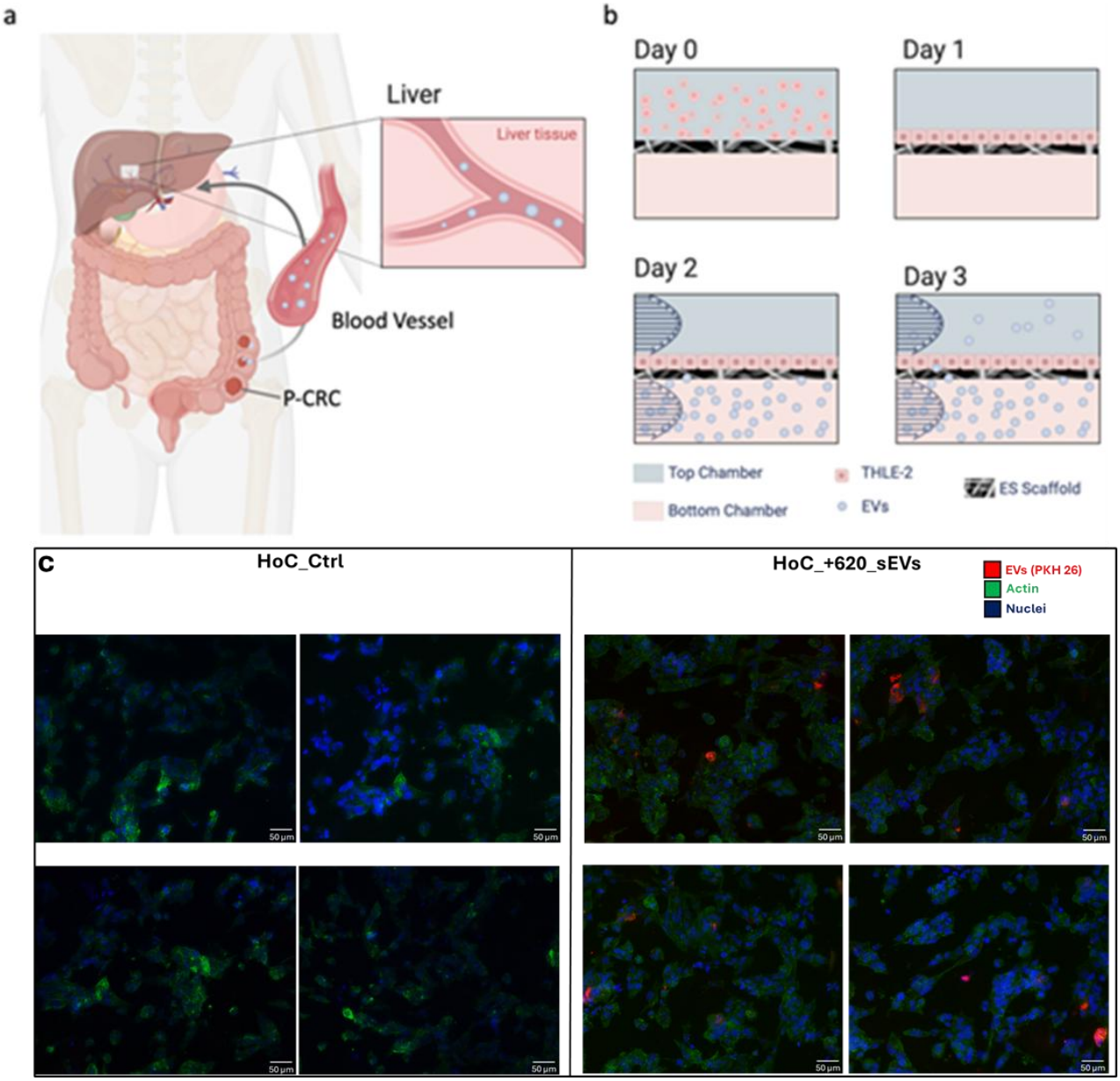

Figure 26 (a) *Schematic representation of the in vivo systemic condition depicting tumor-derived small extracellular vesicles released from the primary colorectal cancer (P-CRC) site and transported via the bloodstream to distant tissues, such as the liver. These EVs contribute to the establishment of the pre-metastatic niche (PMN), acting as key mediators between primary tumors and potential metastatic sites.* ***(b)*** *Schematic timeline of the HoC experiment: hepatocytes seeding on Day 0, adhesion to the PLA scaffold on Day 1, dynamic delivery of culture medium in the top chamber and EVs in the bottom chamber on Day 2, and interaction between sEVs and hepatocytes on Day 3.* ***(c)*** *Uptake assay of PKH 26/SW620_sEVs by THLE2 cells. (scale bar = 50 µM). HoC_Ctrl: untreated cells. For each condition four different fields are shown.*

The potential use of this system was assessed by confirming results obtained in our previous study where we described the ability of the EVs released by cancer colorectal cells SW620 (SW620_sEVs) to activate the EMT of the hepatocytes, as demonstrated by the increase of the mesenchymal markers (Vimentin and a-SMA) and the decrease of the epithelial markers (E-Cadherin, CK8-18) [5]. Similar to these results, here we found that the increase of the expression of Vimentin (red signal) induced by the acute treatment with 20 µg/ml of SW620-EVs for 48h performed in the 2D system [5], was obtained in the HoC system where the whole dose of 20 µg/ml was delivered over a 48h period with a constant flux of 41.7 µl/h (0.830 µg/hour of

SW620_sEVs) (***Fig. 27a-b***). This result suggests that the HoC developed is an effective system for the chronic-low dose delivery of EVs to target cells that can better mimic the real systemic contest in which cells and tissues are exposed to the EVs stimuli, with the purpose to better simulate the in vivo systemic condition in which the PMN.

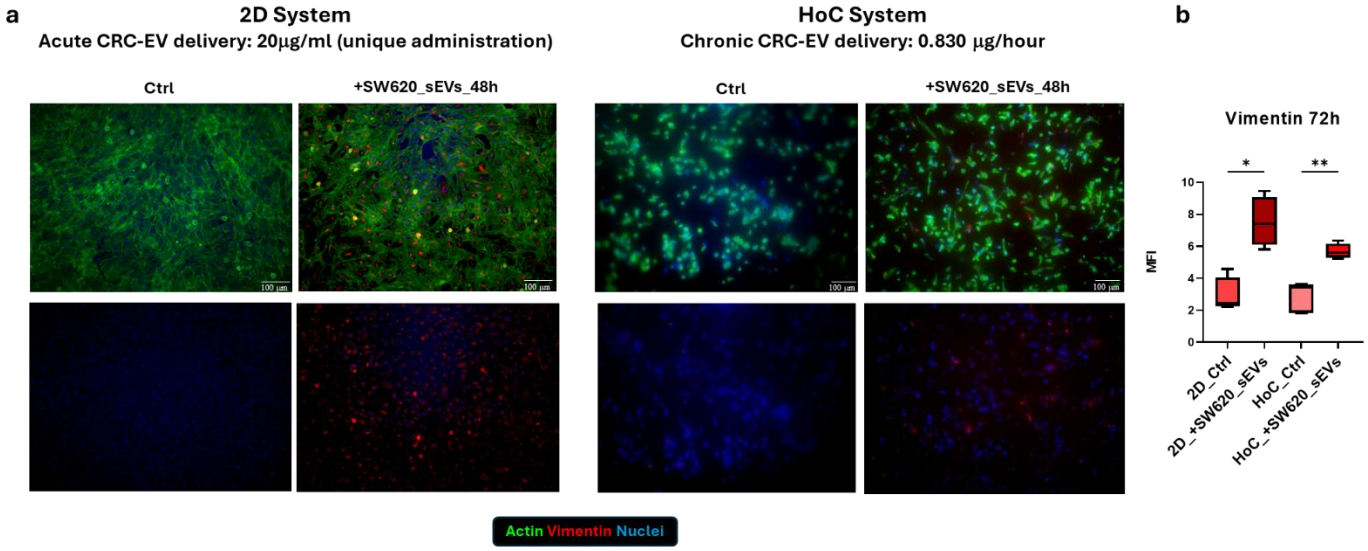

Figure 27 (a) *Fluorescence microscopy images of THLE2 cells grown in 2D system (left panel) and in HoC system (right panel), treated for 48h with 20µg/ml of SW620_sEVs respectively in acute (unique administration) and chronic manner (0.830 µg/hour over 48h). Nuclear staining was performed using Hoescht.* ***(b)*** *Mean Fluorescence Intensity (MFI) ±SD of Vimentin expression in 2D and HoC (Ctrl and + SW620_sEVs) conditions measured with ImageJ Software. (*p ≤ 0.05; **p ≤ 0.01).*

Supplementary Information

Click here to access/download
Supporting Information
Supplementary Table S2.xlsx

Click here to access/download
Supporting Information
Supplementary Table S3.xlsx

Click here to access/download
Supporting Information
Supplementary Table S5.xlsx

CHAPTER 8

CONCLUSIONS

Recent evidence highlighted the role of CRC_sEVs in priming the PMN in the liver, mainly focusing on their role on the non-parenchymal component of the liver, mostly HSC and Kupffer cells, while the involvement of the hepatocytes at this stage has been mostly neglected [4]. Moreover, the role of ncRNAs inside the EVs has gained particular interest, due to their molecular activity on gene expression regulation [154]. In our previous study, we have demonstrated the role of CRC_sEVs in the activation of the EMT program in the hepatocytes, but the subtle molecular alterations underlying this process have not been completely elucidated yet [5]. One of the missing steps in gaining a deeper understanding of the effects of CRC_sEVs on hepatocytes probably lies in the administration "experimental platform". In fact, as previously explained, common acute treatment with the EVs cannot simulate the realistic effect of the vesicles released by primary tumour, since this common methodology, adopted in most of the studies, can elicit unspecific responses in cells, burdening them with significant lipid overload. In this context, OoC devices are emerging as interesting tools for the possibility of co-culturing different cell type and performing prolonged delivery with the CRC_sEVs, reproducing more realistically their effects *in vivo* [155].

For my PhD studies, I have investigated the biological effects induced by CRC_sEVs on the hepatocytes, reporting the role of EV-H19 in the induction of AS mechanism associated with the EMT phenotype, a molecular mechanism often underestimated in literature. H19 could induce in the hepatocytes, acting together with RBFOX2, an AS program, which lead to the formation of splicing variants of different mRNAs strictly associated with the regulation of cell shape and cytoskeleton. Even though further studies still need to be conducted to confirm the association of this AS induction with the establishment of a pro metastatic microenvironment, the data reported highlight their role on H19 in a previously underestimated molecular process. Moreover, in this study I successfully developed a novel Hepatocyte-on-Chip platform composed of laser-patterned poly (methyl methacrylate) layers integrated with an electrospun poly-lactic acid scaffold. This device, designed to investigate the chronic effect of colorectal cancer-derived extracellular vesicles in the formation of pre-metastatic niches in the human liver, demonstrated enhanced hepatocyte differentiation compared to traditional 2D cultures, as revealed by proteomic profiling. Furthermore, dynamic delivery of EVs through the HoC induced epithelial to mesenchymal transition, supporting its application in modelling chronic EV exposure and tumour-liver interactions. This innovative HoC platform addresses limitations of conventional static and 2D culture systems by offering improved material properties, reproducibility, and biomimetic relevance. Overall, this study highlights the HoC as a powerful tool for cancer research, offering new insights into the molecular mechanisms driving metastatic progression and opening pathways for therapeutic advancements.

CHAPTER 9

RESEARCH VISITING

From July to December 2024, I performed my research activities in the "cancer exosome research laboratories" under the supervision of PD Dr. Basant Kumar Thakur, located in the paediatric oncology Department III at Essen University Hospital. I focused my research on different methodologies for isolating EVs from adhesion and suspension cells using a combination of Tangential Flow Filtration (TFF), Size Exclusion Chromatography (SEC), and Ultrafiltration (UF). This combined Isolation method, called from now on TFU (TFF+SEC+UF), was already optimized by the research group and allowed to obtain high purity EVs [156]. After acquiring new skills regarding these Isolation methods, I studied and developed assays for tracking the RNA packaged inside the EVs and follow its delivery to recipient cells, mainly focusing on Imaging techniques, but with possible new applications for immunoprecipitations and pull-down assays in order to gain a deeper knowledge on the interactions between ncRNAs and RBPs inside the EVs.

9.1 EVs Isolation with TFU and Eu signal Optimization

In the previous studies the research group coordinated by Dr. Thakur already demonstrated the role of sEVs derived from acute myeloid leukaemia (AML) in affecting the differentiation of bone marrow-derived mesenchymal stem cells (BM-MSCs), reducing their osteoblastic differentiation [157]. Thakur's research group focused their attention on the DNA and DNA-binding proteins inside TD_sEVs, and how this could affect tumor progression and the possibility to deploy it as a future biomarker. For EVs isolation, the cell supernatant was collected 72 hours after seeding and after differential centrifugations, according to the protocol already established in Kumar Thakur lab [157, 158]. Consistently with the research group already published studies, Fraction 2 and Fraction 3 of the EVs were collected and stored at -80 °C. To study the RNA content inside the vesicles, the EV-progenitor cells were preincubated with 5-Ethynyl-uridine (Eu) (CLK-N002-10, Jena Bioscience). Eu is a uridine analog which can replace uracil (U) and be incorporated into the newly synthesized RNA molecules, it reacts with fluorescent dye or biotin azide, through fluorescence detection or capture and can be used to analyze de novo RNA synthesis in proliferating cells. The resulting ethynyl-functionalized RNA can subsequently be detected via Cu(I)-catalyzed click chemistry that offers the choice to introduce a Biotin group (via Azides of Biotin) for subsequent purification tasks or a fluorescent group (via Azides of fluorescent dyes) for subsequent microscopic imaging. Before applying the protocol, I evaluated the different concentrations of Eu and CuSO4-Copper Protectant needed to catalyze the Click-iT chemistry, in order to reduce the signal background. C2C12 cell line was used for the signal evaluation through the following protocol: after the different incubations for 24h, cells were fixed with 4%PFA for 15 minutes, rinsed three times in PBS, membraned were stained with WGA (Cat. No. W11261, ThermoFisher Scientific) for 20 min, and after three washed with HBSS buffer, Click-iT® RNA Imaging Kits (Cat. no. C10330, Invitrogen) was utilized according to manufacturer's Instructions. Finally, nuclei were stained with dapi, and after three washes in PBS samples were stored at 4 ° overnight and subsequently analysed at confocal microscopy (Zeiss ELYRA PS.1). As shown in ***Figure 28***, among the different

combinations, 10µM of Eu and medium concentration of CuSO4-Copper Protectant were chosen for the Imaging protocols, giving lower signal background compared to the other conditions.

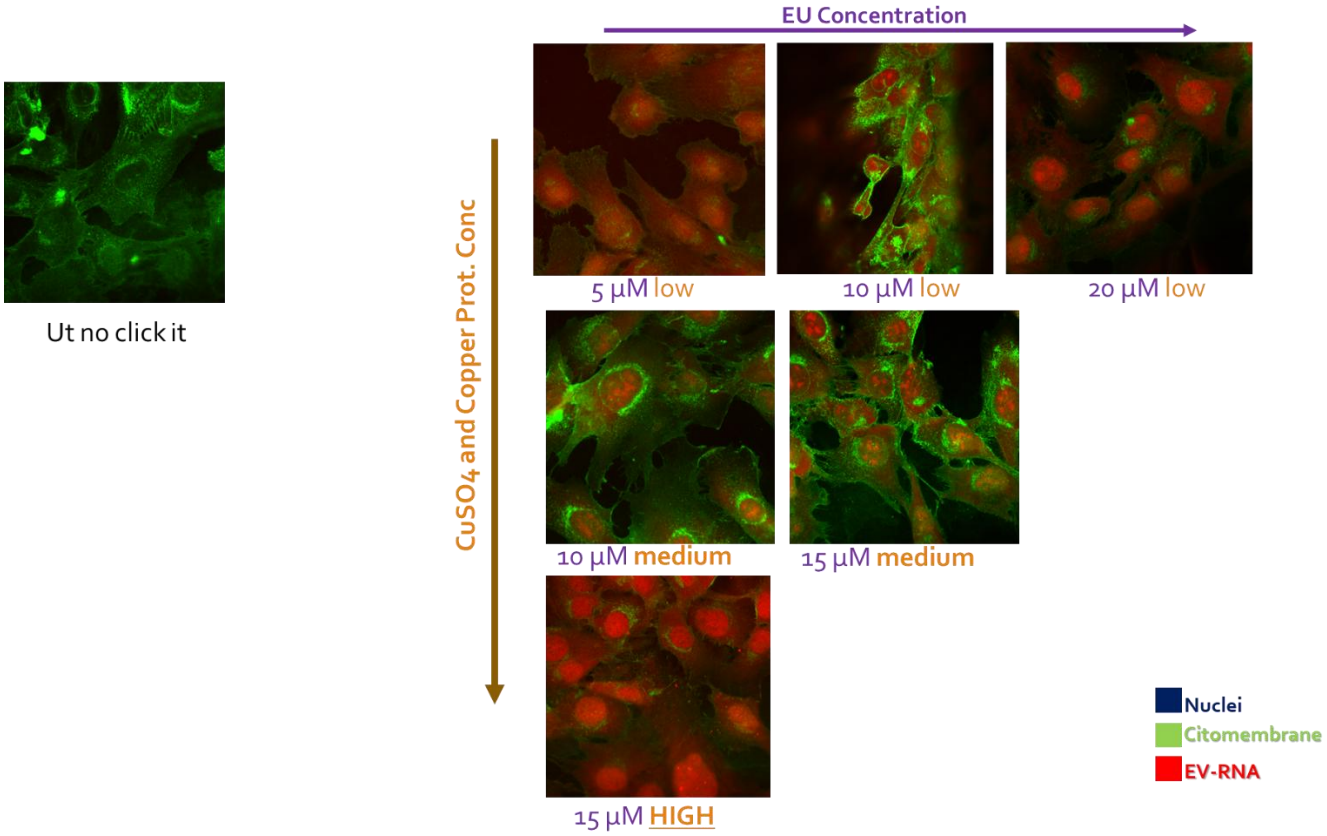

Figure 28 *Confocal Micrographs showing C2C12 cell line stained with Eu and CuSo4 at different concentrations in order evaluate the RNA signal. Eu concentrations: 15µM, 10µM, 5µM. CuSO4 and Copper protectant concentrations: High (8µL+2µL), Medium (6µL+4µL), Low (5µL+5µL). Membrane is shown in red, nuclei in blue.*

9.1 HEK293T and HCT-116 EV isolation and EV-RNA delivery evaluation

Before Isolating the EVs from a CRC cell line as the HCT-116, I evaluated the EV-RNA delivery in two prototypes of EV-releasing and EV-recipient cells, the HEK293T (Cat. No. CRL-3216 ™, ATCC) and Hela cell line (Cat. No. CCL-2 ™ ATCC), respectively. After incubating the HEK293T with medium supplemented with FBS deprived of EVs, the supernatant was collected after 48h with or without the incubation with Eu at the concentration of 10µM. After applying the TFU isolation protocol, the collected EVs were used to treat The Hela at different concentrations, particularly the dose of 30µL/ml of EVs (2,25 x 10^9 particles/ml) and 50 µL/ml (2,25 x 10^9 particles/ml) of Fractions 2 and 3 (F2 and F3), which were found to be extremely enriched in high purity vesicles according to the research group previous studies[156]. After 24h of treatment, cells were fixed as previously described and Click-iT® RNA Imaging Kits (Cat. no. C10330, Invitrogen) was utilized to evaluate the Eu-stained RNA delivered to the recipient cells. As shown in ***Figure 29***, Hela cells educated by sEVs show an increased EV-RNA signal (red).

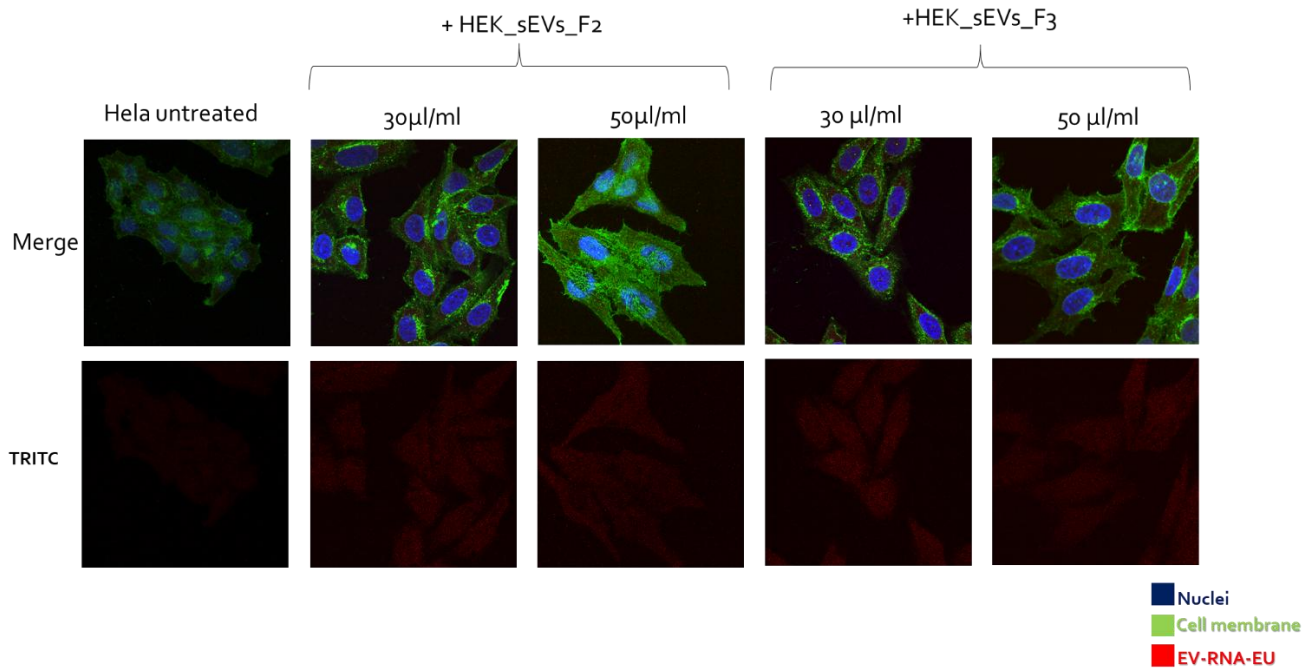

Figure 29 *Confocal Images showing Hela cells treated with two different doses of the single Fractions of the HEK293T_sEVs stained with Eu in order to evaluate the signal relative to the RNA in the sEVs.*

After applying the previously described protocol for culturing the HEK293T, HCT-116_sEVs F2 and F3 were used to treat an Immortalized human fetal liver cell line, the cBAL111 (Cat. numb. ABMT0789 abm). After 24h of treatment, cells were fixed as previously described and Click-iT® RNA Imaging Kits (Cat. no. C10330, Invitrogen) was utilized to evaluate the Eu-stained RNA delivered to the recipient cells. In order to evaluate the Eu signal, cells were also incubated with the Eu to show a positive control of the reaction. As shown in ***Figure 30*****,** the treatment with HCT-116_sEVs could induce an increase in the RNA delivery in the cBAL111.

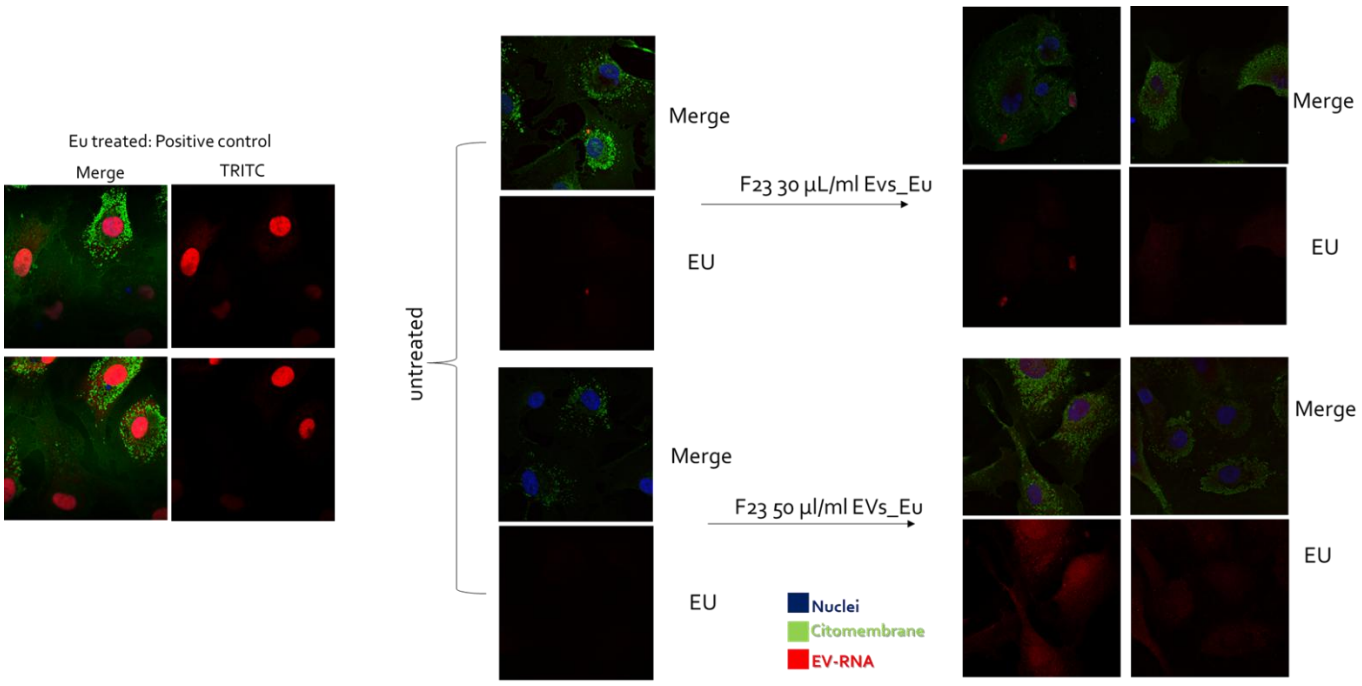

Figure 30 *Confocal micrographs showing cBAL 111 treated with different concentrations of Fraction 2 and 3 of HCT-116_sEVs_Eu stained. Eu treated Positive control: cells incubated only with Eu.*

References

[1] C. Santucci *et al.*, "European cancer mortality predictions for the year 2024 with focus on colorectal cancer," *Annals of Oncology*, vol. 35, no. 3, pp. 308–316, Mar. 2024, doi: 10.1016/j.annonc.2023.12.003.

[2] Y. Li, H. Wang, D. Mao, X. Che, Y. Chen, and Y. Liu, "Understanding pre-metastatic niche formation: implications for colorectal cancer liver metastasis," Dec. 01, 2025, *BioMed Central Ltd*. doi: 10.1186/s12967-025-06328-2.

[3] B. Wang, Z. Tan, and F. Guan, "Tumor-derived exosomes mediate the instability of cadherins and promote tumor progression," Aug. 01, 2019, *MDPI AG*. doi: 10.3390/ijms20153652.

[4] K. A. Paschos, A. W. Majeed, and N. C. Bird, "Natural history of hepatic metastases from colorectal cancer - Pathobiological pathways with clinical significance," *World J Gastroenterol*, vol. 20, no. 14, pp. 3719–3737, 2014, doi: 10.3748/wjg.v20.i14.3719.

[5] M. Pucci *et al.*, "Colorectal cancer-derived small extracellular vesicles induce TGFβ1-mediated epithelial to mesenchymal transition of hepatocytes," *Cancer Cell Int*, vol. 23, no. 1, Dec. 2023, doi: 10.1186/s12935-023-02916-8.

[6] A. Ferro *et al.*, "Extracellular Vesicles as Delivery Vehicles for Non-Coding RNAs: Potential Biomarkers for Chronic Liver Diseases," Mar. 01, 2024, *Multidisciplinary Digital Publishing Institute (MDPI)*. doi: 10.3390/biom14030277.

[7] C. Gu *et al.*, "Technological Advances of 3D Scaffold-Based Stem Cell/Exosome Therapy in Tissues and Organs," Sep. 09, 2021, *Frontiers Media S.A.* doi: 10.3389/fcell.2021.709204.

[8] J. Huang, J. Xiong, L. Yang, J. Zhang, S. Sun, and Y. Liang, "Cell-free exosome-laden scaffolds for tissue repair," *Nanoscale*, vol. 13, no. 19, pp. 8740–8750, May 2021, doi: 10.1039/d1nr01314a.

[9] H. Zhao, R. Jiang, C. Zhang, Z. Feng, and X. Wang, "LncRNA H19-rich extracellular vesicles derived from gastric cancer stem cells facilitate tumorigenicity and metastasis via mediating intratumor communication network," *J Transl Med*, vol. 21, no. 1, Dec. 2023, doi: 10.1186/s12967-023-04055-0.

[10] A. Vilaça *et al.*, "Extracellular vesicle transfer of lncRNA H19 splice variants to cardiac cells," *Mol Ther Nucleic Acids*, vol. 35, no. 3, Sep. 2024, doi: 10.1016/j.omtn.2024.102233.

[11] Y. Xi and P. Xu, "Global colorectal cancer burden in 2020 and projections to 2040," Oct. 01, 2021, *Neoplasia Press, Inc.* doi: 10.1016/j.tranon.2021.101174.

[12] F. A. Haggar and R. P. Boushey, "Colorectal cancer epidemiology: Incidence, mortality, survival, and risk factors," *Clin Colon Rectal Surg*, vol. 22, no. 4, pp. 191–197, 2009, doi: 10.1055/s-0029-1242458.

[13] G. Roshandel, F. Ghasemi-Kebria, and R. Malekzadeh, "Colorectal Cancer: Epidemiology, Risk Factors, and Prevention," Apr. 01, 2024, *Multidisciplinary Digital Publishing Institute (MDPI)*. doi: 10.3390/cancers16081530.

[14] T. Sawicki, M. Ruszkowska, A. Danielewicz, E. Niedźwiedzka, T. Arłukowicz, and K. E. Przybyłowicz, "A review of colorectal cancer in terms of epidemiology, risk factors, development, symptoms and diagnosis," May 01, 2021, *MDPI AG*. doi: 10.3390/cancers13092025.

[15] P. Piña-Sánchez *et al.*, "Cancer Biology, Epidemiology, and Treatment in the 21st Century: Current Status and Future Challenges From a Biomedical Perspective," 2021, *SAGE Publications Ltd*. doi: 10.1177/10732748211038735.

[16] H. T. Nguyen and H. Q. Duong, “The molecular characteristics of colorectal cancer: Implications for diagnosis and therapy (review),” Jul. 01, 2018, *Spandidos Publications*. doi: 10.3892/ol.2018.8679.

[17] C. C. Murphy and T. A. Zaki, “Changing epidemiology of colorectal cancer — birth cohort effects and emerging risk factors,” Jan. 01, 2024, *Nature Research*. doi: 10.1038/s41575-023-00841-9.

[18] R. Marcellinaro *et al.*, “Colorectal Cancer: Current Updates and Future Perspectives,” Jan. 01, 2024, *Multidisciplinary Digital Publishing Institute (MDPI)*. doi: 10.3390/jcm13010040.

[19] L. H. Che *et al.*, “A single-cell atlas of liver metastases of colorectal cancer reveals reprogramming of the tumor microenvironment in response to preoperative chemotherapy,” *Cell Discov*, vol. 7, no. 1, Dec. 2021, doi: 10.1038/s41421-021-00312-y.

[20] M. S. Hossain *et al.*, “Colorectal Cancer: A Review of Carcinogenesis, Global Epidemiology, Current Challenges, Risk Factors, Preventive and Treatment Strategies,” Apr. 01, 2022, *MDPI*. doi: 10.3390/cancers14071732.

[21] J. Engstrand, H. Nilsson, C. Strömberg, E. Jonas, and J. Freedman, “Colorectal cancer liver metastases - a population-based study on incidence, management and survival,” *BMC Cancer*, vol. 18, no. 1, Jan. 2018, doi: 10.1186/s12885-017-3925-x.

[22] T. Shasha, M. Gruijs, and M. van Egmond, “Mechanisms of colorectal liver metastasis development,” Dec. 01, 2022, *Springer Science and Business Media Deutschland GmbH*. doi: 10.1007/s00018-022-04630-6.

[23] J. Guinney *et al.*, “The Consensus Molecular Subtypes of Colorectal Cancer”, doi: 10.7303/syn2623706.

[24] Z. Liu, X. Zhou, and F. Tang, “Epigenetic regulators as the foundation for molecular classification of colorectal cancer,” Jul. 16, 2024. doi: 10.20892/j.issn.2095-3941.2024.0176.

[25] M. Schmitt and F. R. Greten, “The inflammatory pathogenesis of colorectal cancer,” Oct. 01, 2021, *Nature Research*. doi: 10.1038/s41577-021-00534-x.

[26] M. E. Salem, A. Puccini, and J. Tie, “GASTROINTESTINAL CANCER-COLORECTAL AND ANAL Redefining Colorectal Cancer by Tumor Biology,” 2024, doi: 10.1200/EDBK_.

[27] A. M. Khaliq *et al.*, “Refining colorectal cancer classification and clinical stratification through a single-cell atlas,” *Genome Biol*, vol. 23, no. 1, Dec. 2022, doi: 10.1186/s13059-022-02677-z.

[28] A. M. Zaborowski, D. C. Winter, and L. Lynch, “The therapeutic and prognostic implications of immunobiology in colorectal cancer: a review,” Nov. 09, 2021, *Springer Nature*. doi: 10.1038/s41416-021-01475-x.

[29] J. Li, X. Ma, D. Chakravarti, S. Shalapour, and R. A. Depinho, “Genetic and biological hallmarks of colorectal cancer,” 2021, doi: 10.1101/gad.348226.

[30] R. Chandra *et al.*, “The colorectal cancer tumor microenvironment and its impact on liver and lung metastasis,” Dec. 01, 2021, *MDPI*. doi: 10.3390/cancers13246206.

[31] H. Zhou *et al.*, “Colorectal liver metastasis: molecular mechanism and interventional therapy,” Dec. 01, 2022, *Springer Nature*. doi: 10.1038/s41392-022-00922-2.

[32] R. R. Langley and I. J. Fidler, “The seed and soil hypothesis revisited-The role of tumor-stroma interactions in metastasis to different organs,” *Int J Cancer*, vol. 128, no. 11, pp. 2527–2535, Jun. 2011, doi: 10.1002/ijc.26031.

[33] L. Mathot and J. Stenninger, “Behavior of seeds and soil in the mechanism of metastasis: A deeper understanding,” Apr. 2012. doi: 10.1111/j.1349-7006.2011.02195.x.

[34] Y. Wang *et al.*, “Liver metastasis from colorectal cancer: pathogenetic development, immune landscape of the tumour microenvironment and therapeutic approaches,” Dec. 01, 2023, *BioMed Central Ltd*. doi: 10.1186/s13046-023-02729-7.

[35] C. L. Stewart *et al.*, “Cytoreduction for colorectal metastases: liver, lung, peritoneum, lymph nodes, bone, brain. When does it palliate, prolong survival, and potentially cure?,” *Curr Probl Surg*, vol. 55, no. 9, pp. 330–379, Sep. 2018, doi: 10.1067/j.cpsurg.2018.08.004.

[36] A. Cañellas-Socias *et al.*, “Metastatic recurrence in colorectal cancer arises from residual EMP1+ cells,” *Nature*, vol. 611, no. 7936, pp. 603–613, Nov. 2022, doi: 10.1038/s41586-022-05402-9.

[37] M. C. Pavel *et al.*, “The Impact of Molecular Biology in the Seeding, Treatment Choices and Follow-Up of Colorectal Cancer Liver Metastases—A Narrative Review,” Jan. 01, 2023, *MDPI*. doi: 10.3390/ijms24021127.

[38] A. E. Shin, F. G. Giancotti, and A. K. Rustgi, “Metastatic colorectal cancer: mechanisms and emerging therapeutics,” Apr. 01, 2023, *Elsevier Ltd*. doi: 10.1016/j.tips.2023.01.003.

[39] W. Zhao *et al.*, “Emerging mechanisms progress of colorectal cancer liver metastasis,” Dec. 08, 2022, *Frontiers Media S.A.* doi: 10.3389/fendo.2022.1081585.

[40] B. E. Ueberroth, M. Kriss, J. R. Burton, and W. A. Messersmith, “Liver transplantation for colorectal cancer with liver metastases,” Jan. 01, 2025, *Oxford University Press*. doi: 10.1093/oncolo/oyae367.

[41] A. Conigliaro and C. Cicchini, “Exosome-mediated signaling in epithelial to mesenchymal transition and tumor progression,” Jan. 01, 2019, *MDPI*. doi: 10.3390/jcm8010026.

[42] C. Ciardiello, R. Migliorino, A. Leone, and A. Budillon, “Large extracellular vesicles: Size matters in tumor progression,” Feb. 01, 2020, *Elsevier Ltd*. doi: 10.1016/j.cytogfr.2019.12.007.

[43] J. A. Welsh *et al.*, “Minimal information for studies of extracellular vesicles (MISEV2023): From basic to advanced approaches,” *J Extracell Vesicles*, vol. 13, no. 2, Feb. 2024, doi: 10.1002/jev2.12404.

[44] F. Khazaei, L. Rezakhani, M. Alizadeh, E. Mahdavian, and M. Khazaei, “Exosomes and exosome-loaded scaffolds: Characterization and application in modern regenerative medicine,” Feb. 01, 2023, *Elsevier Ltd*. doi: 10.1016/j.tice.2022.102007.

[45] S. Gurung, D. Perocheau, L. Touramanidou, and J. Baruteau, “The exosome journey: from biogenesis to uptake and intracellular signalling,” Dec. 01, 2021, *BioMed Central Ltd*. doi: 10.1186/s12964-021-00730-1.

[46] M. Yáñez-Mó *et al.*, “Biological properties of extracellular vesicles and their physiological functions,” 2015, *Co-Action Publishing*. doi: 10.3402/jev.v4.27066.

[47] Y. Zhang, Y. Liu, H. Liu, and W. H. Tang, “Exosomes: Biogenesis, biologic function and clinical potential,” Feb. 15, 2019, *BioMed Central*. doi: 10.1186/s13578-019-0282-2.

[48] J. Gao, A. Li, J. Hu, L. Feng, L. Liu, and Z. Shen, “Recent developments in isolating methods for exosomes,” Jan. 13, 2023, *Frontiers Media S.A.* doi: 10.3389/fbioe.2022.1100892.

[49] C. Yang, Y. Xue, Y. Duan, C. Mao, and M. Wan, “Extracellular vesicles and their engineering strategies, delivery systems, and biomedical applications,” Jan. 01, 2024, *Elsevier B.V.* doi: 10.1016/j.jconrel.2023.11.057.

[50] N. Dilsiz, “A comprehensive review on recent advances in exosome isolation and characterization: Toward clinical applications,” Dec. 01, 2024, *Neoplasia Press, Inc.* doi: 10.1016/j.tranon.2024.102121.

[51] R. Crescitelli *et al.*, “Subpopulations of extracellular vesicles from human metastatic melanoma tissue identified by quantitative proteomics after optimized isolation,” *J Extracell Vesicles*, vol. 9, no. 1, Jan. 2020, doi: 10.1080/20013078.2020.1722433.

[52] E. R. Abels and X. O. Breakefield, “Introduction to Extracellular Vesicles: Biogenesis, RNA Cargo Selection, Content, Release, and Uptake,” Apr. 01, 2016, *Springer New York LLC*. doi: 10.1007/s10571-016-0366-z.

[53] R. J. Simpson, H. Kalra, and S. Mathivanan, “Exocarta as a resource for exosomal research,” *J Extracell Vesicles*, vol. 1, no. 1, 2012, doi: 10.3402/jev.v1i0.18374.

[54] S. V. Chitti *et al.*, “Vesiclepedia 2024:ãn extracellular vesiclesãnd extrãcellular par ticles reposit ory,” *Nucleic Acids Res*, vol. 52, no. D1, pp. D1694–D1698, Jan. 2024, doi: 10.1093/nar/gkad1007.

[55] M. I. Sandira *et al.*, “Nanoscopic Profiling of Small Extracellular Vesicles via High-Speed Atomic Force Microscopy (HS-AFM) Videography,” *J Extracell Vesicles*, vol. 14, no. 4, Apr. 2025, doi: 10.1002/jev2.70050.

[56] T. Skotland, K. Sagini, K. Sandvig, and A. Llorente, “An emerging focus on lipids in extracellular vesicles,” Jan. 01, 2020, *Elsevier B.V.* doi: 10.1016/j.addr.2020.03.002.

[57] S. Ghadami and K. Dellinger, “The lipid composition of extracellular vesicles: applications in diagnostics and therapeutic delivery,” 2023, *Frontiers Media SA*. doi: 10.3389/fmolb.2023.1198044.

[58] R. C. Lai and S. K. Lim, “Membrane lipids define small extracellular vesicle subtypes secreted by mesenchymal stromal cells,” 2019, *American Society for Biochemistry and Molecular Biology Inc.* doi: 10.1194/jlr.R087411.

[59] J. Ghanam, V. K. Chetty, L. Barthel, D. Reinhardt, P. F. Hoyer, and B. K. Thakur, “DNA in extracellular vesicles: from evolution to its current application in health and disease,” Dec. 01, 2022, *BioMed Central Ltd*. doi: 10.1186/s13578-022-00771-0.

[60] J. Elzanowska, C. Semira, and B. Costa-Silva, “DNA in extracellular vesicles: biological and clinical aspects,” Jun. 01, 2021, *John Wiley and Sons Ltd*. doi: 10.1002/1878-0261.12777.

[61] H. Shi *et al.*, “Exosomal non-coding RNAs: Emerging insights into therapeutic potential and mechanisms in bone healing,” Jan. 01, 2024, *SAGE Publications Ltd*. doi: 10.1177/20417314241286606.

[62] Y. Qiu, P. Li, Z. Zhang, and M. Wu, “Insights Into Exosomal Non-Coding RNAs Sorting Mechanism and Clinical Application,” Apr. 27, 2021, *Frontiers Media S.A.* doi: 10.3389/fonc.2021.664904.

[63] C. Corrado, M. M. Barreca, C. Zichittella, R. Alessandro, and A. Conigliaro, “Molecular mediators of rna loading into extracellular vesicles,” Dec. 01, 2021, *MDPI*. doi: 10.3390/cells10123355.

[64] S. Yang and X. Li, “Recent advances in extracellular vesicles enriched with non-coding RNAs related to cancers,” Mar. 01, 2018, *Chongqing University*. doi: 10.1016/j.gendis.2017.12.001.

[65] M. Samuels, W. Jones, B. Towler, C. Turner, S. Robinson, and G. Giamas, “The role of non-coding RNAs in extracellular vesicles in breast cancer and their diagnostic implications,” Oct. 06, 2023, *Springer Nature*. doi: 10.1038/s41388-023-02827-y.

[66] H. Yao *et al.*, “Extracellular vesicle-packaged lncRNA from cancer-associated fibroblasts promotes immune evasion by downregulating HLA-A in pancreatic cancer,” *J Extracell Vesicles*, vol. 13, no. 7, Jul. 2024, doi: 10.1002/jev2.12484.

[67] S. Rahmati, A. Moeinafshar, and N. Rezaei, “The multifaceted role of extracellular vesicles (EVs) in colorectal cancer: metastasis, immune suppression, therapy resistance, and autophagy crosstalk,” Dec. 01, 2024, *BioMed Central Ltd*. doi: 10.1186/s12967-024-05267-8.

[68] K. Lin *et al.*, “Comprehensive proteomic profiling of serum extracellular vesicles in patients with colorectal liver metastases identifies a signature for non-invasive risk stratification and early-response evaluation,” Dec. 01, 2022, *BioMed Central Ltd*. doi: 10.1186/s12943-022-01562-4.

[69] A. Kogure, Y. Yoshioka, and T. Ochiya, “Extracellular vesicles in cancer metastasis: Potential as therapeutic targets and materials,” Jun. 23, 2020, *MDPI AG*. doi: 10.3390/ijms21124463.

[70] X. Yang *et al.*, “Colorectal cancer-derived extracellular vesicles induce liver premetastatic immunosuppressive niche formation to promote tumor early liver metastasis,” Dec. 01, 2023, *Springer Nature*. doi: 10.1038/s41392-023-01384-w.

[71] L. M. Channon *et al.*, “Small extracellular vesicles (exosomes) and their cargo in pancreatic cancer: Key roles in the hallmarks of cancer,” May 01, 2022, *Elsevier B.V.* doi: 10.1016/j.bbcan.2022.188728.

[72] Z. Zhou *et al.*, “Extracellular vesicles activated cancer-associated fibroblasts promote lung cancer metastasis through mitophagy and mtDNA transfer,” *Journal of Experimental and Clinical Cancer Research*, vol. 43, no. 1, Dec. 2024, doi: 10.1186/s13046-024-03077-w.

[73] E. Willms, C. Cabañas, I. Mäger, M. J. A. Wood, and P. Vader, “Extracellular vesicle heterogeneity: Subpopulations, isolation techniques, and diverse functions in cancer progression,” Apr. 30, 2018, *Frontiers Media S.A.* doi: 10.3389/fimmu.2018.00738.

[74] L. M. Desrochers, M. A. Antonyak, and R. A. Cerione, “Extracellular Vesicles: Satellites of Information Transfer in Cancer and Stem Cell Biology,” May 23, 2016, *Cell Press*. doi: 10.1016/j.devcel.2016.04.019.

[75] D. M. Hermann, W. Xin, M. Bähr, B. Giebel, and T. R. Doeppner, “Emerging roles of extracellular vesicle-associated non-coding RNAs in hypoxia: Insights from cancer, myocardial infarction and ischemic stroke,” 2022, *Ivyspring International Publisher*. doi: 10.7150/thno.73931.

[76] Q. Dong, X. Liu, K. Cheng, J. Sheng, J. Kong, and T. Liu, “Pre-metastatic Niche Formation in Different Organs Induced by Tumor Extracellular Vesicles,” Sep. 20, 2021, *Frontiers Media S.A.* doi: 10.3389/fcell.2021.733627.

[77] J. Zhou *et al.*, “Targeting circ-0034880-enriched tumor extracellular vesicles to impede SPP1highCD206+ pro-tumor macrophages mediated pre-metastatic niche formation in colorectal cancer liver metastasis,” *Mol Cancer*, vol. 23, no. 1, Dec. 2024, doi: 10.1186/s12943-024-02086-9.

[78] B. Ormseth, A. Onuma, H. Zhang, and A. Tsung, “The Hepatic Pre-Metastatic Niche,” Aug. 01, 2022, *MDPI*. doi: 10.3390/cancers14153731.

[79] L. Kotelevets and E. Chastre, “Extracellular Vesicles in Colorectal Cancer: From Tumor Growth and Metastasis to Biomarkers and Nanomedications,” Feb. 01, 2023, *MDPI*. doi: 10.3390/cancers15041107.

[80] J. S. Mattick *et al.*, “Long non-coding RNAs: definitions, functions, challenges and recommendations,” *Nat Rev Mol Cell Biol*, vol. 24, no. 6, pp. 430–447, Jun. 2023, doi: 10.1038/s41580-022-00566-8.

[81] X. Zhang *et al.*, “Mechanisms and functions of long non-coding RNAs at multiple regulatory levels,” Nov. 02, 2019, *MDPI AG*. doi: 10.3390/ijms20225573.

[82] M. Sebastian-Delacruz, I. Gonzalez-Moro, A. Olazagoitia-Garmendia, A. Castellanos-Rubio, and I. Santin, “non-coding RNA The Role of lncRNAs in Gene Expression Regulation through mRNA Stabilization,” 2021, doi: 10.3390/ncrna.

[83] F. P. Marchese, I. Raimondi, and M. Huarte, “The multidimensional mechanisms of long noncoding RNA function,” Oct. 31, 2017, *BioMed Central Ltd.* doi: 10.1186/s13059-017-1348-2.

[84] R. Z. He, D. X. Luo, and Y. Y. Mo, “Emerging roles of lncRNAs in the post-transcriptional regulation in cancer,” Mar. 01, 2019, *Chongqing University*. doi: 10.1016/j.gendis.2019.01.003.

[85] S. Zhao *et al.*, “LncRNA MIR17HG promotes colorectal cancer liver metastasis by mediating a glycolysis-associated positive feedback circuit,” *Oncogene*, vol. 40, no. 28, pp. 4709–4724, Jul. 2021, doi: 10.1038/s41388-021-01859-6.

[86] G. Pisignano and M. Ladomery, “Epigenetic regulation of alternative splicing: How lncrnas tailor the message,” 2021, *MDPI AG*. doi: 10.3390/ncrna7010021.

[87] X. Wang *et al.*, “Mechanisms of non-coding RNA-modulated alternative splicing in cancer,” 2022, *Taylor and Francis Ltd.* doi: 10.1080/15476286.2022.2062846.

[88] J. Ouyang *et al.*, “Long non-coding RNAs are involved in alternative splicing and promote cancer progression,” May 03, 2022, *Springer Nature*. doi: 10.1038/s41416-021-01600-w.

[89] I. Gonzalez *et al.*, “A lncRNA regulates alternative splicing via establishment of a splicing-specific chromatin signature,” *Nat Struct Mol Biol*, vol. 22, no. 5, pp. 370–376, May 2015, doi: 10.1038/nsmb.3005.

[90] D. Ranieri, B. Rosato, M. Nanni, A. Magenta, F. Belleudi, and M. R. Torrisi, “Expression of the FGFR2 mesenchymal splicing variant in epithelial cells drives epithelial-mesenchymal transition.” [Online]. Available: www.impactjournals.com/oncotarget

[91] M. Hashemi *et al.*, “Long non-coding RNA (lncRNA) H19 in human cancer: From proliferation and metastasis to therapy,” Oct. 01, 2022, *Academic Press*. doi: 10.1016/j.phrs.2022.106418.

[92] X. Zhang *et al.*, “The role of lncRNA H19 in tumorigenesis and drug resistance of human Cancers,” Sep. 27, 2022, *Frontiers Media S.A.* doi: 10.3389/fgene.2022.1005522.

[93] E. Raveh, I. J. Matouk, M. Gilon, and A. Hochberg, “The H19 Long non-coding RNA in cancer initiation, progression and metastasis - a proposed unifying theory,” Nov. 04, 2015, *BioMed Central Ltd.* doi: 10.1186/s12943-015-0458-2.

[94] I. J. Matouk, D. Halle, E. Raveh, M. Gilon, V. Sorin, and A. Hochberg, “Oncotarget 3748 www.impactjournals.com/oncotarget The role of the oncofetal H19 lncRNA in tumor metastasis: orchestrating the EMT-MET decision.” [Online]. Available: www.impactjournals.com/oncotarget/

[95] R. Kalluri and R. A. Weinberg, “The basics of epithelial-mesenchymal transition,” Jun. 01, 2009. doi: 10.1172/JCI39104.

[96] T. Chen, Y. You, H. Jiang, and Z. Z. Wang, “Epithelial–mesenchymal transition (EMT): A biological process in the development, stem cell differentiation, and tumorigenesis,” Dec. 01, 2017, *Wiley-Liss Inc.* doi: 10.1002/jcp.25797.

[97] P. Nisticò, M. J. Bissell, and D. C. Radisky, “Epithelial-mesenchymal transition: General principles and pathological relevance with special emphasis on the role of matrix metalloproteinases,” *Cold Spring Harb Perspect Biol*, vol. 4, no. 2, Feb. 2012, doi: 10.1101/cshperspect.a011908.

[98] J. Yang *et al.*, “Guidelines and definitions for research on epithelial–mesenchymal transition,” Jun. 01, 2020, *Nature Research*. doi: 10.1038/s41580-020-0237-9.

[99] B. Wu *et al.*, “Long Noncoding RNA H19: A Novel Therapeutic Target Emerging in Oncology Via Regulating Oncogenic Signaling Pathways,” Dec. 16, 2021, *Frontiers Media S.A.* doi: 10.3389/fcell.2021.796740.

[100] Y. Xia *et al.*, “Long noncoding RNA H19: functions and mechanisms in regulating programmed cell death in cancer,” Dec. 01, 2024, *Springer Nature*. doi: 10.1038/s41420-024-01832-8.

[101] Z. Huang *et al.*, "H19 Promotes HCC Bone Metastasis Through Reducing Osteoprotegerin Expression in a Protein Phosphatase 1 Catalytic Subunit Alpha/p38 Mitogen-Activated Protein Kinase-Dependent Manner and Sponging microRNA 200b-3p," *Hepatology*, vol. 74, no. 1, p. 2021, 2020, doi: 10.1002/hep.31673/suppinfo.

[102] P. R. Chowdhury, S. Salvamani, B. Gunasekaran, H. B. Peng, and V. Ulaganathan, "H19: An Oncogenic Long Non-coding RNA in Colorectal Cancer," 2023.

[103] J. Xie, Y. Hu, D. Sun, C. Liu, Z. Li, and J. Zhu, "Targeting non-coding RNA H19: A potential therapeutic approach in pulmonary diseases," Sep. 16, 2022, *Frontiers Media S.A.* doi: 10.3389/fphar.2022.978151.

[104] L. Saieva *et al.*, "Hypoxia-induced MiR-675-5p supports β-catenin nuclear localization by regulating GSK3-β activity in colorectal cancer cell lines," *Int J Mol Sci*, vol. 21, no. 11, Jun. 2020, doi: 10.3390/ijms21113832.

[105] A. Conigliaro *et al.*, "CD90+ liver cancer cells modulate endothelial cell phenotype through the release of exosomes containing H19 lncRNA," *Mol Cancer*, vol. 14, no. 1, Aug. 2015, doi: 10.1186/s12943-015-0426-x.

[106] C. Poulet *et al.*, "Molecular Sciences Exosomal Long Non-Coding RNAs in Lung Diseases", doi: 10.3390/ijms21100000.

[107] X. Wang *et al.*, "Exosome-mediated transfer of long noncoding RNA H19 induces doxorubicin resistance in breast cancer," *J Cell Physiol*, vol. 235, no. 10, pp. 6896–6904, Oct. 2020, doi: 10.1002/jcp.29585.

[108] Y. Song, N. Guo, F. Zi, J. Zheng, and J. Cheng, "lncRNA H19 plays a role in multiple myeloma via interacting with hnRNPA2B1 to stabilize BET proteins by targeting osteoclasts and osteoblasts," *Int Immunopharmacol*, vol. 142, Dec. 2024, doi: 10.1016/j.intimp.2024.113080.

[109] R. Liu *et al.*, "Cholangiocyte-Derived Exosomal Long Noncoding RNA H19 Promotes Hepatic Stellate Cell Activation and Cholestatic Liver Fibrosis," *Hepatology*, vol. 70, no. 4, pp. 1317–1335, Oct. 2019, doi: 10.1002/hep.30662.

[110] M. Ismail *et al.*, "Dynamic role of exosomal long non-coding RNA in liver diseases: pathogenesis and diagnostic aspects," Dec. 01, 2024, *Springer*. doi: 10.1007/s12072-024-10722-1.

[111] J. Zhang *et al.*, "A Transforming Growth Factor-β and H19 Signaling Axis in Tumor-Initiating Hepatocytes That Regulates Hepatic Carcinogenesis," *Hepatology*, vol. 69, no. 4, pp. 1549–1563, Apr. 2019, doi: 10.1002/hep.30153.

[112] D. Singh, A. Mathur, S. Arora, S. Roy, and N. Mahindroo, "Journey of organ on a chip technology and its role in future healthcare scenario," *Applied Surface Science Advances*, vol. 9, Jun. 2022, doi: 10.1016/j.apsadv.2022.100246.

[113] P. L. Candarlioglu *et al.*, "Organ-on-a-chip: current gaps and future directions," *Biochem Soc Trans*, vol. 50, no. 2, pp. 665–673, Apr. 2022, doi: 10.1042/BST20200661.

[114] H. Kimura, Y. Sakai, and T. Fujii, "Organ/body-on-a-chip based on microfluidic technology for drug discovery," Feb. 01, 2018, *Japanese Society for the Study of Xenobiotics*. doi: 10.1016/j.dmpk.2017.11.003.

[115] N. Azizipour, R. Avazpour, D. H. Rosenzweig, M. Sawan, and A. Ajji, "Evolution of biochip technology: A review from lab-on-a-chip to organ-on-a-chip," *Micromachines (Basel)*, vol. 11, no. 6, pp. 1–15, Jun. 2020, doi: 10.3390/mi11060599.

[116] M. C. Koyilot *et al.*, "Breakthroughs and Applications of Organ-on-a-Chip Technology," Jun. 01, 2022, *MDPI*. doi: 10.3390/cells11111828.

[117] M. Mendes *et al.*, “Organ-on-a-chip: Quo vademus? Applications and regulatory status,” May 01, 2025, *Elsevier B.V.* doi: 10.1016/j.colsurfb.2025.114507.

[118] Q. Wu *et al.*, “Organ-on-a-chip: Recent breakthroughs and future prospects,” Feb. 12, 2020, *BioMed Central Ltd.* doi: 10.1186/s12938-020-0752-0.

[119] A. Aazmi *et al.*, “Engineered Vasculature for Organ-on-a-Chip Systems,” Feb. 01, 2022, *Elsevier Ltd*. doi: 10.1016/j.eng.2021.06.020.

[120] S. K. Srivastava, G. W. Foo, N. Aggarwal, and M. W. Chang, “Organ-on-chip technology: Opportunities and challenges,” Jan. 01, 2024, *KeAi Communications Co.* doi: 10.1016/j.biotno.2024.01.001.

[121] J. Deng *et al.*, “Engineered liver-on-a-chip platform to mimic liver functions and its biomedical applications: A review,” Oct. 01, 2019, *MDPI AG*. doi: 10.3390/mi10100676.

[122] Z. Yang, X. Liu, E. M. Cribbin, A. M. Kim, J. J. Li, and K. T. Yong, “Liver-on-a-chip: Considerations, advances, and beyond,” Dec. 01, 2022, *American Institute of Physics Inc.* doi: 10.1063/5.0106855.

[123] V. Mehta, G. Karnam, and V. Madgula, “Liver-on-chips for drug discovery and development,” Aug. 01, 2024, *Elsevier B.V.* doi: 10.1016/j.mtbio.2024.101143.

[124] H. Liu *et al.*, “Standard: human liver-on-a-chip,” Dec. 01, 2025, *Springer*. doi: 10.1186/s13619-025-00226-0.

[125] S. Kawakita *et al.*, “Rapid integration of screen-printed electrodes into thermoplastic organ-on-a-chip devices for real-time monitoring of trans-endothelial electrical resistance,” *Biomed Microdevices*, vol. 25, no. 4, p. 37, 2023.

[126] O. R. F. Mook, J. Van Marie, R. Jonges, H. Vreeling-Sindelarova, W. M. Frederiks, and C. J. F. Van Noorden, “Interactions between colon cancer cells and hepatocytes in rats in relation to metastasis,” *J Cell Mol Med*, vol. 12, no. 5B, pp. 2052–2061, Oct. 2008, doi: 10.1111/j.1582-4934.2008.00242.x.

[127] F. Lopresti *et al.*, “Effect of Polyhydroxyalkanoate (PHA) Concentration on Polymeric Scaffolds Based on Blends of Poly-L-Lactic Acid (PLLA) and PHA Prepared via Thermally Induced Phase Separation (TIPS),” *Polymers (Basel)*, vol. 14, no. 12, Jun. 2022, doi: 10.3390/polym14122494.

[128] Q. Feng *et al.*, “Engineering the cellular mechanical microenvironment to regulate stem cell chondrogenesis: Insights from a microgel model,” *Acta Biomater*, vol. 113, pp. 393–406, Sep. 2020, doi: 10.1016/j.actbio.2020.06.046.

[129] M. Tweedie and P. D. Maguire, “Microfluidic ratio metering devices fabricated in PMMA by CO2 laser,” *Microsystem Technologies*, vol. 27, no. 1, pp. 47–58, Jan. 2021, doi: 10.1007/s00542-020-04902-w.

[130] F. Lopresti, I. Keraite, A. E. Ongaro, N. M. Howarth, V. La Carrubba, and M. Kersaudy-Kerhoas, “Engineered membranes for residual cell trapping on microfluidic blood plasma separation systems. A comparison between porous and nanofibrous membranes,” *Membranes (Basel)*, vol. 11, no. 9, Sep. 2021, doi: 10.3390/membranes11090680.

[131] G. Varnavides, M. Madern, D. Anrather, N. Hartl, W. Reiter, and M. Hartl, “In Search of a Universal Method: A Comparative Survey of Bottom-Up Proteomics Sample Preparation Methods,” *J Proteome Res*, vol. 21, no. 10, pp. 2397–2411, Oct. 2022, doi: 10.1021/acs.jproteome.2c00265.

[132] J. Rappsilber, Y. Ishihama, and M. Mann, “Stop And Go Extraction tips for matrix-assisted laser desorption/ionization, nanoelectrospray, and LC/MS sample pretreatment in proteomics,” *Anal Chem*, vol. 75, no. 3, pp. 663–670, Feb. 2003, doi: 10.1021/ac026117i.

[133] N. Prianichnikov *et al.*, “Maxquant software for ion mobility enhanced shotgun proteomics,” *Molecular and Cellular Proteomics*, vol. 19, no. 6, pp. 1058–1069, Mar. 2020, doi: 10.1074/mcp.TIR119.001720.

[134] P. Fonseka, M. Pathan, S. V. Chitti, T. Kang, and S. Mathivanan, “FunRich enables enrichment analysis of OMICs datasets,” *J Mol Biol*, vol. 433, no. 11, May 2021, doi: 10.1016/j.jmb.2020.166747.

[135] O. Palasca, A. Santos, C. Stolte, J. Gorodkin, and L. J. Jensen, “TISSUES 2.0: an integrative web resource on mammalian tissue expression,” *Database*, vol. 2018, p. bay003, 2018.

[136] O. Schillaci *et al.*, “Exosomes from metastatic cancer cells transfer amoeboid phenotype to non-metastatic cells and increase endothelial permeability: Their emerging role in tumor heterogeneity,” *Sci Rep*, vol. 7, no. 1, Dec. 2017, doi: 10.1038/s41598-017-05002-y.

[137] A. Cordaro *et al.*, “Regulatory role of lncH19 in RAC1 alternative splicing: implication for RAC1B expression in colorectal cancer,” *Journal of Experimental and Clinical Cancer Research*, vol. 43, no. 1, Dec. 2024, doi: 10.1186/s13046-024-03139-z.

[138] J. P. Venables *et al.*, “RBFOX2 Is an Important Regulator of Mesenchymal Tissue-Specific Splicing in both Normal and Cancer Tissues,” *Mol Cell Biol*, vol. 33, no. 2, pp. 396–405, Jan. 2013, doi: 10.1128/mcb.01174-12.

[139] P. J. Gardina *et al.*, “Alternative splicing and differential gene expression in colon cancer detected by a whole genome exon array,” *BMC Genomics*, vol. 7, 2006, doi: 10.1186/1471-2164-7-325.

[140] F. Di Modugno *et al.*, “Splicing program of human MENA produces a previously undescribed isoform associated with invasive, mesenchymal-like breast tumors,” *Proc Natl Acad Sci U S A*, vol. 109, no. 47, pp. 19280–19285, Nov. 2012, doi: 10.1073/pnas.1214394109.

[141] D. Zhou, S. Couture, M. S. Scott, and S. Abou Elela, “RBFOX2 alters splicing outcome in distinct binding modes with multiple protein partners,” *Nucleic Acids Res*, vol. 49, no. 14, pp. 8370–8383, Aug. 2021, doi: 10.1093/nar/gkab595.

[142] S. C. Tao, J. Y. Huang, Z. X. Li, S. Zhan, and S. C. Guo, “Small extracellular vesicles with LncRNA H19 ‘overload’: YAP Regulation as a Tendon Repair Therapeutic Tactic,” *iScience*, vol. 24, no. 3, Mar. 2021, doi: 10.1016/j.isci.2021.102200.

[143] C. Zichittella *et al.*, “Long non-coding RNA H19 enhances the pro-apoptotic activity of ITF2357 (a histone deacetylase inhibitor) in colorectal cancer cells,” *Front Pharmacol*, vol. 14, 2023, doi: 10.3389/fphar.2023.1275833.

[144] W.-C. Liang *et al.*, “The lncRNA H19 promotes epithelial to mesenchymal transition by functioning as miRNA sponges in colorectal cancer.” [Online]. Available: www.impactjournals.com/oncotarget

[145] S. Kaja, A. J. Payne, Y. Naumchuk, and P. Koulen, “Quantification of lactate dehydrogenase for cell viability testing using cell lines and primary cultured astrocytes,” *Curr Protoc Toxicol*, vol. 2017, pp. 1–10, May 2017, doi: 10.1002/cptx.21.

[146] Z. Heydari *et al.*, “Standard Protocols for Characterising Primary and In Vitro-Generated Human Hepatocytes,” Feb. 01, 2025, *John Wiley and Sons Inc*. doi: 10.1111/jcmm.70390.

[147] R. J. Schulze, M. B. Schott, C. A. Casey, P. L. Tuma, and M. A. McNiven, “The cell biology of the hepatocyte: A membrane trafficking machine,” 2019, *Rockefeller University Press*. doi: 10.1083/jcb.201903090.

[148] S. Ruijtenberg and S. van den Heuvel, “Coordinating cell proliferation and differentiation: Antagonism between cell cycle regulators and cell type-specific gene expression,” Jan. 17, 2016, *Taylor and Francis Inc.* doi: 10.1080/15384101.2015.1120925.

[149] A. Asai *et al.*, “Paracrine signals regulate human liver organoid maturation from induced pluripotent stem cells,” *Development (Cambridge)*, vol. 144, no. 6, pp. 1056–1064, Mar. 2017, doi: 10.1242/dev.142794.

[150] S. J. Mun *et al.*, “Generation of expandable human pluripotent stem cell-derived hepatocyte-like liver organoids,” *J Hepatol*, vol. 71, no. 5, pp. 970–985, Nov. 2019, doi: 10.1016/j.jhep.2019.06.030.

[151] S. Agarwal, K. L. Holton, and R. Lanza, “Efficient Differentiation of Functional Hepatocytes from Human Embryonic Stem Cells,” *Stem Cells*, vol. 26, no. 5, pp. 1117–1127, May 2008, doi: 10.1634/stemcells.2007-1102.

[152] X. Huang *et al.*, “Current Advances in 3D Dynamic Cell Culture Systems,” Dec. 01, 2022, *MDPI*. doi: 10.3390/gels8120829.

[153] C. Li *et al.*, “Roles and mechanisms of exosomal non-coding RNAs in human health and diseases,” Dec. 01, 2021, *Springer Nature*. doi: 10.1038/s41392-021-00779-x.

[154] J. Kim *et al.*, “Three-dimensional human liver-chip emulating premetastatic niche formation by breast cancer-derived extracellular vesicles,” *ACS Nano*, vol. 14, no. 11, pp. 14971–14988, Nov. 2020, doi: 10.1021/acsnano.0c04778.

[155] V. K. Chetty *et al.*, “Efficient Small Extracellular Vesicles (EV) Isolation Method and Evaluation of EV-Associated DNA Role in Cell–Cell Communication in Cancer,” *Cancers (Basel)*, vol. 14, no. 9, May 2022, doi: 10.3390/cancers14092068.

[156] V. K. Chetty, J. Ghanam, K. Lichá, A. Brenzel, D. Reinhardt, and B. K. Thakur, “Y-box binding protein 1 in small extracellular vesicles reduces mesenchymal stem cell differentiation to osteoblasts—implications for acute myeloid leukaemia,” *J Extracell Vesicles*, vol. 13, no. 3, Mar. 2024, doi: 10.1002/jev2.12417.

[157] J. Ghanam *et al.*, “Extracellular vesicles transfer chromatin-like structures that induce non-mutational dysfunction of p53 in bone marrow stem cells,” Dec. 01, 2023, *Springer Nature*. doi: 10.1038/s41421-022-00505-z.

Acknowledgements

Alla fine di questo intenso e ricco percorso, di cui sono profondamente grato, intendo porgere i miei ringraziamenti a tutte le persone che mi hanno accompagnato e senza le quali non sarei probabilmente arrivato a questo traguardo. Il dottorato di ricerca è stato un percorso travagliato, costellato di gioie e dolori, che ha profondamente cambiato il mio modo di affrontare le sfide e gli ostacoli che la vita inevitabilmente presenta.

Ringrazio il Professore Riccardo Alessandro per essere stato il mio tutor di dottorato e per aver consentito di svolgere la mia attività di ricerca presso i laboratori da lui diretti. Il Professore è stato per me un esempio di instancabilità, forza, amore per la ricerca e di attenzione verso noi studenti. Ringrazio il Professore per essere sempre riuscito a trasmetterci la passione per questo lavoro, lo sguardo critico che ogni ricercatore deve avere, e per averci sempre guidato verso la giusta direzione attraverso le sue indicazioni e "richiami", mantenendo sempre umanità e fermezza.

Ringrazio la Professoressa Alice Conigliaro, co-tutor del mio progetto di dottorato, per avermi trasmesso grande passione per la ricerca e dedizione al lavoro. Grazie alla Prof ho capito l'importanza del diventare pienamente indipendenti nella propria attività di ricerca, e del sapere dare fondo alle proprie forze quando alcune strade sembrano chiuse, riuscendo ad aprirne di nuove.

Ringrazio la Professoressa Simona Fontana, co-tutor di questa tesi di dottorato. Ringrazio la Prof per avermi trasmesso, sin dalla tesi magistrale, l'amore ardente per questo lavoro, la sua grande etica professionale e rigore metodologico. Ringrazio ulteriormente la Prof per essere sempre stata attenta ai travagli e alle inquietudini che a volte accompagnano noi studenti in questo percorso, riuscendo sempre a trovare le parole giuste per motivarci ed ispirarci a fare di meglio.

Ringrazio le dottoresse Marzia Pucci e Stefania Raimondo per essere state delle fonti di grande ispirazione nell'attività di laboratorio, mostrando sempre grande disponibilità, spirito di sacrificio, amore per la ricerca ed energie incrollabili.

Ringrazio i colleghi che mi hanno affiancato per parte o per tutto il percorso, contribuendo, in un modo o nell'altro, alla mia crescita professionale. Grazie ai nostri confronti e scambi di opinione, a volte anche accesi, la mia attività si è arricchita di quella componente importante che à la collaborazione tra colleghi ed il saper lavorare in gruppo. Non per ultimo, grazie per aver reso questo percorso, a volte difficile, più leggero con le nostre risate e gli scherzi insieme. A Denise e Chiara, grazie per la vostra amicizia e per il vostro prezioso contributo nell'avanzamento di questo progetto; a Ornella e Marta, con cui ho iniziato da tirocinante; a Gabriele, Giulia, Nima, Roberta, Antonio, Martina, Aurora, Marilena. A Elisa e Vichi in particolare, oltre che valide colleghe, siete diventate delle preziosissime amiche: grazie a Vichi per tutti gli scambi di opinioni nei momenti delicati di questi tre anni. A Elisa per essere stata di grande aiuto nell'avanzamento di questo progetto, e per aver sempre provato ad affrontare positivamente le situazioni avverse, riuscendo a vedere il buono nelle persone. Grazie ai tesisti, a cui abbiamo cercato di fornire gli strumenti di base allo studio dei processi biologici, ma da cui abbiamo anche tratto grande insegnamenti e condiviso momenti goliardici: ad Anna, Angelo, Francesca, Giuliana, Arianna e Simone. Grazie ai ricercatori dello IOR per i nostri scambi di opinioni e per lo spirito collaborativo e di cordialità che ha contraddistinto la nostra convivenza in Dipartimento.

Ringrazio l'ingegnere Francesco Lopresti ed il suo gruppo di ricerca per la loro energia vulcanica e per il progetto di ricerca che abbiamo portato avanti con grande entusiasmo.

Ringrazio il dottor Basant Kumar Thakur per avermi ospitato durante il periodo di ricerca in Germania, la sua grande ospitalità, e quella del suo gruppo di ricerca, hanno reso la mia permanenza ad Essen molto stimolante e gradevole. Ad Anna, Venki e Jamal. Estendo il ringraziamento a tutti i ricercatori che ho avuto l'onore di conoscere attraverso Congressi, corsi di formazione e altri eventi scientifici, in particolar modo alla dottoressa Rossella Crescitelli e al dottor Frederik Verweij.

Grazie al mio ragazzo, Giovanni, per avermi sempre sostenuto e per essermi stato vicino in questi tre anni, la tua presenza è stata preziosa.

Alla mia famiglia, ed in particolar modo ai miei genitori e ai miei fratelli, Giuseppe e Andrea, per il loro enorme supporto e per tutto l'affetto e la serenità che ci siamo trasmessi.

Ai miei amici e alle persone care che in questi anni hanno accompagnato la mia vita fuori dal laboratorio, la vostra presenza non è stata affatto secondaria. A Davide, Vincenzo, Adriano, Federico, Claudio, Fabio, Salvo, Sarah, Katarina, Julia, Alice, Gabriele, Elena, Enrico, Dario, Francesco, Licia, Chiara, Irene e Noemi.

A conclusione di questi tre anni, sono profondamente grato per il percorso che ho fatto, tutte le avversità e i sacrifici fatti sono stati fondamentali a temprare la mia determinazione, in loro assenza questo risultato non sarebbe stato altrettanto significativo. Anche se il mio dottorato di ricerca finisce oggi, spero non finisca mai il mio l'impegno e la mia dedizione per il bellissimo mondo della ricerca scientifica.

Grazie.